



## FULLERENE NANODISCS: FROM CHEMISTRY TO COMBINATORICS

Mariana Martins Ferreira da Cruz

Dissertação de Mestrado apresentada ao Programa de Pós-graduação em Engenharia de Sistemas e Computação, COPPE, da Universidade Federal do Rio de Janeiro, como parte dos requisitos necessários à obtenção do título de Mestre em Engenharia de Sistemas e Computação.

Orientadores: Celina Miraglia Herrera de  
Figueiredo  
Diana Sasaki Nobrega

Rio de Janeiro  
Junho de 2022

FULLERENE NANODISCS: FROM CHEMISTRY TO COMBINATORICS

Mariana Martins Ferreira da Cruz

DISSERTAÇÃO SUBMETIDA AO CORPO DOCENTE DO INSTITUTO ALBERTO LUIZ COIMBRA DE PÓS-GRADUAÇÃO E PESQUISA DE ENGENHARIA DA UNIVERSIDADE FEDERAL DO RIO DE JANEIRO COMO PARTE DOS REQUISITOS NECESSÁRIOS PARA A OBTENÇÃO DO GRAU DE MESTRE EM CIÊNCIAS EM ENGENHARIA DE SISTEMAS E COMPUTAÇÃO.

Orientadores: Celina Miraglia Herrera de Figueiredo  
Diana Sasaki Nobrega

Aprovada por: Prof. Celina Miraglia Herrera de Figueiredo  
Prof. Diana Sasaki Nobrega  
Prof. Sulamita Klein  
Prof. Luerbio Faria

RIO DE JANEIRO, RJ – BRASIL  
JUNHO DE 2022

Cruz, Mariana Martins Ferreira da  
Fullerene nanodiscs: From Chemistry to  
Combinatorics/Mariana Martins Ferreira da Cruz. –  
Rio de Janeiro: UFRJ/COPPE, 2022.

XIII, 94 p.: il.; 29, 7cm.

Orientadores: Celina Miraglia Herrera de Figueiredo  
Diana Sasaki Nobrega

Dissertação (mestrado) – UFRJ/COPPE/Programa de  
Engenharia de Sistemas e Computação, 2022.

Referências Bibliográficas: p. 59 – 61.

1. Graph Theory. 2. Total Coloring. 3. Conformable  
Coloring. 4. Combinatorics. 5. Fullerenes. 6.  
Nanodiscs. I. Figueiredo, Celina Miraglia Herrera de  
*et al.* II. Universidade Federal do Rio de Janeiro, COPPE,  
Programa de Engenharia de Sistemas e Computação. III.  
Título.

*Dedico essa dissertação a todos  
que estiveram comigo durante  
esta jornada.*

# Agradecimentos

Agradeço à minha família por todo apoio que sempre recebi.

Às minhas orientadoras Celina e Diana, pela orientação e pela ótima trajetória que tivemos juntas durante todo o mestrado. A experiência adquirida por mim graças à essa experiência é de extrema importância para meu desenvolvimento acadêmico e profissional.

Ao meu companheiro Rafael, pelo apoio, por ouvir meus desabaços e estar comigo sempre que precisei. Ao meu companheiro de mestrado Matheus, por todos os momentos que compartilhamos ao longo dessa experiência.

Ao professor Marcus Tovar, que esteve conosco durante todo o mestrado, participando ativamente dos resultados dessa dissertação.

Ao professor Diego Nicodemos, que também tem um papel fundamental neste trabalho.

Aos membros da banca, por aceitarem avaliar este trabalho.

Ao PESC, por sua excelência e por me dar boas condições para obtenção dessa dissertação.

À CAPES, pelo suporte financeiro.

Resumo da Dissertação apresentada à COPPE/UFRJ como parte dos requisitos necessários para a obtenção do grau de Mestre em Ciências (M.Sc.)

## NANODISCOS DE FULERENO: DA QUÍMICA PARA A COMBINATÓRIA

Mariana Martins Ferreira da Cruz

Junho/2022

Orientadores: Celina Miraglia Herrera de Figueiredo  
Diana Sasaki Nobrega

Programa: Engenharia de Sistemas e Computação

Um grafo é um modelo matemático utilizado para representar relações entre objetos. O estudo formal desses objetos combinatórios e suas relações levou à criação da chamada Teoria de Grafos, que foi aplicada a problemas de grande escala em diversas áreas, como matemática, física, informática, engenharia, química e psicologia. Grafos fulerenos são modelos matemáticos para moléculas compostas exclusivamente por átomos de carbono, descobertas experimentalmente no início da década de 1980. Diversos parâmetros associados a estes grafos vêm sendo discutidos, buscando descrever a estabilidade destas moléculas. Por definição, grafos fulerenos são cúbicos, planares, 3-conexos formados por faces pentagonais e hexagonais. Uma coloração total de um grafo  $G$  atribui cores aos vértices e arestas de  $G$  tal que elementos adjacentes ou incidentes tenham cores distintas. A famosa Conjectura da Coloração Total permanece aberta há mais de 50 anos e está provada para grafos cúbicos, mas ainda não foi demonstrada para grafos regulares e nem para grafos planares arbitrários. O comprimento do menor ciclo de um grafo é denominado cintura. Nosso objetivo é estudar a coloração total de uma subfamília infinita de grafos fulerenos, os nanodiscos de fulerenos  $D_r$ , com distância entre a camada interna (externa) e a camada central dada pelo parâmetro raio  $r \geq 2$ , motivados por uma conjectura de que a cintura de um grafo é um parâmetro relevante no estudo da coloração total. Para destacar a escolha da classe de grafos estudada, apresentamos um aporte histórico da descoberta da molécula de carbono que pode ser modelada através de um grafo cúbico planar especial que possui cintura 5. Fornecemos a primeira descrição combinatória para os nanodiscos para aprimorar a compreensão desta classe, e em seguida estudamos a coloração harmônica em subfamílias infinitas de nanodiscos, para que então possamos enfrentar a desafiadora coloração total nesses grafos.

Abstract of Dissertation presented to COPPE/UFRJ as a partial fulfillment of the requirements for the degree of Master of Science (M.Sc.)

## FULLERENE NANODISCS: FROM CHEMISTRY TO COMBINATORICS

Mariana Martins Ferreira da Cruz

June/2022

Advisors: Celina Miraglia Herrera de Figueiredo

Diana Sasaki Nobrega

Department: Systems Engineering and Computer Science

A graph is a mathematical model used to represent relationships between objects. The general characteristics that objects and their relationships can assume allowed the construction of the (so-called) Graph Theory, which has been applied to model large scale problems in several areas, such as Mathematics, Physics, Computer Science, Engineering, Chemistry and Psychology.

Fullerene graphs are mathematical models for carbon-based molecules experimentally discovered in the early 1980. Many parameters associated with these graphs have been discussed to describe the stability of fullerene molecules. By definition, fullerene graphs are cubic, planar, 3-connected with pentagonal and hexagonal faces. A total coloring of a graph  $G$  assigns colors to the vertices and edges of  $G$  such that adjacent or incident elements have different colors. The famous Total Coloring Conjecture open for 50 years is settled for cubic graphs, but not to arbitrary regular graphs nor to arbitrary planar graphs. The length of the shortest cycle in a graph is called girth. Our goal is to study the total coloring of an infinite subfamily of fullerene graphs, the fullerene nanodiscs  $D_r$ , with distance between the inner (outer) layer and the central layer given by the radius parameter  $r \geq 2$ , motivated by a conjecture that the girth of a graph is a relevant parameter in the study of total coloring. To highlight the choice of the studied graph class, we present a historical scenario of the carbon molecule discovery that can be modeled through a special cubic planar graph of girth 5. We contribute by giving the first combinatorial description for fullerene nanodiscs, aiming to improve the understanding of this class and then a conformable coloring for infinite families of fullerene nanodiscs, so that we are able to tackle the challenging total coloring of these graphs.

# Contents

<b>List of Figures</b>	<b>x</b>
<b>List of Tables</b>	<b>xiii</b>
<b>1 Introduction</b>	<b>1</b>
1.1 Königsberg Bridge Problem . . . . .	1
1.2 Four-Color Problem . . . . .	3
1.3 Basic Definitions . . . . .	4
1.4 Graph Coloring . . . . .	12
1.4.1 Vertex Coloring . . . . .	12
1.4.2 The Conformable Condition . . . . .	14
1.4.3 Edge Coloring . . . . .	14
1.4.4 Total Coloring . . . . .	17
1.4.5 Equitable Total Coloring . . . . .	19
<b>2 Fullerene graphs</b>	<b>21</b>
2.1 A graph class modeling a molecule . . . . .	21
2.2 Graph properties . . . . .	25
<b>3 Fullerene nanodiscs</b>	<b>28</b>
3.1 Knowing the class structure . . . . .	28
3.2 Combinatorial results . . . . .	31
<b>4 On the total coloring of nanodiscs</b>	<b>41</b>
4.1 All nanodiscs are conformable . . . . .	42
4.2 Hunting a Type 2 fullerene nanodisc . . . . .	48
4.2.1 The natural strategy does not work . . . . .	52
<b>5 Conclusion</b>	<b>56</b>
<b>References</b>	<b>59</b>
<b>A Fullerene Nanodisc: The definition through its dual</b>	<b>62</b>

<b>B Attachment: Poster “A result on total coloring of fullerene nanodiscs” presented at LAWCG 2020</b>	<b>71</b>
<b>C Attachment: Manuscript “Hunting a Type 2 fullerene nanodisc”, Matemática Contemporânea volume 48, 2021</b>	<b>73</b>
<b>D Attachment: Poster “Fullerene nanodiscs: from Chemistry to Combinatorics” presented at WPCCG 2021</b>	<b>86</b>
<b>E Attachment: Extended abstract “The conformable condition for Nanodiscs” to be presented at ETC 2022</b>	<b>88</b>
<b>F Attachment: Abstract “Hunting a conformable fullerene nanodisc that is not 4-total colorable” accepted for participation in LAWCG 2022</b>	<b>93</b>

# List of Figures

1.1	Region of Königsberg. The seven bridges are labeled a, b, c, d, e, f and g. . . . .	2
1.2	Graph representation. The seven bridges correspond to the seven edges connecting the four vertices A, B, C and D. . . . .	2
1.3	The map of the districts of England colored with four colors. . . . .	3
1.4	A graph with $\Delta = 3$ . . . . .	4
1.5	The cycle graphs $C_4$ and $C_7$ , respectively. . . . .	5
1.6	A connected graph and a disconnected graph, respectively. . . . .	6
1.7	A graph (a), its induced subgraph (b) and its subgraph (c) that is not induced. . . . .	6
1.8	Two isomorphic graphs. . . . .	6
1.9	A 2-regular graph and a 3-regular graph, respectively. . . . .	7
1.10	A bipartite graph with 5 vertices and a complete bipartite graph with 6 vertices, respectively. . . . .	7
1.11	The complete graphs up to 5 vertices. . . . .	8
1.12	Vertices in blue and labeled with number 1 form an independent set in the graph. Note that this independent set is maximum. . . . .	8
1.13	Edges in blue and labeled with number 1 form a matching in the graph. Note that this matching is perfect. . . . .	8
1.14	A graph with $\kappa(G) = 1$ and $\kappa'(G) = 2$ . . . . .	9
1.15	The edge $e$ is a bridge in this graph. . . . .	10
1.16	Two representations of the $K_4$ graph, where the representation on the right is planar. . . . .	10
1.17	A planar graph with five faces, where $f_1$ is the external face. . . . .	11
1.18	The dual representation of the graph of the Figure 1.17. . . . .	12
1.19	A graph with $\chi(G) = 3$ . . . . .	13
1.20	On the left, a $(\Delta + 1)$ -vertex coloring of $C_4$ , where a color class has cardinality zero. On the right, a $(\Delta + 1)$ -vertex coloring of $C_7$ . . . . .	14
1.21	A graph with $\chi'(G) = 3$ . . . . .	15
1.22	A Class 1 graph and a Class 2 graph, respectively. . . . .	16

1.23	A 2-regular Class 1 graph and a cubic Class 2 graph, respectively. . . . .	16
1.24	A graph with $\chi''(G) = 4$ . . . . .	17
1.25	A Type 1 and a Type 2 graph, respectively. . . . .	18
1.26	An equitable 4-total coloring for the cycle graph $C_5$ . . . . .	19
2.1	Molecular structure of diamond, graphite and lonsdaleite, respectively. . . . .	22
2.2	Robert Curl, Harold Kroto and Richard Smalley. . . . .	22
2.3	Montreal Biosphere. . . . .	23
2.4	Molecular structure of $C_{60}$ . . . . .	23
2.5	Structure of some fullerene molecules. . . . .	24
2.6	Fullerene graph of $C_{60}$ with the pentagons highlighted in blue. . . . .	25
2.7	Molecular structure (a) and fullerene graph (b) of $C_{20}$ . . . . .	26
3.1	The smallest fullerene nanodisc graphs. . . . .	28
3.2	Two consecutive pentagons partitioned differently. . . . .	30
3.3	Three-dimensional view of the nanodisc $D_5$ , the smallest nanodisc that contradicts the Conjecture 5. . . . .	30
3.4	Balanced and unbalanced hexagons, respectively. . . . .	31
3.5	When two consecutive faces are such that each face has 2 vertices in the same auxiliary cycle, we obtain a large forbidden face. . . . .	31
3.6	Three pentagons arranged alternately in the central layer of $D_r$ . . . . .	32
3.7	Two consecutive pentagons followed by an unbalanced hexagon in the central layer of $D_3$ contradicts the large forbidden face lemma. . . . .	33
3.8	A balanced hexagon between two pentagons partitioned in the same way in the central layer of $D_3$ contradicts the large forbidden face lemma. . . . .	34
3.9	The three possible cases to have at least 3 hexagons between the pentagons in the central layer of $D_4$ . . . . .	35
3.10	The two possibilities of having an unbalanced hexagon between the pentagons in the central layer of $D_4$ . . . . .	36
3.11	Case in which there are two hexagons between the pentagons. . . . .	37
3.12	The possibilities of having mixed pentagons when $r = 4$ . . . . .	39
3.13	Two possible representations of fullerene nanodisc $D_4$ . . . . .	40
4.1	(a) A Type 2 girth 3 cubic graph; (b) a Type 2 girth 4 cubic graph. . . . .	41
4.2	A 4-total coloring of fullerene graph $C_{20}$ . . . . .	42
4.3	Conformable colorings for $D_2$ and $D_4$ , respectively. . . . .	42
4.4	A 4-vertex coloring that does not give a conformable coloring of $D_3$ . . . . .	43
4.5	An optimal 3-vertex coloring that gives a conformable coloring of $D_3$ . . . . .	44

4.6	On the left, a 3-vertex coloring for $D_5$ , with $ \mathcal{C}_1  = 141$ , $ \mathcal{C}_2  = 140$ , $ \mathcal{C}_3  = 19$ and on the right, a conformable 4-vertex coloring for $D_5$ , where $ \mathcal{C}_1  = 140$ , $ \mathcal{C}_2  = 140$ , $ \mathcal{C}_3  = 18$ , $ \mathcal{C}_4  = 2$ . Note that the non-adjacent vertices $u \in \mathcal{C}_1$ and $v \in \mathcal{C}_3$ received color $\mathcal{C}_4$ during the procedure. . . . .	45
4.7	A pair of pentagons in the central layer of $D_r$ , $r \geq 3$ and their neighboring vertices. . . . .	46
4.8	Attempt to extend a vertex coloring into a 4-total coloring whose adjacent auxiliary cycles are colored with two colors. . . . .	47
4.9	A 5-total coloring of $D_4$ . . . . .	49
4.10	A 5-total coloring of $D_3$ . . . . .	50
4.11	A 5-total coloring of $D_3$ . . . . .	51
4.12	A 4-total coloring of fullerene nanodisc $D_2$ . . . . .	52
4.13	A 3-total coloring of $C_6$ and $C_{18}$ , respectively. . . . .	53
4.14	(a) A 3-total coloring for $D_r[C] \setminus M_1$ ; (b) Color conflict after the inclusion of radial edges that form 6 unbalanced hexagons. . . . .	54
A.1	(a) the subgraph $T_2(N)$ , where its border consists of 12 vertices, where the vertices of degree 3 are: $u_1, u_3, u_5, u_7, u_9$ and $u_{11}$ ; (b), the subgraph $T_3(N)$ , where its border consists of 18 vertices, where the vertices of degree 3 are: $u_1, u_4, u_7, u_{10}, u_{13}$ and $u_{16}$ . . . . .	63
A.2	On the left, the $T_3(N)$ subgraph. On the right, the $T_3(S)$ subgraph. . . . .	64
A.3	On the left, the planar triangulation $D_{3,1}^*$ . On the right, its corresponding fullerene nanodisc $D_{3,1}$ . . . . .	64
A.4	Two possible representations of fullerene nanodisc $D_4$ . . . . .	67
A.5	Two possible representations of fullerene nanodisc $D_5$ . . . . .	69

# List of Tables

3.1	Number of vertices, faces, edges and layers in a fullerene nanodisc $D_r$ , according to parameter $r \geq 2$ . . . . .	29
-----	--	----

# Chapter 1

## Introduction

We understand by graph a mathematical model used to represent relations between objects, having applications in the resolution of problems of several areas, modeling problems and large situations. Graph Theory studies combinatorial objects, as they are good models for many problems in various branches of Mathematics, Computer Science, Engineering, Chemistry, Psychology, and Industry.

This text is divided into five chapters. In Chapter 1, we briefly introduce Graph Theory and some motivating problems, as well as basic definitions necessary for understanding the text, in order to make it self-sufficient. In Chapter 2 we describe the fullerene graphs, which are mathematical models for molecules composed exclusively of carbon atoms, making a brief historical exposition of their origin and some properties of these graphs. Chapter 3 is dedicated to the fullerene nanodiscs, a sub-family of fullerene graphs that is the main object of study of this dissertation. We present combinatorial and structural properties of this class unpublished in the literature. In Chapter 4, we contextualized the search for a Type 2 fullerene nanodisc and presented the conformable condition, showing results about vertex coloring and total coloring of fullerene nanodiscs. Finally, in the last chapter, we will summarize the results obtained and future steps.

### 1.1 Königsberg Bridge Problem

Leonhard Euler's paper published in 1736 [16] on the "Königsberg Bridge Problem" is considered the first result of Graph Theory. Königsberg was a city in ancient Prussia (See Figure 1.1<sup>1</sup>), today called Kaliningrad, in present-day Russia. In the central part of Königsberg, slopes of the Pregel River flowed, forming two islands. Seven bridges, connecting parts of the city, were built. The problem was originated by the curiosity of the inhabitants of not finding a route (with departure and arrival at the same place) that allowed them to cross only once each of the bridges.

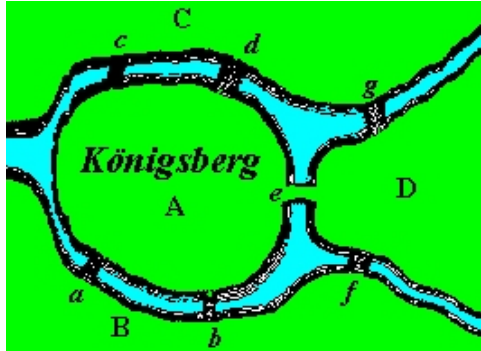


Figure 1.1: Region of Königsberg. The seven bridges are labeled a, b, c, d, e, f and g.

To solve the Königsberg Bridge Problem, the Swiss mathematician Leonhard Euler eliminated details that did not influence the problem, such as distance and size of islands. He focused only on what he considered important. With this, Euler represented the problem in a rather simple, diagrammatic form, and this diagram is considered to have been the first example of a graph (See Figure 1.2<sup>2</sup>). In his diagram, Euler identified each bridge as an edge and each island and margin as a vertex. With this, the problem was reduced to verifying whether it would be possible to find a trajectory on the diagram that met each edge only once, returning to the starting point. In other words, the problem has been reduced to an analysis of the degrees of the vertices of the graph, and it has been proved that the Königsberg Bridge Problem has no solution.

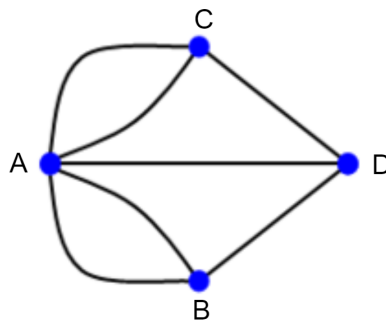


Figure 1.2: Graph representation. The seven bridges correspond to the seven edges connecting the four vertices A, B, C and D.

<sup>1</sup>Figure from <https://www.inf.ufsc.br/grafos/problema/pontes/grafos.html>. Accessed on 03 Mai. 2022.

<sup>2</sup>Figure from <https://m3.ime.unicamp.br/arquivos/1258/pontes-guia.pdf>. Accessed on: 18 Out. 2021.

## 1.2 Four-Color Problem

The Four-Color Problem deals with determining the minimum number of colors needed to color a map, from real or imaginary countries so that countries with common borders have different colors. In 1852, Francis Guthrie, while trying to color several districts on the map of England in such a way that two neighboring districts did not have the same color, concluded that any map could be colored with only four colors, formulating the Four-Color Conjecture. As the Königsberg Bridge Problem, the Four-Color Problem is also extremely important for the theoretical foundation of graph theory, since it is the first known coloring problem. Figure 1.3<sup>3</sup> illustrates the map of the English districts colored with four colors.



Figure 1.3: The map of the districts of England colored with four colors.

For 124 years, various methods have been developed to try to solve the Four-Color Problem, until the Graph Theory emerged to address the problem. Finally, in 1976, Kenneth Appel and Wolfgang Haken, using an IBM 360, presented a proof for the Four-Color Theorem. The demonstration, however, generated much controversy, as it depended, in an essential way, on the use of large computers. In 1990, a new proof of the Four Color Theorem was developed by four mathematicians, Neil Robertson, Dan Sanders, Paul Seymour and Robin Thomas [26]. Their demonstration still made use of computers, but the computational part can be performed, on a laptop, in just a few hours. The Four-Color Theorem was the first theorem to be demonstrated using computers. Note that we can model this problem from a graph, where each region of

<sup>3</sup>Figure from <http://onlinemaps.blogspot.com/2012/08/map-of-england-with-counties.html>. Accessed on: 03 Mai. 2022.

the map is represented by a vertex and the boundary between neighboring regions is represented by an edge, and assign distinct colors to the vertices that are adjacent, thus setting up a vertex coloring problem, topic that will be addressed later.

### 1.3 Basic Definitions

In this section, we bring basic definitions and Theorems of Graph Theory that will be used throughout this dissertation. Such definitions and results were obtained in [5] and [35].

**Definition 1.** A simple graph  $G = ((V(G), E(G)))$  is an ordered pair, where  $V(G)$  is a nonempty finite set of vertices and  $E(G)$  is a set, disjoint with  $V(G)$  of edges, formed by unordered pairs of distinct elements of  $V(G)$ , i.e., for every edge  $e(G)$  there are  $u$  and  $v \in V(G)$  such that  $e = uv$ . We can denote a graph as  $G = (V, E)$  or just  $G$ .

If  $uv \in E(G)$ , we say that  $u$  and  $v$  are adjacent vertices or that  $u$  is neighbor of  $v$ , and that the edge  $e$  is incident of  $u$  and  $v$ , and  $u$  and  $v$  are extremes of  $e$ . We define  $N(v) = \{u, uv \in E(G)\}$  as the open neighborhood of  $v$  in  $G$ . The closed neighborhood is  $N[v] = N(v) \cup \{v\}$  in  $G$ . If  $S$  is a subset of  $V(G)$ , we denote by  $N_s(v) = N(v) \cap S$  the neighborhood of  $v$  at  $S$ . Two edges that have the same ends are called adjacent edges.

**Definition 2.** The degree of a vertex  $v$  in a simple graph  $G$ , denoted by  $d(v)$ , is given by the number of edges incident to  $v$ , or similarly, the number of vertices adjacent to  $v$ . The maximum degree of  $G$ , denoted by  $\Delta(G)$ , is the highest degree of all vertices, i.e.,  $\Delta(G) = \max \{d(v) : v \in V(G)\}$ . See Figure 1.4.

**Observation 1.** When there is no ambiguity, we will just use  $\Delta$  to represent the maximum degree of a graph  $G$ .

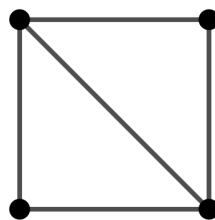


Figure 1.4: A graph with  $\Delta = 3$ .

**Theorem 2** (The handshaking Lemma). For any graph  $G$ ,

$$\sum_{v \in V} d(v) = 2m.$$

*Proof.* Summing the degrees counts each edge twice, since each edge has two ends and contributes to the degree at each endpoint.  $\square$

**Corollary 1.** *In any graph, the number of vertices of odd degree is even.*

*Proof.* If we had an odd number of vertices of odd degree, a sum of degrees would be odd. But the sum of degrees is twice the number of edges and therefore is an even number.  $\square$

**Definition 3.** *A walk of a graph  $G$  is a sequence of vertices  $S = (v_1, v_2, \dots, v_k)$ , where  $v_i, i = 1, \dots, k$  belongs to the vertex set  $V(G)$  and  $v_i v_{i+1}$  is an edge of  $G$ .*

*A path or track is a walk without repeated edges. A path is said closed if the walk  $S = (v_1, v_2, \dots, v_k)$  has  $v_1 = v_k$ .*

**Definition 4.** *A cycle in a graph  $G$  is a closed path, with a single repetition of vertices and no repetition of edges.*

**Definition 5.** *The girth of a graph  $G$ , denoted by  $g(G)$  is the length of the shortest cycle in  $G$ .*

**Definition 6.** *The cycle graph is a graph that consists of a single cycle, or in other words, some number of vertices (at least 3, if the graph is simple) connected in a closed chain. The cycle graph with  $n$  vertices is called  $C_n$ . See Figure 1.5.*

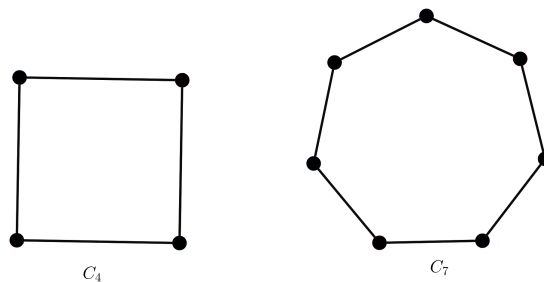


Figure 1.5: The cycle graphs  $C_4$  and  $C_7$ , respectively.

**Observation 3.** *In this work, we denote the cycle  $C_3$  as triangle, the  $C_4$  as square, the  $C_5$  as pentagon and the  $C_6$  as hexagon.*

**Definition 7.** *A graph  $G$  is called connected when there is a path between each pair of vertices of  $G$ . Otherwise, the graph is called disconnected. See Figure 1.6.*

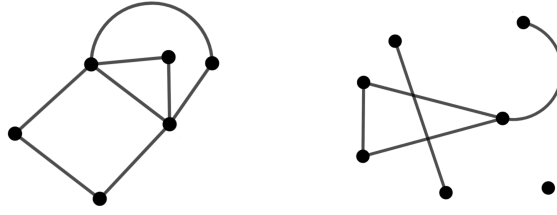


Figure 1.6: A connected graph and a disconnected graph, respectively.

**Definition 8.** A subgraph  $G' = (V', E')$  of a graph  $G$  is a graph obtained from  $G$  such that  $V(G') \subseteq V(G)$  e  $E(G') \subseteq E(G)$ .

**Definition 9.** Let  $G$  be a graph and  $S$  be a subset of vertices. We say that  $G[S]$  is the subgraph induced by  $S$  when  $G[S] = (S, \{uv; u, v \in S \text{ e } uv \in E(G)\}) = (V(G[S]), E(G[S]))$ . See Figure 1.7.

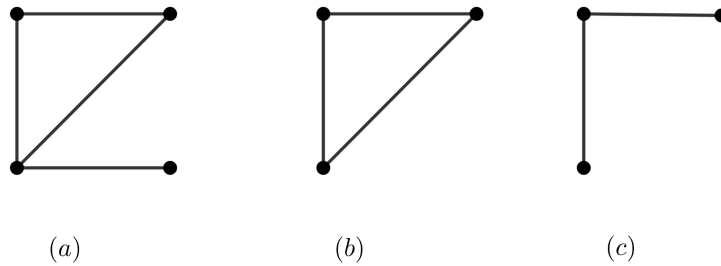


Figure 1.7: A graph (a), its induced subgraph (b) and its subgraph (c) that is not induced.

**Definition 10.** Given two graphs  $G_1$  and  $G_2$ .  $G_1$  and  $G_2$  are isomorphic if there is a biunivocal function  $f : V(G_1) \rightarrow V(G_2)$  such that  $uv \in E(G_1) \Leftrightarrow f(u)f(v) \in E(G_2)$ . See Figure 1.8.

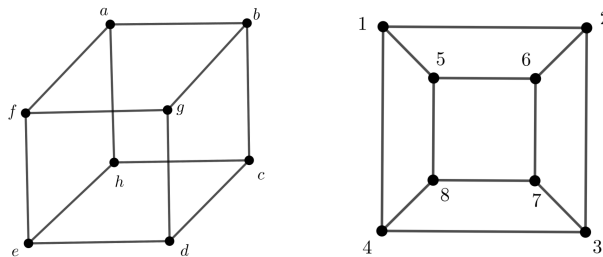


Figure 1.8: Two isomorphic graphs.

**Definition 11.** A graph  $G$  is called regular of degree  $r$  or  $r$ -regular when all its vertices have the same degree  $r$ . See Figure 1.9.

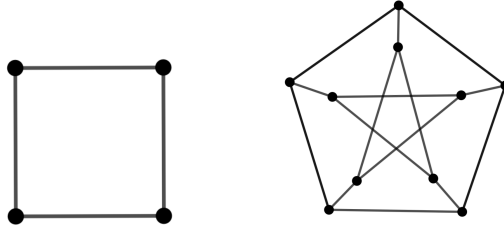


Figure 1.9: A 2-regular graph and a 3-regular graph, respectively.

For  $r = 0, 1, 2$ , the  $r$ -regular graphs have very simple structures and are easily characterized. On the other hand, 3-regular graphs can be remarkably complex. These graphs, also known as cubic, play a fundamental role in the Graph Theory. If no vertex is connected to more than three edges, then  $G$  is called subcubic.

**Definition 12.** A graph  $G$  is bipartite when its vertex set  $V$  can be partitioned into two subsets  $V_1, V_2$  so that every edge of  $G$  joins a vertex of  $V_1$  to a vertex of  $V_2$ . In this case,  $V_1$  and  $V_2$  are called partition sets.  $G$  is called complete bipartite when it has an edge for each pair of vertices  $v_1 \in V_1$  and  $v_2 \in V_2$ . Indicating  $n_1$  as the number of vertices of  $V_1$  and  $n_2$  the number of vertices of  $V_2$ , a complete bipartite graph is denoted by  $K_{n_1, n_2}$  and has  $n_1 n_2$  edges. See Figure 1.10.

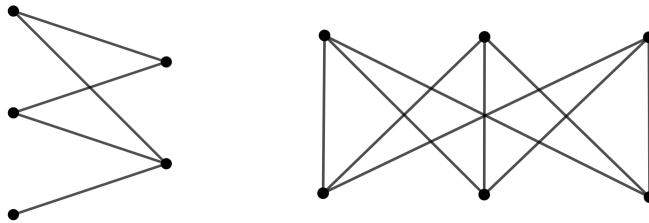


Figure 1.10: A bipartite graph with 5 vertices and a complete bipartite graph with 6 vertices, respectively.

**Definition 13.** A graph  $G$  is called complete when there is an edge between each pair of its vertices. We use the  $K_n$  notation for complete graphs with  $n$  vertices. Note that in a complete graph,  $d(v) = n - 1$  for all  $v \in V(K_n)$ . In other words, every complete graph is  $n - 1$ -regular. See Figure 1.11.

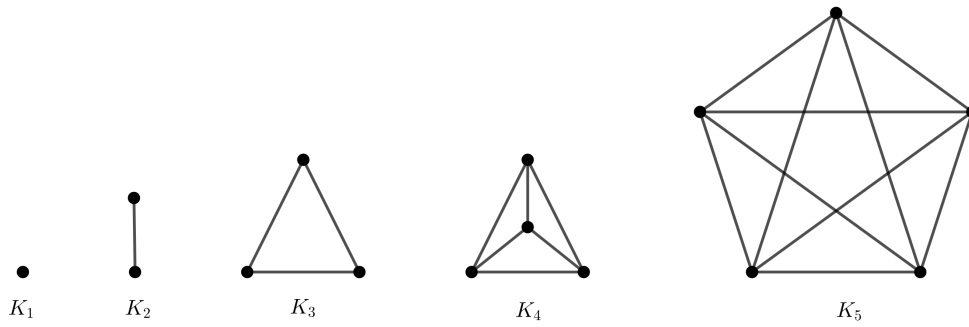


Figure 1.11: The complete graphs up to 5 vertices.

**Definition 14.** A set of vertices  $S \subseteq V(G)$  is called independent set if no two vertices in  $S$  are adjacent to each other. The independence number of  $G$  is the maximum size of an independent set and is denoted  $\alpha(G)$ . See Figure 1.12.

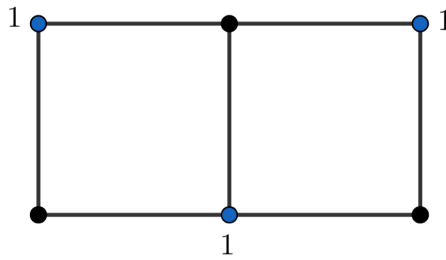


Figure 1.12: Vertices in blue and labeled with number 1 form an independent set in the graph. Note that this independent set is maximum.

**Definition 15.** A matching is a subset of edges  $M \subseteq E(G)$  in a graph  $G$  such that no two edges share the same vertex. If a matching involves all vertices of  $G$ , then  $M$  is called perfect matching. The independence edge number of  $G$  is the maximum size of a matching and is denoted by  $\alpha'(G)$ . See Figure 1.13.

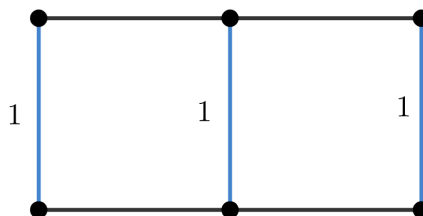


Figure 1.13: Edges in blue and labeled with number 1 form a matching in the graph. Note that this matching is perfect.

**Definition 16.** A vertex cut of a graph  $G$  is a subset  $V' \subset V(G)$  such that  $G \setminus V'$  is disconnected. A  $k$ -vertex cut is a vertex cut of  $k$  elements.

**Definition 17.** The vertex connectivity  $\kappa(G)$  of a graph  $G$  is the cardinality of the minimum vertex cut of  $G$ , and  $G$  is said  $k$ -vertex-connected if  $\kappa(G) \geq k$ .

**Definition 18.** Let  $G$  be a graph. If  $S, T$  are vertex subsets of  $G$ , so  $[S, T]$  is the set of all the edges of  $G$  that has one extreme on  $S$  and another on  $T$ .

**Definition 19.** An edge cut of a graph  $G$  is a nonempty set  $E' \subset E(G)$  of the form  $E' = [S, \bar{S}]$ , where  $S \subset V(G)$  e  $\bar{S} = V(G) \setminus S$ , such that  $G \setminus E'$  is disconnected. A  $k$ -edge cut is a edge cut of  $k$  elements.

**Definition 20.** The edge connectivity  $\kappa'(G)$  of a graph  $G$  is the cardinality of the minimum edge cut of  $G$ , and  $G$  is said  $k$ -edge-connected if  $\kappa'(G) \geq k$ .

Figure 1.14 displays a graph whose minimum vertex cut is given by the vertex subset  $V' = \{w\}$  and minimum edge cut given by the edge subset  $E' = \{uw, vw\}$ .

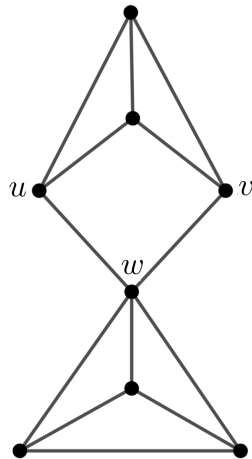


Figure 1.14: A graph with  $\kappa(G) = 1$  and  $\kappa'(G) = 2$ .

**Definition 21.** An edge  $e \in E(G)$  is called bridge when  $G \setminus e$  is a disconnected graph. See Figure 1.15.

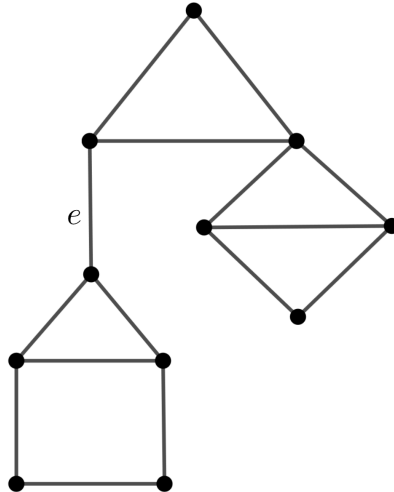


Figure 1.15: The edge  $e$  is a bridge in this graph.

**Definition 22.** A graph  $G$  is called *bridgeless* if it cannot be disconnected by deleting any one edge. See Figure 1.14.

Julius Petersen in 1891 established a relationship between bridgeless cubic graphs and perfect matchings, culminating in the following result.

**Theorem 4** (Petersen’s Theorem, 1891 [25]). *Any bridgeless cubic graph has a perfect matching.*

**Definition 23.** A graph  $G$  is said to be *planar* if there is a representation (embedding) in the plane so that the edges do not intersect. Such a representation is called a *planar embedding* of  $G$ . We also refer to a planar embedding of a planar graph as a *plane graph*. See Figure 1.16.

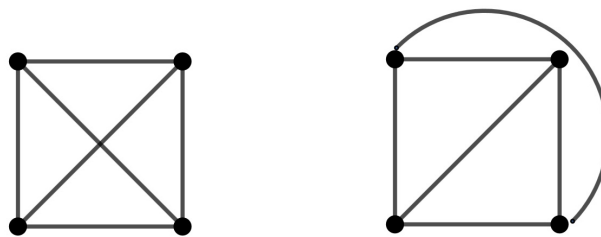


Figure 1.16: Two representations of the  $K_4$  graph, where the representation on the right is planar.

The solution of the “Königsberg Bridge Problem”, mentioned in detail in Section 1.1 was not Leonhard Euler’s only contribution to the development of Graph Theory. He also established a formula for polyhedral graphs that relates the number of vertices, edges and faces in a planar connected graph. This formula became known as Euler’s Formula, and will be enunciated below.

**Theorem 5** (Euler's Formula, 1752 [5]). *If  $G$  is a connected plane graph with  $f$  faces,  $m$  edges and  $n$  vertices, then*

$$n - m + f = 2.$$

**Definition 24.** *A planar graph  $G$  divides the plane into regions. Such regions are called faces of  $G$ .*

**Definition 25.** *The border or outer cycle of a face  $f$  of a connected planar graph is a closed edge walk that limits and determines  $f$  and is denoted by  $\partial(f)$ . Two faces  $f$  and  $g$  are adjacent if they have a common edge between their borders.*

There is always a face that is not limited, that is, has infinite area. This face is called external or infinite face. See Figure 1.17.

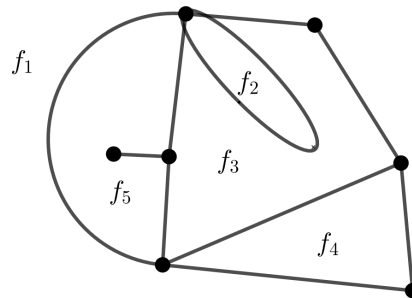


Figure 1.17: A planar graph with five faces, where  $f_1$  is the external face.

**Definition 26.** *Let  $G$  be a planar graph. We define the dual graph of  $G$ , denoted by  $G^*$  as follows: each  $f$  face of  $G$  corresponds to a vertex  $f^*$  of  $G^*$ , and each  $e$  edge of  $G$  corresponds to an  $e^*$  edge of  $G^*$ . Two vertices  $f^*, g^* \in G^*$  are adjacent if and only if it has an edge between its corresponding faces  $f, g \in G$ . See Figure 1.18.<sup>4</sup>*

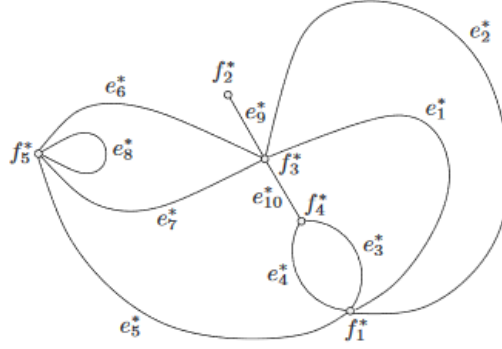


Figure 1.18: The dual representation of the graph of the Figure 1.17.

Once we have introduced the basic definitions of Graph Theory, we can resume the topic of graph coloring, which is extremely important in this dissertation.

## 1.4 Graph Coloring

In Graph Theory, graph coloring is an assignment of colors to elements of the graph, subject to certain restrictions. The coloring study was started with the Four-Color Problem, as mentioned in the Section 1.2. As was done in the previous section, we will bring basic concepts of graph coloring, as well as important results. This section is divided into four subjects: vertex coloring, edge coloring, total coloring and equitable total coloring. Such results were obtained in [9],[10],[30] and [36].

### 1.4.1 Vertex Coloring

**Definition 27.** Let  $G$  be a graph and  $\mathcal{C} = \{\mathcal{C}_1, \mathcal{C}_2, \dots, \mathcal{C}_k\}$ ,  $k \in \mathbb{N}$  be a set of colors. A vertex coloring of  $G$  is an assignment of some color of  $\mathcal{C}$  for each vertex  $v$  of  $G$  so that the adjacent vertices are assigned distinct colors.

A  $k$ -coloring of  $G$  is a vertex coloring with  $k$  colors. We say then that  $G$  is  $k$ -colorable.

**Definition 28.** We define as chromatic number of a graph  $G$  the smallest number of colors  $k$  for which there is a  $k$ -coloring of  $G$ , and is denoted by  $\chi(G)$ . See Figure 1.19.

---

<sup>4</sup>Figure from [5].

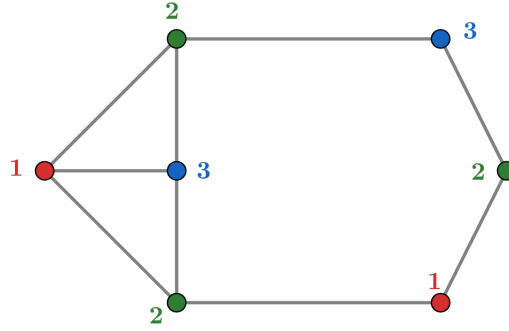


Figure 1.19: A graph with  $\chi(G) = 3$ .

It is possible to establish the chromatic number  $\chi(G)$  for some special classes of graphs, as follows.

**Theorem 6** ([9]). *A graph  $G$  is 2-colorable if and only if  $G$  is bipartite.*

*Proof.* If  $G$  is a bipartite graph, let  $V_1, V_2 \subseteq V$  be the subsets of  $V$  that partition it. Thus, just assign the color  $\mathcal{C}_1$  to the vertices of  $V_1$  and the color  $\mathcal{C}_2$  to the vertices of  $V_2$ . Conversely, if  $G$  is 2-colorable, consider a 2-vertex coloring of  $G$  with the colors  $\mathcal{C}_1$  and  $\mathcal{C}_2$ , in this order. Let  $V_1$  and  $V_2$  be the vertex subsets that have the colors  $\mathcal{C}_1$  and  $\mathcal{C}_2$ , respectively. Then  $V_1$  and  $V_2$  are bipartitions of  $G$ . □

**Theorem 7** ([9]). *Let  $G$  be the cycle graph  $C_n$  with  $n$  vertices. Then*

$$\chi(G) = \begin{cases} 2, & \text{if } n \text{ is even;} \\ 3, & \text{if } n \text{ is odd.} \end{cases}$$

**Theorem 8** ([9]). *Let  $K_n$  be the complete graph with  $n$  vertices. Then  $\chi(K_n) = n$ .*

**Theorem 9** (Brooks' Theorem, 1941 [8]). *If  $G$  is a connected simple graph,  $\chi(G) \leq \Delta$  unless  $G$  is an odd cycle or a complete graph. In these cases, the chromatic number is  $\Delta + 1$ .*

Since the pairs of adjacent vertices of a planar graph correspond to the pairs of adjacent faces of its dual, the Four-Color Problem is equivalent to the following statement.

**Conjecture 1** (The Four-Color Conjecture for vertices [5]). *Every loopless planar graph is 4-colorable.*

## 1.4.2 The Conformable Condition

**Definition 29.** *The deficiency of a graph  $G$ , denoted by  $def(G)$ , is defined as*

$$def(G) = \sum_{v \in V(G)} (\Delta - d(v)).$$

Let  $C$  be a  $(\Delta + 1)$ -vertex coloring of  $G$ , and  $r$  the number of coloring classes of  $C$ , where the size has the same parity as  $|V(G)|$ . If

$$def(G) \geq \Delta + 1 - r,$$

this vertex coloring is said conformable [10]. If  $G$  has some conformable vertex coloring, then  $G$  is called conformable.

We can restrict the conformable coloring definition to a regular graphs, as following.

**Lemma 10** (Chetwynd and Hilton, 1988 [10]). *Let  $G$  be a regular graph.  $G$  is conformable if and only if it has a vertex coloring with  $\Delta + 1$  colors and each color class has the same parity of  $|V(G)|$ .*

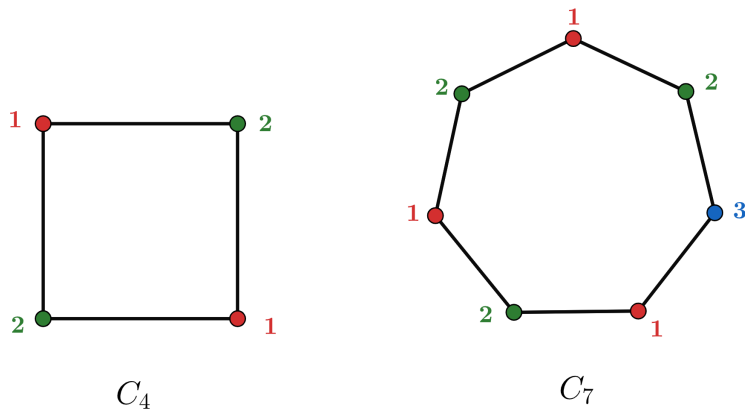


Figure 1.20: On the left, a  $(\Delta + 1)$ -vertex coloring of  $C_4$ , where a color class has cardinality zero. On the right, a  $(\Delta + 1)$ -vertex coloring of  $C_7$ .

The two colorings exhibited in Figure 1.20 are conformable vertex colorings. This special vertex coloring will be very important in this work, as it is one of our tools to establish some results in our target class.

## 1.4.3 Edge Coloring

**Definition 30.** *Let  $G$  be a graph and be a set of colors. An edge coloring of  $G$  is an assignment of some color of  $\mathcal{C} = \{C_1, C_2, \dots, C_k\}$ ,  $k \in \mathbb{N}$  for each edge  $e$  of  $G$  so that the adjacent edges are assigned distinct colors.*

A  $k$ -edge coloring of  $G$  is an edge coloring with  $k$  colors. We say then that  $G$  is  $k$ -edge colorable.

**Definition 31.** We define as chromatic index of a graph  $G$  the smallest number of colors  $k$  for which there is a  $k$ -edge coloring of  $G$ , and is denoted by  $\chi'(G)$ . See Figure 1.21.

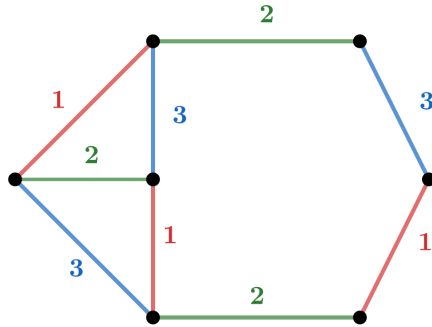


Figure 1.21: A graph with  $\chi'(G) = 3$ .

It is possible to establish the chromatic index  $\chi'(G)$  for some classes of graphs previously defined.

**Theorem 11** (König, 1916 [9]). *If  $G$  is a bipartite graph with maximum degree  $\Delta$ , then  $\chi'(G) = \Delta$ .*

**Theorem 12** ([9]). *Let  $G$  be the cycle graph  $C_n$ . Then*

$$\chi'(G) = \begin{cases} 2, & \text{if } n \text{ is even}; \\ 3, & \text{if } n \text{ is odd.} \end{cases}$$

**Theorem 13** (Baranyai, 1975 [9]). *Let  $G$  be the complete graph  $K_n$ . Then*

$$\chi'(G) = \begin{cases} n, & \text{if } n \text{ is odd}; \\ n - 1, & \text{if } n \text{ is even.} \end{cases}$$

The following theorem is considered the most important result of the study of edge coloring.

**Theorem 14** (Vizing's Theorem, 1964). *Let  $G$  be a simple graph with maximum degree  $\Delta$ . Then*

$$\Delta \leq \chi'(G) \leq \Delta + 1.$$

Vizing's theorem originated the classification of graphs into two classes, such as:

- $G$  is Class 1, if  $\chi'(G) = \Delta$ ;

- $G$  is Class 2, if  $\chi'(G) = \Delta + 1$ .

See Figure 1.22.

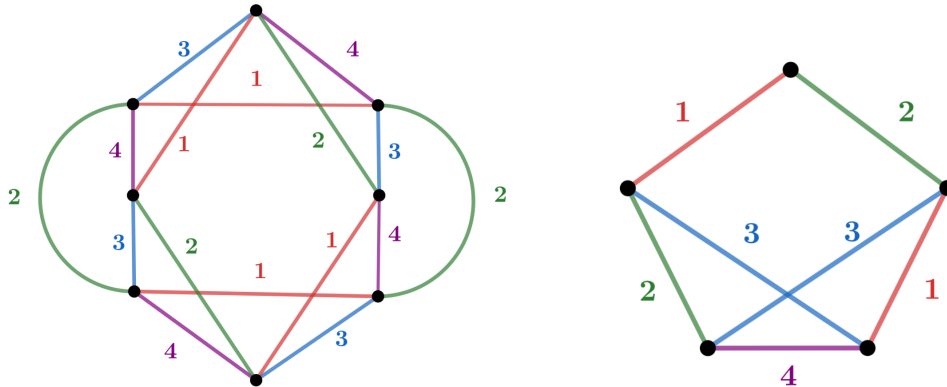


Figure 1.22: A Class 1 graph and a Class 2 graph, respectively.

**Theorem 15** ([9]). *Every regular graph of odd order is of Class 2.*

From this result, we know that regular graphs of odd order are Class 2, but regular graphs of even order can be either Class 1 or Class 2. See Figure 1.23.

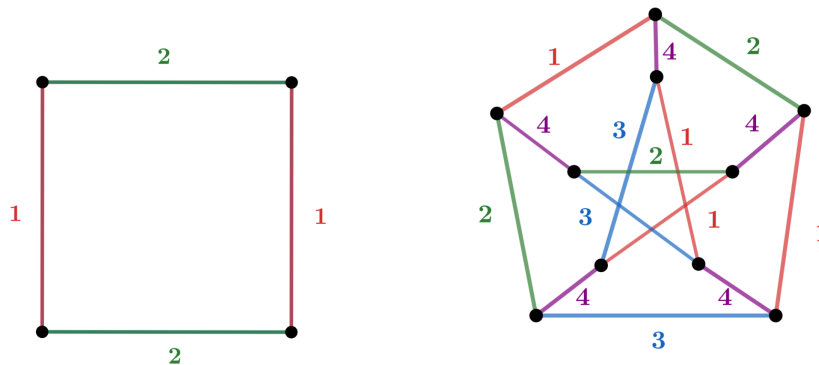


Figure 1.23: A 2-regular Class 1 graph and a cubic Class 2 graph, respectively.

In 1880, Tait found a relationship between face coloring and edge coloring in 3-connected planar cubic graphs [32].

**Theorem 16** (Tait's Theorem, 1880 [32]). *A 3-connected cubic planar graph is 4-face colorable if and only if it is 3-edge-colorable.*

By virtue of Tait's Theorem, The Four-Color Conjecture can be reformulated in terms of edge coloring.

**Conjecture 2** (The Four-Color Conjecture for edges [5]). *Every 3-connected cubic planar graph is Class 1.*

### 1.4.4 Total Coloring

**Definition 32.** A total coloring  $\mathcal{C}^T$  of a graph  $G$  is a color assignment to the set  $E \cup V$  in a color set  $\mathcal{C} = \{\mathcal{C}_1, \mathcal{C}_2, \dots, \mathcal{C}_k\}$ ,  $k \in \mathbb{N}$ , such that distinct colors are assigned to:

- Every pair of vertices that are adjacent;
- All edges that are adjacent;
- Each vertex and its incident edges.

A  $k$ -total coloring of a graph  $G$  is a total coloring of  $G$  that uses a set of  $k$  colors, and a graph is  $k$ -total colorable if there is a  $k$ -total coloring of  $G$ .

**Definition 33.** We define as the total chromatic number of a graph  $G$  the smallest natural  $k$  for which  $G$  admits a  $k$ -total coloring, and is denoted by  $\chi''(G)$ . See Figure 1.24.

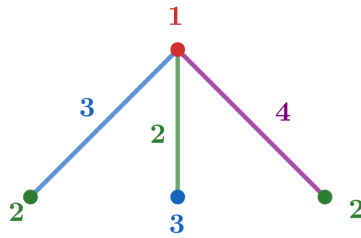


Figure 1.24: A graph with  $\chi''(G) = 4$ .

A graph  $G$  with vertex  $v$  such that  $d(v) = \Delta$ , needs  $\Delta$  colors to color the edges incident to  $v$  and, in addition, needs one more color to be assigned to  $v$ . Then, for any graph  $G$ ,

$$\chi''(G) \geq \Delta + 1.$$

Behzad and Vizing [4, 33] independently conjectured the same upper bound for the total chromatic number.

**Conjecture 3** (Total Coloring Conjecture (TCC)). For every simple graph  $G$ ,

$$\chi''(G) \leq \Delta + 2.$$

Knowing that  $\chi''(G) \geq \Delta + 1$ , and from the TCC, we have the following classification:

- If  $\chi''(G) = \Delta + 1$ , the graph is Type 1;
- If  $\chi''(G) = \Delta + 2$ , the graph is Type 2.

See Figure 1.25.

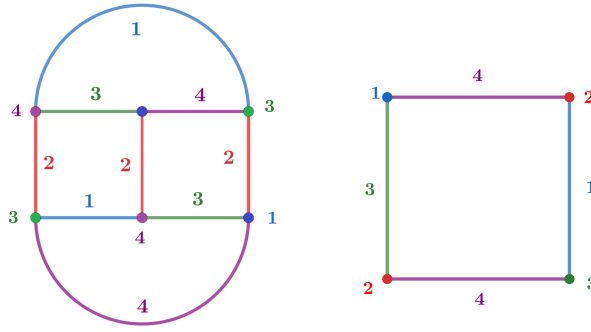


Figure 1.25: A Type 1 and a Type 2 graph, respectively.

To determine that a graph is Type 1, simply display the total coloring with  $\Delta + 1$  colors. To determine that a graph is Type 2, it is necessary to prove the TCC for the class of the graph in question and then prove that there is no total coloring with  $\Delta + 1$  colors, and finally display a total coloring that uses  $\Delta + 2$  colors.

The TCC is open for regular graphs, and has been verified for some particular classes of graphs. For cubic graphs that are graphs where every vertex has degree 3, the TCC has already been settled [18], but it is not yet settled for all planar graphs [21]. Deciding whether a cubic bipartite graph is Type 1 is NP-complete [28]. It is also possible to establish the total chromatic number for some classes of graphs previously defined.

**Theorem 17** ([36]). *Let  $G$  be the cycle graph  $C_n$ . Then*

$$\chi''(G) = \begin{cases} 3, & \text{if } n \equiv 0 \pmod{3}; \\ 4, & \text{otherwise.} \end{cases}$$

**Theorem 18** ([36]). *Let  $G$  be the complete graph  $K_n$ . Then*

$$\chi''(G) = \begin{cases} \Delta + 1, & \text{if } n \text{ is odd;} \\ \Delta + 2, & \text{if } n \text{ is even.} \end{cases}$$

The following lemma relates total coloring and a conformable vertex coloring.

**Lemma 19** (Chetwynd and Hilton, 1988 [10]). *If  $G$  is a Type 1 graph, then  $G$  is conformable.*

By Lemmas 10 and 19, a necessary step towards proving that a cubic graph is Type 1 is to define a 4-vertex coloring where the cardinality of each vertex color class has the same parity when compared to the cardinality of the entire vertex set. By the Handshaking Lemma, every cubic graph has an even number of vertices. Thus, all color classes must have an even number of vertices.

## 1.4.5 Equitable Total Coloring

**Definition 34.** A total coloring  $\mathcal{C}^T$  is equitable if the cardinalities of any two color classes differ by at most 1.

An equitable  $k$ -total coloring of a graph  $G$  is an equitable total coloring of  $G$  that uses a set of  $k$  colors, and a graph is equitable  $k$ -total colorable if there is an equitable  $k$ -total coloring of  $G$ .

**Definition 35.** We define as the equitable total chromatic number of a graph  $G$  the smallest natural  $k$  for which  $G$  admits an equitable  $k$ -total coloring, and is denoted by  $\chi_e''(G)$ . See Figure 1.26.

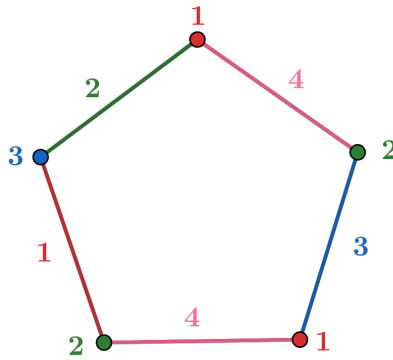


Figure 1.26: An equitable 4-total coloring for the cycle graph  $C_5$ .

In 2002, Wang [34] conjectured an upper bound for the equitable total chromatic number.

**Conjecture 4.** For every graph  $G$ ,

$$\chi_e''(G) \leq \Delta + 2.$$

The following result guarantee that Conjecture 4 holds for cubic graphs.

**Theorem 20** ([34]). *If  $G$  is a multigraph with  $\Delta \leq 3$ , then  $G$  has an equitable total 5-coloring.*

**Theorem 21** ([30]). *The problem of determining whether a bipartite cubic graph has an equitable 4-total coloring is NP-complete.*

The equitable total chromatic number was determined for some classes of graphs, such as the complete graphs  $K_n$ .

**Theorem 22** ([20]). *Let  $G$  be the complete graph  $K_n$ . Then*

$$\chi_e''(G) = \begin{cases} \Delta + 1, & \text{if } n \text{ is odd;} \\ \Delta + 2, & \text{otherwise.} \end{cases}$$

The first Type 1 cubic graphs such that  $\chi_e'' = \Delta + 2$  known in literature was displayed in [30]. However, all the displayed graphs have a small girth. Thus, in this same work, the following question was proposed.

**Question 1** (Sasaki, 2013 [30]). *Is there a Type 1 cubic graph such that  $\chi_e'' = 5$  with girth at least 5?*

This question is relevant because the class of graphs studied in this dissertation are graphs that have girth 5. Thus, this open question can also be seen as a motivation for class choice, which will be presented in the following chapters.

# Chapter 2

## Fullerene graphs

We investigate the total coloring problem considering cubic planar graphs with large girth that model chemical structures: the fullerene nanodiscs. The length of the shortest cycle in a graph is called girth and has been considered for total coloring planar graphs [6]. Our goal is to study a conjecture proposed by Brinkmann, Preissmann and Sasaki [7] which states that every Type 2 cubic graph has girth less than 5, and suggests that the girth of a graph is a relevant parameter in the study of total coloring. The hunting of special Type 2 cubic graphs has been considered for nonplanar graphs as well [31]. We contribute by giving a combinatorial description of the *small fullerene nanodiscs* according with  $r$  parameter in Chapter 3, and then by showing that they are conformable in the Chapter 4, a necessary step towards proving that they are Type 1.

To motivate the choice of the studied graph class, we first give a historical account of the discovery of the carbon molecule which can be modeled through a special cubic planar graph of girth 5, and we bring some properties of this class of graphs so special, so that in Chapter 3 we can introduce our target fullerene subfamily.

### 2.1 A graph class modeling a molecule

Allotrope substances are those that are simple and formed by the same chemical element but have distinct physical properties, such as red phosphorus ( $P_n$ ) and white phosphorus ( $P_4$ ), which differ in atomicity. Another type of allotropy arises from the spatial arrangement of atoms, as in the case of carbon atoms, which vary their geometric aspect forming different substances, as illustrated in the Figure 2.1<sup>1</sup>. Carbon can be found in different stable crystalline structures, which differ in the spatial arrangement of carbon atoms or in the sequence of packing layers in the crystal lattice. These distinctions define important differences in the physical and chemical properties of these substances.

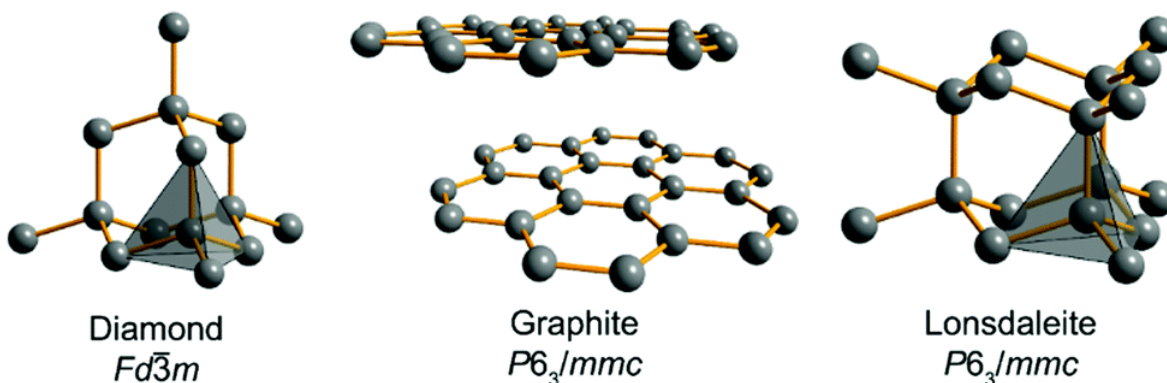


Figure 2.1: Molecular structure of diamond, graphite and lonsdaleite, respectively.

In 1985, the scientific community witnessed the appearance of a new carbon allotrope: the  $C_{60}$ [19].

In attempt to understand the spectroscopy data obtained from astronomical objects as giant red carbon stars, which indicates the formation of long chains of carbon atoms, Harold Kroto and coworkers [19] (see Figure 2.2<sup>2</sup>) performed a series of experiments vaporizing and cooling highly pure carbon samples discovering a new carbon allotrope highly symmetrical stable molecule, composed of 60 tertiary carbon atoms.

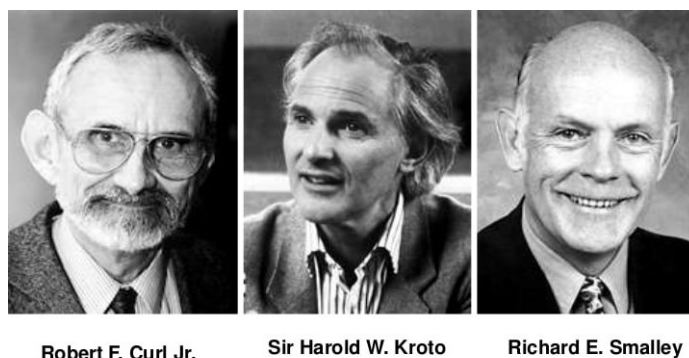


Figure 2.2: Robert Curl, Harold Kroto and Richard Smalley.

Initially, the researchers thought that the most likely form of this molecule would be plans of carbon atoms arranged in hexagonal vertices, similar to graphite, of which the molecule has been vaporised. Kroto, an admirer of American architect Richard Buckminster Fuller, famous for his geodesic dome constructions, which were composed of hexagonal and pentagonal faces, such as the Montreal Biosphere at EXPO67 in Montreal, illustrated in Figure 2.3<sup>3</sup>, suggested to coworkers that the

<sup>1</sup>Figure from <https://pubs.rsc.org/en/content/articlehtml/2019/cp/c8cp07592a>. Accessed on: 03 Mai. 2022.

<sup>2</sup>Figure from <https://hemanth-99.medium.com/fullerenes-and-their-applications-49313545d23a>. Accessed on: 21 Mar. 2021.

molecule could have a structure such as the domes created by Fuller.

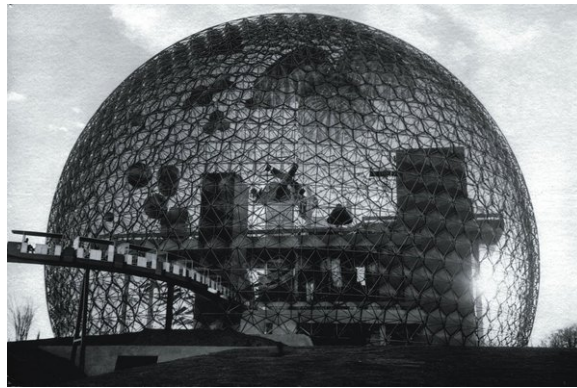


Figure 2.3: Montreal Biosphere.

As the only way to maintain this amount of carbon atoms stable, Richard Smalley proposed a spheroid structure, with 32 faces, being 20 hexagonal and 12 pentagonal (see Figure 2.4<sup>4</sup>) later named by them as “ $C_{60}$  buckminsterfullerene”, or simply “buckyball” since the molecule structure is shaped like a soccer ball.

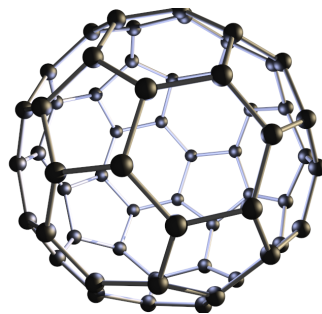


Figure 2.4: Molecular structure of  $C_{60}$ .

At the end of the 1980s, other carbon allotrope molecules with similar spatial structure to the  $C_{60}$ , which is the most stable representative of the fullerene family, other allotrope forms of carbon with structure similar to the  $C_{60}$  molecule were also found (see Figure 2.5<sup>5</sup>). These structures were called fullerene molecules. The number of carbon atoms in a fullerene molecule can vary, forming hexagons as well as pentagons. As the number of hexagons grows larger than 20, which is the case of  $C_{60}$ , the stability of the molecule decreases, as pentagons occupy increasingly tense positions and are therefore more vulnerable to chemical attacks. For example, the fullerene molecule  $C_{70}$  is similar to a rugby ball, with 12 pentagons and 25 hexagons [1]. In the case of  $C_{60}$ , each pentagon is surrounded by six-membered ring [27].

---

<sup>3</sup>Figure from <https://www.maison.com/architecture/portraits/richard-buckminster-fuller-architecte-visionnaire-7490/galerie/33942/>. Accessed on: 03 Mai. 2022.

<sup>4</sup>Figure from <https://arxiv.org/pdf/1510.01642.pdf>. Accessed on: 03 Mai. 2022.

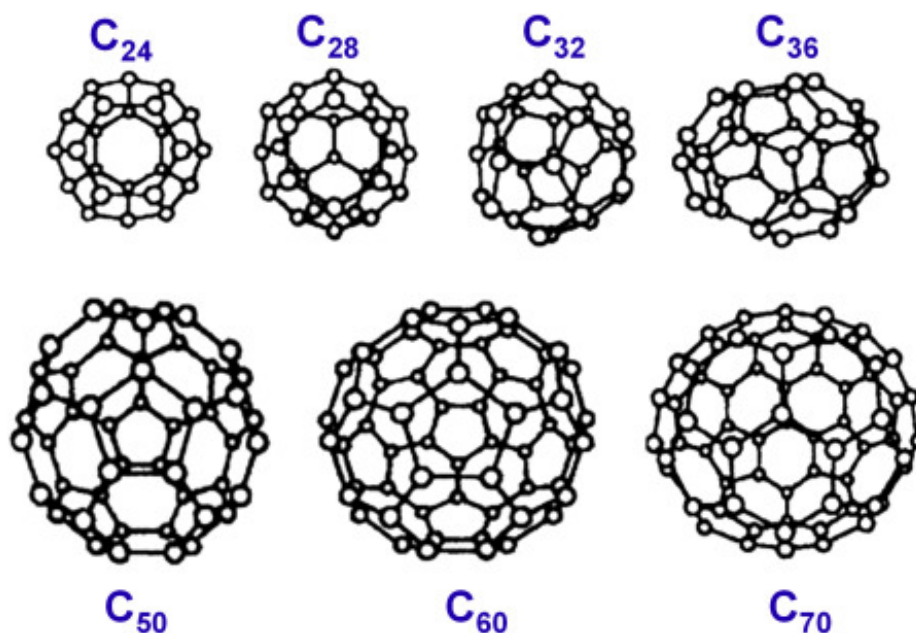


Figure 2.5: Structure of some fullerene molecules.

The discovery of these molecular species has deeply animated the scientific community. For this contribution Harold Kroto, Robert Curl and Richard Smalley earned the 1996 Chemistry Nobel Prize.

Fullerene molecules are widely studied by different branches of science, from medicine to mathematics. These molecules are supposed to contribute to transport chemotherapy, antibiotics or antioxidant agents, and are released in contact with deficient cells [29].

Fullerenes have unique physical and chemical properties, which can be explored in various areas of biochemistry and medicine. [29]. One of its possible uses would be to transport medicines through the human body. Among the wide range of biomedical applications of fullerenes, the following stand out in development:

- Antiviral activity;
- Antioxidant activity and free radical traps;
- Photodynamic therapy;
- Photo-cleavage of the DNA;
- Antimicrobial activity;
- Transport of drugs with radiotherapy effect and contrast for diagnostic imaging;

---

<sup>5</sup>Figure from <https://www.sciencedirect.com/science/article/pii/B9780323461528000184>. Accessed on: 03 Mai. 2022.

- Technologies of energy storage.

Recent advances in organic Chemistry have allowed the functionalization and adaptation of fullerene molecules for medical applications, overcoming its non-polar character and its repulsion by water. The hydrosolubility of fullerenes was a milestone in the research and development of biomedical applications of these molecules.

## 2.2 Graph properties

Each fullerene molecule can be described as a planar graph in which the atoms and the bonds are represented by the vertices and edges of the graph, respectively, preserving the geometric properties of the original fullerene molecule. Thus, we define a fullerene graph as cubic, planar, 3-connected graph whose faces are pentagonal or hexagonal (see Figure 2.6).

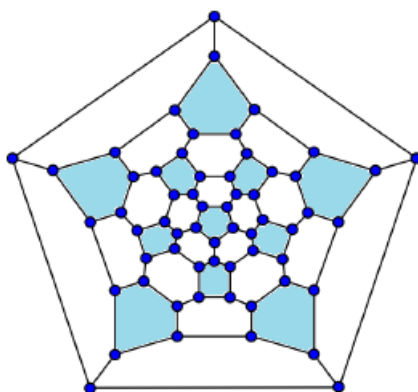


Figure 2.6: Fullerene graph of  $C_{60}$  with the pentagons highlighted in blue.

The famous Euler's formula for connected planar graphs  $n + f - m = 2$  relates the number  $f$  of faces, the number  $m$  of edges and the number  $n$  of vertices, and implies the following Lemma.

**Lemma 23** ([22]). *Every fullerene graph has exactly 12 pentagons.*

*Proof.* Let  $G$  be a fullerene graph with  $p$  pentagonal faces and  $h$  hexagonal faces. So,  $G$  has  $p + h$  faces,  $\frac{5p + 6h}{2}$  edges, because every edge belongs to two faces and  $G$  is a simple cubic graph, so  $G$  has  $\frac{5p + 6h}{3}$  vertices. As  $G$  is planar and connected, by Euler's formula we have

$$\frac{5p + 6h}{3} + p + h - \frac{5p + 6h}{2} = 2.$$

From there, we get:

$$10p + 12h + 6p + 6h - 15p - 18h = 12,$$

and therefore  $p = 12$ . □

The smallest fullerene molecule known is  $C_{20}$ , which contains only the 12 pentagons, without hexagons. Thus, its graph representation can be schematized by the dodecahedron with 20 vertices where all faces are pentagons [22]. See Figure 2.7<sup>6</sup>.

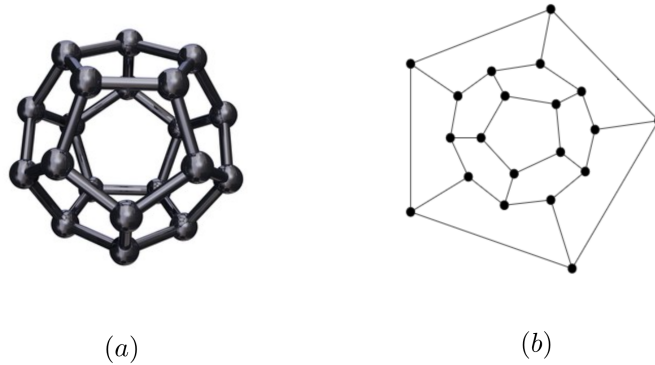


Figure 2.7: Molecular structure (a) and fullerene graph (b) of  $C_{20}$ .

A connected graph  $G$  with  $|V(G)| = 2n$  is  $k$ -extendable ( $1 \leq k \leq n - 1$ ) if any matching  $M$  such that  $|M| = k$  can be extended to a perfect matching of  $G$ . For fullerene graphs, Zhang [37] proved the following result.

**Theorem 24** (Zhang, 2001 [37]). *Every fullerene graph is 2-extendable.*

A pair of disjoint odd cycles  $C_1$  and  $C_2$  in a graph  $G$  with a perfect matching is called a *nice pair* if  $G - V(C_1) - V(C_2)$  still has a perfect matching. In 2020, Došlić [15] proved the following result.

**Theorem 25** (Došlić, 2020 [15]). *Every fullerene graph contains a nice pair of disjoint odd cycles.*

In 2021, Zhang [38] proved that if a fullerene graph satisfies that each pentagon is adjacent to at most two pentagons, then any pair of disjoint pentagons is nice, except for only fullerene graph with 36 vertices.

An edge cut  $S$  of a graph  $G$  is cyclic if  $G \setminus S$  contains two components with cycles.  $G$  with  $e(G) > k$  is cyclically  $k$ -edge connected if  $G$  has no cyclic edge cuts with fewer than  $k$  edges. Došlić [14] proved the following result.

---

<sup>6</sup>(a) Figure from <https://nanotube.msu.edu/fullerene/fullerene.php?C=20>. Accessed on 03 Mai 22. (b) Figure from [22].

**Theorem 26** (Došlić, 2002 [14]). *Every fullerene graph is cyclically 5-edge-connected.*

The diameter of a graph  $G$  is the maximum distance between two vertices of  $G$ , and is denoted by  $diam(G)$ . In [3], Andova et al. proved the following result.

**Theorem 27** (Andova et al., 2012 [3]). *If  $G$  is a fullerene graph on  $n$  vertices, then*

$$diam(G) \leq \sqrt{\frac{2n}{3} - \frac{5}{18}} - \frac{1}{2}.$$

In a subsequent paper, believing that fullerene graphs with icosahedral symmetry (which have “spherical shape”) would minimize the diameter, Andova and Škrekovski [2] proposed the following conjecture.

**Conjecture 5** (Andova and Škrekovski, 2013 [2]). *If  $G$  is any fullerene graph on  $n$  vertices, then*

$$diam(G) \leq \lfloor \sqrt{\frac{5n}{3}} - 1 \rfloor.$$

However, in [23], Diego Nicodemos and Matěj Stehlík disproved Conjecture 5, whose smallest counterexample is a fullerene graph with 300 vertices. Such a graph belongs to the class of fullerene nanodiscs, our target class, which will finally be presented in the following chapter.

# Chapter 3

## Fullerene nanodiscs

We shall consider a particular family of fullerene graphs: the *fullerene nanodiscs*. The choice of this subfamily is motivated by the girth with length 5 that all graphs in this class have. In this chapter, we define the fullerene nanodiscs, denoted by  $D_r$  and contribute with combinatorial and quantitative results for this class, from their planar representation.

### 3.1 Knowing the class structure

According to the 3-dimensional structure, the fullerene nanodiscs, or nanodiscs  $D_r$  of radius  $r \geq 2$ , are structures composed of two identical flat covers connected by a strip along their borders. While in the nanodisc covers there are only hexagonal faces, in the connecting strip, besides the hexagonal faces, additional 12 pentagonal faces are arranged. Please refer to Figure 3.1 where the smallest fullerene nanodisc graphs are depicted. In each fullerene nanodisc graph, we highlight in the connecting strip the 12 pentagons.

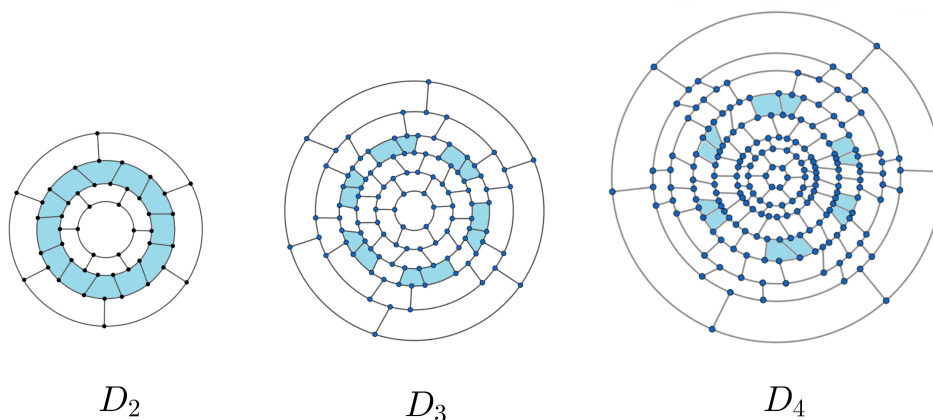


Figure 3.1: The smallest fullerene nanodisc graphs.

A nanodisc graph of radius  $r \geq 2$ , denoted by  $D_r$ , has its faces arranged into

layers, one layer next the nearest previous layer starting from an hexagonal cover until we reach the other hexagonal cover.

The sequence  $\{1, 6, 12, \dots, 6(r-1), 6r, 6(r-1), \dots, 12, 6, 1\}$  provides the amount of faces on each layer of the nanodisc graph  $D_r$ . Note that there is an odd number of  $2r + 1$  layers, and the layer with  $6r$  faces is called *central layer*. For  $D_2$  the layer sequence is  $\{1, 6, 12, 6, 1\}$ , for  $D_3$  is  $\{1, 6, 12, 18, 12, 6, 1\}$  and for  $D_4$  is  $\{1, 6, 12, 18, 24, 18, 12, 6, 1\}$  (see Figure 3.1). The auxiliary cycle sequence provides the sizes of the auxiliary cycles that define the layers  $\{C_6, C_{18}, \dots, C_{12r-6}, C_{12r-6}, \dots, C_{18}, C_6\}$ . For example, for  $D_2$  the cycle sequence is  $\{C_6, C_{18}, C_{18}, C_6\}$ , for  $D_{3,t}$  is  $\{C_6, C_{18}, C_{30}, C_{30}, C_{18}, C_6\}$ , and for  $D_4$  is  $\{C_6, C_{18}, C_{30}, C_{42}, C_{42}, C_{30}, C_{18}, C_6\}$  (see Figure 3.1). A nanodisc graph  $D_r$  contains  $12r^2$  vertices and  $18r^2$  edges. Table 3.1 provides the number of vertices, faces, edges and layers in a fullerene nanodisc  $D_r$ .

$r$	Vertices	Faces	Edges	Layers
2	48	26	72	5
3	108	56	162	7
4	192	98	288	9
5	300	152	450	11
$\cdot$	$\cdot$	$\cdot$	$\cdot$	$\cdot$
$\cdot$	$\cdot$	$\cdot$	$\cdot$	$\cdot$
$\cdot$	$\cdot$	$\cdot$	$\cdot$	$\cdot$
$r \geq 2$	$12r^2$	$6r^2 + 2$	$18r^2$	$2r + 1$

Table 3.1: Number of vertices, faces, edges and layers in a fullerene nanodisc  $D_r$ , according to parameter  $r \geq 2$ .

The 12 pentagonal faces are distributed in the central layer among its  $6r$  faces with the other  $(6r - 12)$  hexagonal faces. This is the key property of fullerene nanodiscs. Note that the only value of  $r$  for which  $D_r$  has no hexagons in the central layer is 2, that is, the fullerene nanodisc  $D_2$  has no hexagons in the central layer.

Note that the central layer is defined by two auxiliary cycles, each of size  $12r - 6$ .

The 5 vertices of each pentagon are partitioned such that 3 vertices appear consecutively in one cycle and 2 vertices appear consecutively in the other cycle. We say that two pentagons in the central layer are partitioned in the same way if each pentagon has 3 vertices in the same cycle  $C_{12r-6}$  and partitioned differently otherwise (see Figure 3.2). Note that every fullerene nanodisc has girth 5.

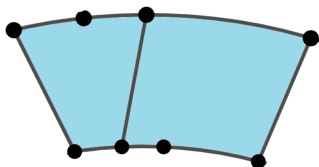


Figure 3.2: Two consecutive pentagons partitioned differently.

**Observation 28.** *Note that by the arrangement of the graph, the radial edges that form the faces and connect the auxiliary cycles involves all vertices of  $D_r$ , forming a perfect matching in  $D_r$ ,  $r \geq 2$ .*

As said in Chapter 2, the fullerene nanodiscs  $D_r$  with  $r \leq 5$  are a counterexample for the Conjecture 5. The following result establishes the existence of the family of nanodiscs and establishes the diameter for this class.

**Theorem 29** ([22, 23]). *For every  $r \geq 2$ , there exists a fullerene graph  $D_{r,t}$ , on  $12r^2$  vertices of diameter at most 4. In particular,  $\text{diam}(D_{r,t}) \leq \sqrt{\frac{4n}{3}}$ .*

**Observation 30.** *Theorem 29 takes into account the parameter  $t$ ,  $1 \leq t \leq r - 1$ , which is defined from the dual  $D_{r,t}^*$  of a nanodisc  $D_{r,t}$ ,  $r \geq 2$ . The definition and representation of the dual  $D_{r,t}^*$  of a nanodisc is found in the Appendix A.*

Figure 3.3<sup>1</sup> displays the smallest nanodisc that contradicts the Conjecture 5.

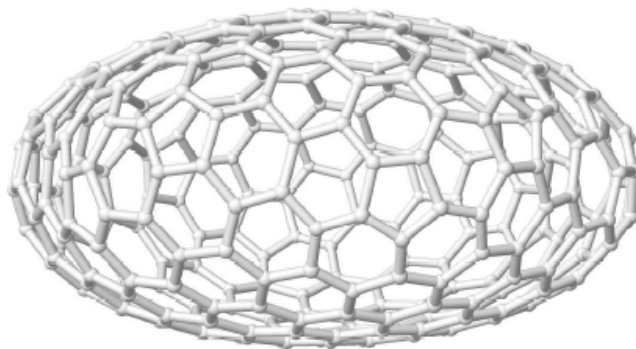


Figure 3.3: Three-dimensional view of the nanodisc  $D_5$ , the smallest nanodisc that contradicts the Conjecture 5.

In the next section, we describe the structure of our target class by first considering the behavior of the hexagonal and pentagonal faces.

---

<sup>1</sup>Figure from [22].

## 3.2 Combinatorial results

Let  $D_r$  be a planar embedding of a fullerene nanodisc  $D_r$ . Observe that there are two ways of partitioning a hexagon in a layer defined by auxiliary cycles  $C$  and  $C'$ . We may place 3 vertices of the hexagon in each auxiliary cycle to obtain a *balanced hexagon*, or we may place 4 vertices of the hexagon in one auxiliary cycle say  $C$  and the other 2 vertices are placed in  $C'$  to obtain an *unbalanced hexagon*. See Figure 3.4.

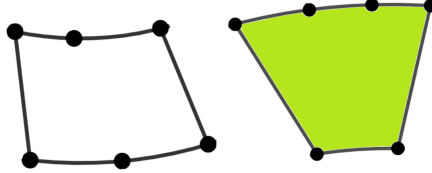


Figure 3.4: Balanced and unbalanced hexagons, respectively.

The regularity of the construction of the hexagonal layers of nanodisc allows us to extract global properties regarding the arrangement of balanced and unbalanced hexagons in the layers, as we increase  $r$ . The first concerns the arrangement of faces containing only two vertices in an auxiliary cycle.

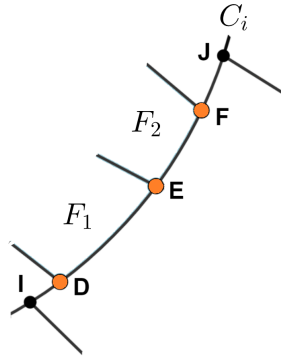


Figure 3.5: When two consecutive faces are such that each face has 2 vertices in the same auxiliary cycle, we obtain a large forbidden face.

**Lemma 31** (Large Forbidden Face Lemma). *Let  $F_1$  and  $F_2$  be two consecutive faces of layer  $L$  containing more than 6 faces. Let  $C_1$  and  $C_2$  be the two cycles defining  $L$ . We cannot have only two vertices of  $F_1$  and only two vertices of  $F_2$  contained in the same cycle  $C_i$ .*

*Proof.* Please refer to Figure 3.5. The faces  $F_1$  and  $F_2$  arranged side by side in  $L$  different than the layers containing 6 hexagons, the vertices  $D, E, F$  belong to the same auxiliary cycle. Consider the layer adjacent to this hexagonal layer, where one of its defining cycles  $C_i$  containing vertices,  $D, E, F$ . By considering vertices  $I$  and

$J$  adjacent respectively to  $D$  and  $F$  in  $C_i$ , we find a path containing five consecutive vertices  $I, D, E, F, J$  in the cycle, leading to a contradiction that  $I, D, E, F, J$  must lie in a forbidden face.  $\square$

As a direct consequence of Lemma 31, we have the following result.

**Corollary 2.** *For every nanodisc  $D_r$ ,  $r \geq 2$ , the only layers that admit consecutive unbalanced hexagons are the layers that contain six hexagons. In this layer, all hexagons are unbalanced.*  $\square$

We have the first result to quantify the fullerene nanodiscs.

**Theorem 32.** *The fullerene nanodisc  $D_2$  has only one non isomorphic representation.*

*Proof.* It occurs from Lemma 31. In this way, there are no hexagons to distribute among the pentagons in the central layer. See the unique  $D_2$  in Figure 3.1.  $\square$

Based on Lemma 31 and Properties about fullerene nanodiscs, we can establish the following result.

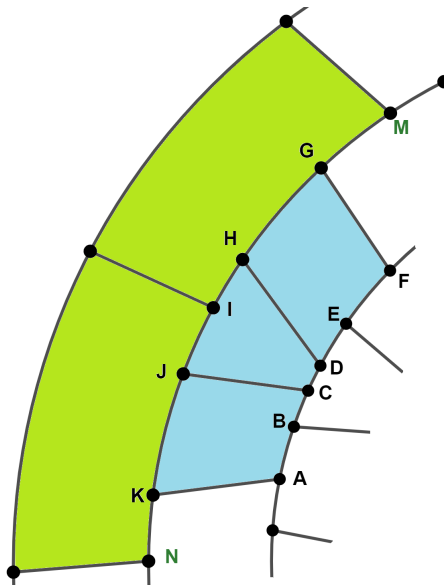


Figure 3.6: Three pentagons arranged alternately in the central layer of  $D_r$ .

**Lemma 33.** *The fullerene nanodisc  $D_r$ ,  $r \geq 3$  cannot have three consecutive pentagons in the central layer.*

*Proof.* Please refer to Figure 3.6. By Lemma 31, we cannot have two consecutive pentagons partitioned in the same way. So the only possible case for distributing three consecutive pentagons is such that between two pentagons containing three consecutive vertices (of the first pentagon,  $A, B, C$  and the second pentagon  $D, E, F$ )

in the auxiliary cycle  $C_{12r-6}$  and two consecutive vertices (from the first pentagon,  $K$  and  $J$ , and from the second pentagon  $H$  and  $G$ ) in the other  $C_{12r-6}$  cycle, there is a pentagon with two consecutive vertices in one  $C_{12r-6}$  and three consecutive vertices in the other  $C_{12r-6}$ .

Note that this distribution will imply two consecutive unbalanced hexagons in the next layer, which contradicts Lemma 31.  $\square$

Thus, there are only two possible groups of distribution of pentagons: in pairs or one in one (isolated). The next results are specific to the central layer of  $D_3$ , where the pentagons must appear in pairs, and between each pair of pentagons there is a hexagon, so that there are not three or more consecutive pentagons in the central layer.

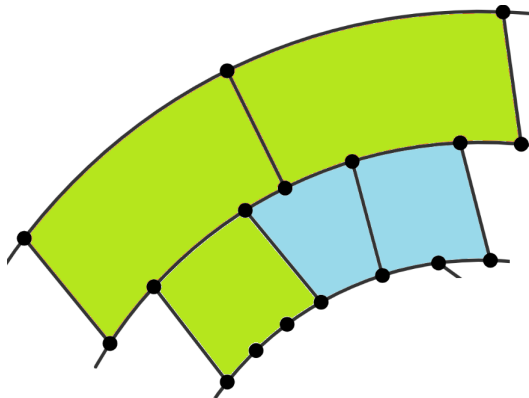


Figure 3.7: Two consecutive pentagons followed by an unbalanced hexagon in the central layer of  $D_3$  contradicts the large forbidden face lemma.

**Lemma 34.** *All the hexagons are balanced in the central layer of  $D_3$ .*

*Proof.* Please refer to Figure 3.7. Suppose there is at least one unbalanced hexagon in the central layer of  $D_3$ . By Lemma 31 this hexagon must appear alongside two consecutive partitioning pentagons in a different way. We can say, without loss of generality, that this representation is unique, up to symmetry.

Note that this arrangement implies two consecutive unbalanced hexagons, highlighted in green, in the hexagonal layer adjacent to the central layer of  $D_3$ , which contradicts Lemma 31. Therefore, there are no unbalanced hexagons in the central layer of  $D_3$ .  $\square$

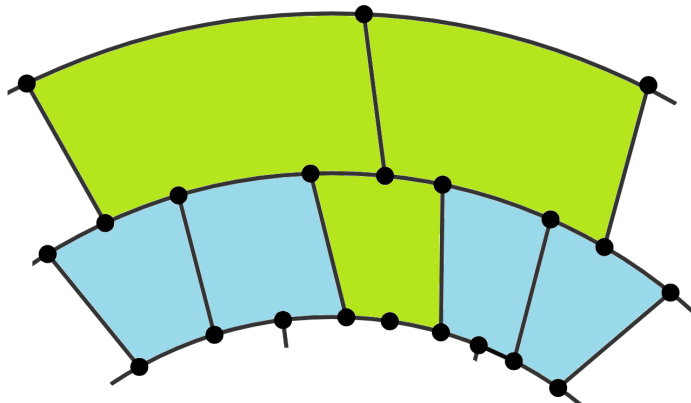


Figure 3.8: A balanced hexagon between two pentagons partitioned in the same way in the central layer of  $D_3$  contradicts the large forbidden face lemma.

**Lemma 35.** *It is not possible to have a balanced hexagon between two pentagons arranged in the same way in the central layer of  $D_3$ .*

*Proof.* Please refer to Figure 3.8. Suppose the central layer of the  $D_3$  has a balanced hexagon whose neighboring faces are pentagons partitioned in the same way. We can say, without loss of generality, that this representation is unique, up to symmetry.

Note that this arrangement implies two consecutive unbalanced hexagons, highlighted in green, in the hexagonal layer adjacent to the central layer of  $D_3$ , which contradicts Lemma 31. Thus, the balanced hexagons of the central layer of the  $D_3$  must have as neighboring faces pentagons partitioned in a different way.  $\square$

**Theorem 36.** *The fullerene nanodisc  $D_3$  has only one non isomorphic representation.*

*Proof.* In the central layer of  $D_3$ , we have 12 pentagons distributed among 6 hexagons. By Lemma 31, we cannot have two consecutive pentagons partitioned in the same way. By Lemma 33, we cannot have three consecutive pentagons such that each pair is not partitioned in the same way. By Lemma 34, all the hexagons are balanced, and by Lemma 35 we have an order to dispose the pairs of pentagons. So the only way is to distribute, among the 6 hexagons, the 12 pentagons in pairs of two consecutive pentagons. See the unique  $D_3$  in Figure 3.1.  $\square$

The Lemma 3.6 sets a limit to the number of consecutive pentagons in the central layer of  $D_r$ , and the only  $D_3$  representation sets its pentagons in pairs. The following result guarantees the existence of a planar representation with pentagons arranged in pairs for every nanodisc with radius greater than 2.

**Theorem 37.** *Every fullerene nanodisc  $D_r$ ,  $r \geq 3$  has a representation where the pentagons are arranged in pairs.*

*Proof.* By definition, the number of faces in the center layer is  $6r$ , where 12 faces are pentagons. Thus, the number of hexagons in the center layer is  $6r - 12$ . Note that the amount of hexagons is divisible by 6, since

$$\frac{6r - 12}{6} = 6(r - 2).$$

Therefore, it is concluded that it is possible to distribute the pentagons in pairs, with  $r - 2$  hexagons between each of the 6 pairs of pentagons.  $\square$

We will do a brief structural analysis of the fullerene nanodisc  $D_4$ . Recalling, the sequence that defines the number of faces in each layer of  $D_4$  is  $\{1.6.12.18.24, 18, 12, 6, 1\}$ . Note also that the central layer of the  $D_4$  nanodisc has 24 faces, being 12 hexagonal and 12 pentagonal. The first result provides limits for the number of hexagons between the pentagons in the central layer.

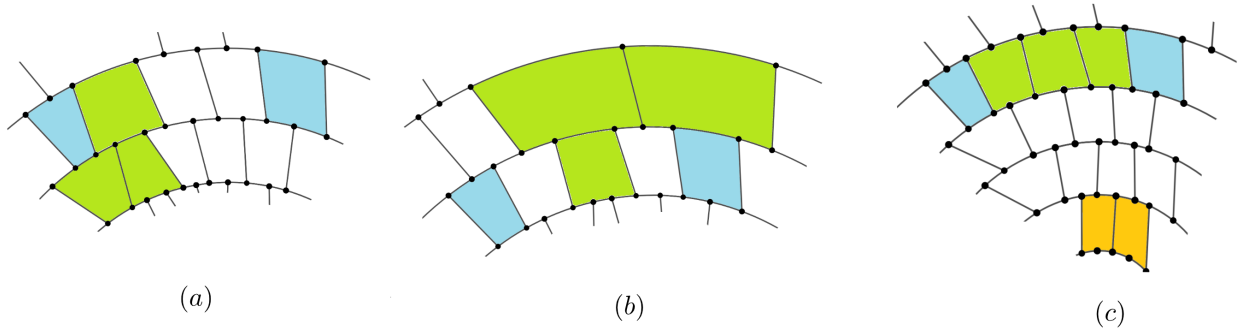


Figure 3.9: The three possible cases to have at least 3 hexagons between the pentagons in the central layer of  $D_4$ .

**Lemma 38.** *It is not possible to have three or more hexagons between the pentagons in the central layer of  $D_4$ .*

*Proof.* Please refer to Figure 3.9.

Note that the pentagonal arrangement is irrelevant to demonstrate this fact, because it is independent of the pentagonal disposition. However, note that in cases where the pentagons are arranged one in one, it is not possible to have more than one hexagon between the pentagons, otherwise contradicts the Lemma 33.

Suppose there are at least 3 hexagons between the pentagons in the central layer of  $D_4$ . If this layer admits unbalanced hexagons, by the Lemma 31 there are two cases to consider: either the hexagon is adjacent to a pentagon (Figure 3.9(a)) or the hexagon is between two balanced hexagons (Figure 3.9(b)). We can say, without loss of generality, that these representations is unique, up to symmetry. Note that in both cases the arrangements implies two consecutive unbalanced hexagons, highlighted in green, in the hexagonal layer adjacent to the central layer of  $D_4$ , which contradicts the Lemma 31.

Now suppose that all three hexagons are balanced (Figure 3.9(c)). Fixed this construction, note that this arrangement implies at least two balanced hexagons, highlighted in orange, in the layer containing 6 hexagons, which contradicts the Corollary 2. Thus, analyzing all possible cases, we concluded that it is not possible to have three or more hexagons between each group of pentagons in the central layer of  $D_4$ .  $\square$

This Lemma is of utmost importance as it restricts our choices to the arrangement of hexagons in the central layer of  $D_4$  in two ways. Also, note that for the arrangement in which pentagons appear isolated, we must have a hexagon between each pentagon, since for  $r = 4$  the number of pentagons and hexagons in the central layer is the same. The hexagonal and pentagonal behavior in the central layer, analyzed in the following results, ensures the uniqueness of this representation.

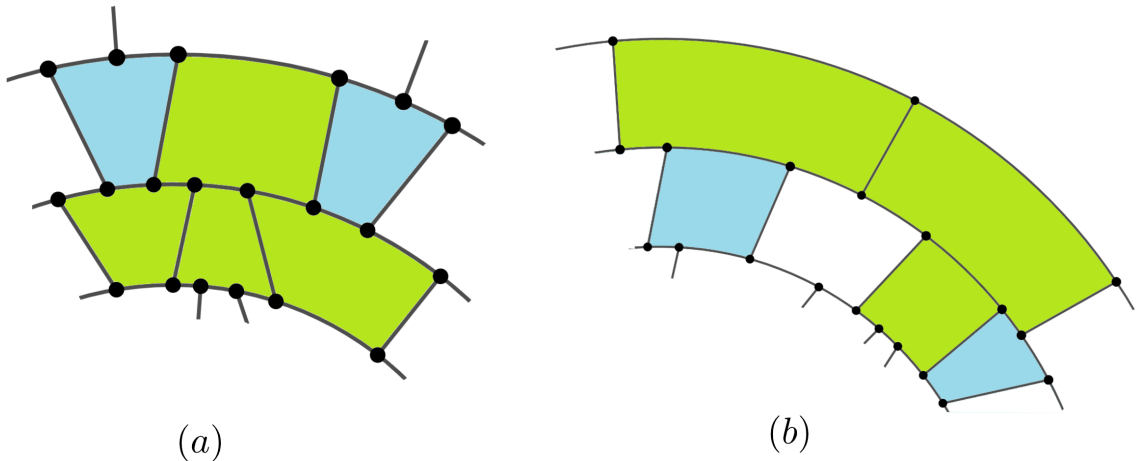


Figure 3.10: The two possibilities of having an unbalanced hexagon between the pentagons in the central layer of  $D_4$ .

**Lemma 39.** *All the hexagons are balanced in the central layer of  $D_4$ .*

*Proof.* Please refer to Figure 3.10. Suppose there is at least one unbalanced hexagon in the central layer of  $D_4$ . There are two cases to consider:

- An unbalanced hexagon between two pentagons. Note that by Lemma 31, the only single pentagon representation possible is such that an unbalanced hexagon is between two partitioned pentagons such that they have two vertices in the auxiliary cycle  $C$ , and the hexagon contains two vertices in the auxiliary cycle  $C'$  (see Figure 3.10(a)). We can say, without loss of generality, that this representation is unique, up to symmetry. Note that this arrangement implies three consecutive unbalanced hexagons, highlighted in green, in the hexagonal layer adjacent to the central layer of  $D_4$ , which contradicts Corollary 2.

- Two hexagons between the pentagons. Suppose one of the hexagons is balanced. By 31, this hexagon must be adjacent to the pentagon that does not have two vertices in the same auxiliary cycle that this hexagon has two vertices (see Figure 3.10(b)). Fixed this construction, note that this arrangement implies three consecutive unbalanced hexagons, highlighted in green, in the hexagonal layer adjacent to the central layer of  $D_4$ , which contradicts Lemma 31.

Therefore, analyzing all possible cases, we concluded that there are no unbalanced hexagons in the central layer of  $D_4$ .  $\square$

The arrangement of the pentagons in the central layer of the fullerene nanodisc  $D_3$  can be generalized for  $D_4$  as follows.

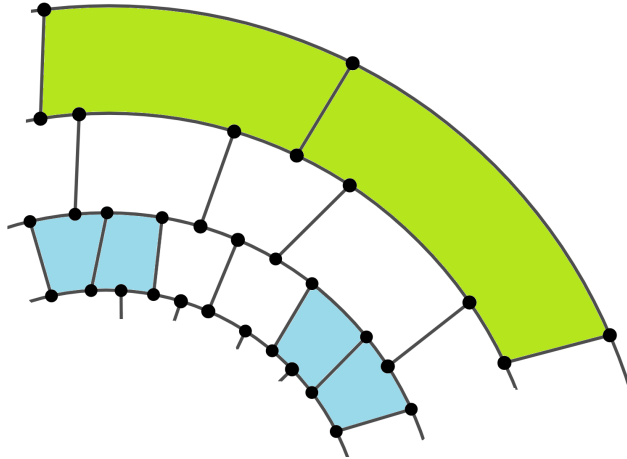


Figure 3.11: Case in which there are two hexagons between the pentagons.

**Lemma 40.** *It is not possible to have balanced hexagons between two pentagons arranged in the same way in the central layer of  $D_4$ .*

*Proof.* Please refer to Figure 3.11. Suppose the central layer of  $D_4$  has balanced hexagons whose neighboring faces are pentagons partitioned in the same way. There are two cases to be examined:

- A balanced hexagon whose neighboring faces are two pentagons partitioned in the same way. Note that this representation is analogous to the nanodisc  $D_3$  (Figure 3.8). Therefore, such representation is not allowed.
- The two balanced hexagons are divided into pentagons partitioned in the same way, as shown in the Figure 3.11. We can say, without loss of generality, that this representation is unique, up to symmetry. Note this arrangement implies

two consecutive unbalanced hexagons, highlighted in green, in the hexagonal layer which contains 12 hexagons. This contradicts the Lemma 31 and Corollary 2 since only the layers containing 6 hexagons have such a distribution.

Therefore, analyzing the possible cases, we concluded that the balanced hexagons of the central layer of  $D_4$  must be arranged between pentagons partitioned in a different way.  $\square$

Lemmas 39 and 40 characterize the uniqueness of the  $D_4$  representation whose pentagons appear isolated in the central layer, and also ensure certain restrictions for the arrangement in which pentagons appear in pairs. Note that by Theorem 37 there is a planar representation for  $D_4$  with pentagons arranged in pairs, where there are 2 balanced hexagons between each pair of pentagons. Thus, a natural thought is a representation where the hexagons appear in different quantities between the pairs of pentagons. Let's see below a result that illustrates the impossibility for  $r = 4$ .

**Theorem 41.** *The representation of the fullerene nanodisc  $D_4$  with pentagons arranged in pairs is unique.*

*Proof.* By Lemma 38, the maximum number of hexagons that can be arranged between each pair of pentagons in the central layer of  $D_4$  is 2 and therefore, to arrange the hexagons in the central layer, the distribution possibilities of the hexagons are necessarily 1 hexagon or 2 hexagons between each pair. Note that  $D_4$  has 12 hexagons to be arranged between 6 pairs of pentagons. This makes a mixed hexagon representation impossible.  $\square$

**Observation 42.** *For  $r = 5$ , we have found a representation where the hexagons are arranged differently in the central layer of this nanodisc. Such evidence can be found in the Appendix A.*

We obtained two different representations for the fullerene nanodisc  $D_4$ . As for  $D_3$ , the representation whose pentagons are arranged in pairs in the central layer of  $D_4$  is also unique, leading to evidence of the uniqueness of the representation given in the Theorem 37. Therefore, we have formulated the following question.

**Question 2.** *The representation of pentagons in pairs given by the Theorem 37 is unique for all fullerene nanodiscs  $D_r$  with  $r \geq 3$ ?*

Since we think of mixed hexagon representation, it is also natural to think that there are fullerene nanodiscs with mixed pentagonal representation. For a simple counting of faces, the nanodiscs  $D_2$  and  $D_3$  does not admit a mixed pentagonal arrangement, that is, a representation where the pentagons in the central layer appear both isolated and in pairs. As we increase the radius parameter, the number

of hexagons to be arranged between pentagons in the central layer increases, and so it is natural to question whether any nanodisc admits a representation in this way. Therefore, we have formulated the following question.

**Question 3.** *Is there a fullerene nanodisc  $D_r$  whose pentagonal representation is mixed for some  $r \geq 4$ ?*

In a first analysis, we found a negative answer for  $r = 4$ .

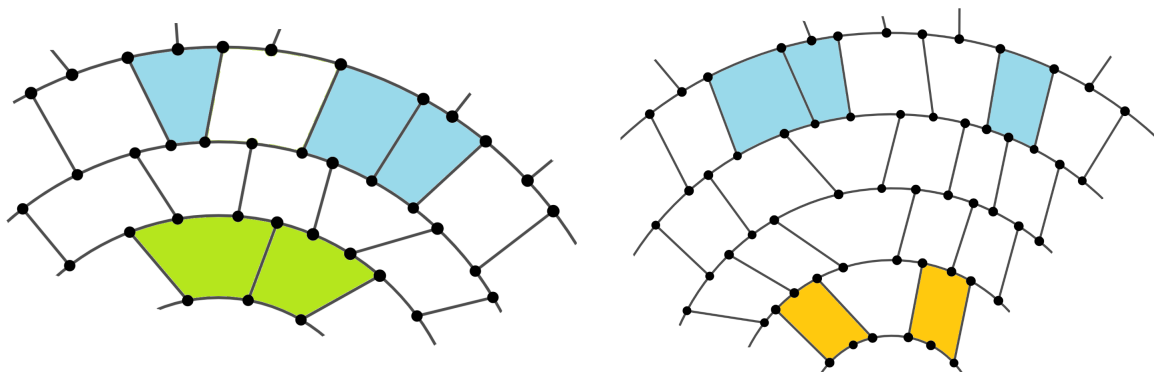


Figure 3.12: The possibilities of having mixed pentagons when  $r = 4$ .

**Lemma 43.** *The fullerene nanodisc  $D_4$  does not admit a mixed pentagonal representation.*

*Proof.* Suppose that the central layer of the fullerene  $D_4$  admits a representation with mixed pentagons. By Lemma 38, the number of cases is limited by the number of hexagons we can have arrange among any group of pentagons. Thus, we are restricted to two possibilities:

- There is only one balanced hexagon between the mixed pentagons (Figure 3.12(a)). We can say, without loss of generality, that this representation is unique, up to symmetry. Note this arrangement implies two consecutive unbalanced hexagons, highlighted in green, in the hexagonal layer which contains 12 hexagons. This contradicts the Lemma 31 and Corollary 2 since only the layers containing 6 hexagons have such a distribution.
- There are two balanced hexagons between the mixed pentagons (Figure 3.12(b)). We can say, without loss of generality, that this representation is unique, up to symmetry. Fixed this construction, note that this arrangement implies at least two balanced hexagons, highlighted in orange, in the layer containing 6 hexagons, which contradicts the Corollary 2.

Therefore, analyzing the possible cases, we concluded that the fullerene nanodisc  $D_4$  does not admit mixed pentagonal representation.  $\square$

We are ready to state the quantitative result for  $D_4$ .

**Theorem 44.** *The fullerene nanodisc  $D_4$  has two non isomorphic representations.*

*Proof.* In the central layer of  $D_4$ , we have 12 pentagons distributed among 12 hexagons. By Lemma 31, we cannot have two consecutive pentagons partitioned in the same way. By Lemma 33, we cannot have three consecutive pentagons such that each pair is not partitioned in the same way. By Lemma 38, we cannot have three or more hexagons between the pentagons. By Lemma 39 all the hexagons are balanced, by Lemma 40 we have an order to dispose the pairs of pentagons, and by Theorem 41 the representation with pentagons arranged in pairs is unique. Also, this central layer does not admit mixed representations, neither of pentagons nor of hexagons. So, we have two forms to distribute:

- A pentagon between each hexagon;
- Among the 12 hexagons arranged in pairs, the 12 pentagons in pairs of two consecutive pentagons such that each pair is not partitioned in the same way.

See the two representations of  $D_4$  in Figure 3.13. □

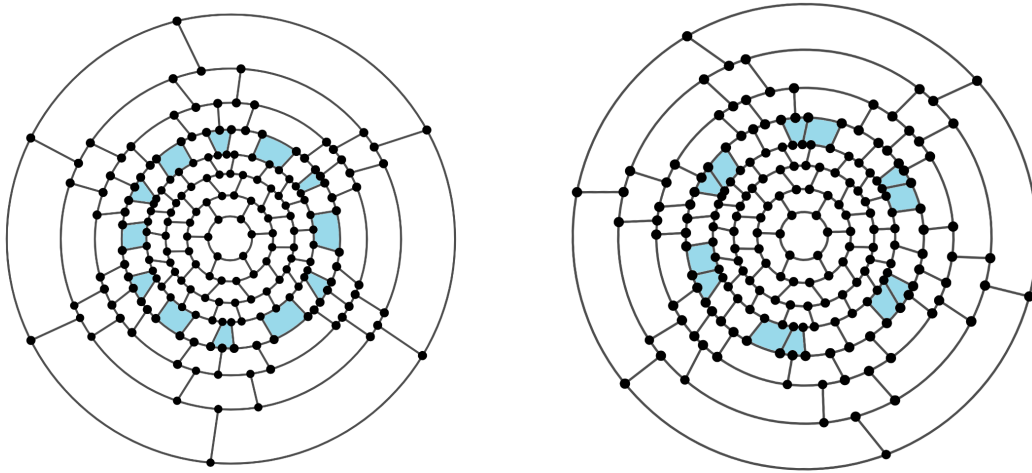


Figure 3.13: Two possible representations of fullerene nanodisc  $D_4$ .

We have evidence that it is possible to generalize most of the results obtained in this chapter to  $D_r$ ,  $r \geq 5$ , which is also an evidence that the Question 3 has a negative answer. However, we have already investigated some results for  $r > 4$ , using the dual representation previously mentioned in this chapter. Such an analysis and some other questions proposed can be found in Appendix A.

Now that we know a little better the structure of this class of graphs, we can venture into the coloring problem, which we will highlight in the following chapter.

# Chapter 4

## On the total coloring of nanodiscs

In 1941, Brooks [8] proved that every graph  $G$  with maximum degree  $\Delta$  has a  $\Delta$ -vertex coloring unless either  $G$  contains  $K_{\Delta+1}$  or  $\Delta = 2$  and  $G$  contains an odd cycle. In particular, this result is valid for cubic graphs. Thus, the optimal vertex coloring of a fullerene nanodisc has 3 colors, that is,  $\chi(D_r) = 3$ . In 1880, Tait [32] proved that the Four-Color Conjecture was equivalent to claim that every bridgeless cubic graph is Class 1 and, in particular,  $\chi'(D_r) = 3$ . In this chapter, we begin the investigation of the problem of total coloring in this class of graphs.

The smallest Type 2 cubic graph is  $K_4$ , and another known Type 2 cubic graph is the generalized Petersen graph  $G(5, 1)$  [10], and both have squares or triangles, as well as all Type 2 cubic graphs found so far [13]. See Figure 4.1.

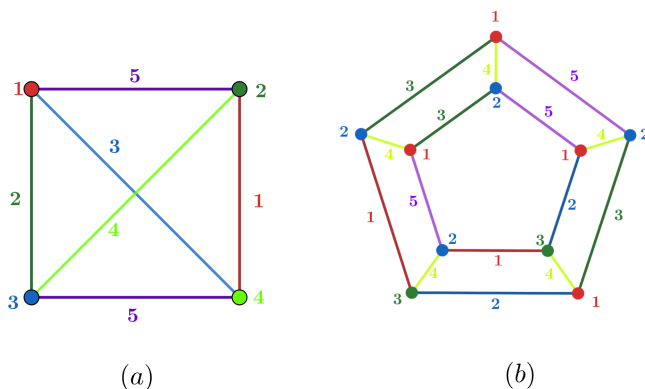


Figure 4.1: (a) A Type 2 girth 3 cubic graph; (b) a Type 2 girth 4 cubic graph.

So, it is natural to think that there are no Type 2 cubic graphs with girth at least 5. Thus the following conjecture was proposed [7]:

**Conjecture 6** (Brinkmann, Preissmann and Sasaki, 2015 [7]). *There is no Type 2 cubic graph with girth at least 5.*

Motivated by this conjecture, searches were started for Type 1 and Type 2 fullerene graphs (see Figure 4.2), which are graphs with girth 5, but so far only

Type 1 fullerene graphs have been obtained [22].

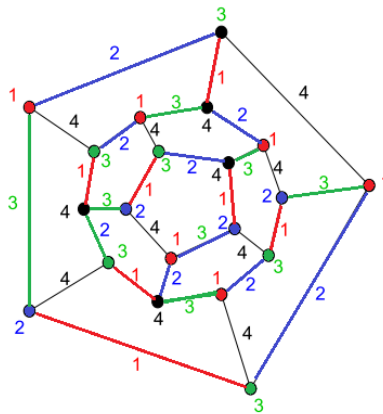


Figure 4.2: A 4-total coloring of fullerene graph  $C_{20}$ .

## 4.1 All nanodiscs are conformable

A strategy to color the vertices of  $D_r$  is to take advantage that the auxiliary cycles have even length and color alternately with colors  $\mathcal{C}_1$  and  $\mathcal{C}_2$  the cycle  $C_6$  defining the inner layer, with colors  $\mathcal{C}_3$  and  $\mathcal{C}_4$  the next cycle  $C_{18}$ , and so on. The strategy does not rely on the unicity of  $D_r$ , and defines for even radius a 4-vertex coloring that is conformable. See Figure 4.3.

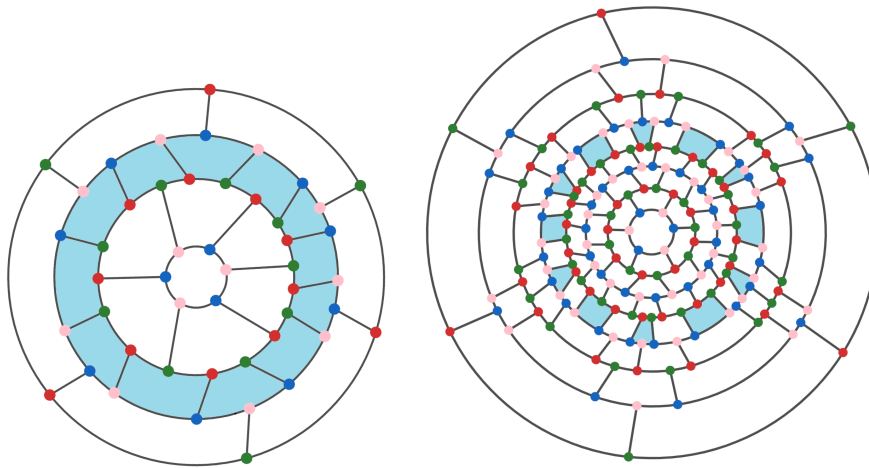


Figure 4.3: Conformable colorings for  $D_2$  and  $D_4$ , respectively.

**Theorem 45.** *Every nanodisc with even radius admits a conformable 4-vertex coloring.*

*Proof.* Let  $\mathcal{C} = \{\mathcal{C}_1, \mathcal{C}_2, \mathcal{C}_3, \mathcal{C}_4\}$  be a set of colors. In a  $D_r$  with even  $r$ , consider the 4-vertex coloring that gives colors  $\mathcal{C}_1$  and  $\mathcal{C}_2$  to the outer cycle  $C_6$ , colors  $\mathcal{C}_3$  and

$\mathcal{C}_4$  to the next cycle  $C_{18}$ , until we reach the central layer, where colors  $\mathcal{C}_3$  and  $\mathcal{C}_4$  are given to cycle  $C_{12r-6}$  and colors  $\mathcal{C}_1$  and  $\mathcal{C}_2$  are given to the next cycle  $C_{12r-6}$ , continue in this fashion until colors  $\mathcal{C}_3$  and  $\mathcal{C}_4$  are given to the inner cycle  $C_6$ . Note that each cycle provides an odd number of colored vertices with the same color, and that every color class has the same number of vertices and that this number is even, given by  $3r^2$ .  $\square$

Note that for  $r$  odd this 4-vertex coloring is not conformable, since  $3r^2$  generates an odd number of vertices for each color class (See Figure 4.4).

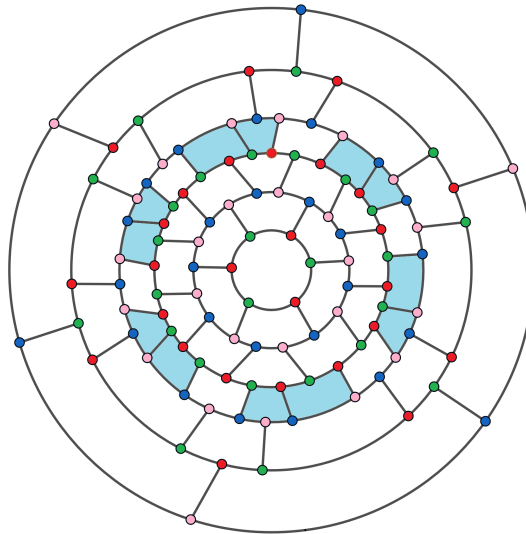


Figure 4.4: A 4-vertex coloring that does not give a conformable coloring of  $D_3$ .

Seeking to prove that all  $D_r$  nanodiscs are conformable, we further studied the  $D_3$  nanodisc and obtained an optimal 3-vertex coloring that gives a conformable 4-vertex coloring, since each of the three color classes has an even number of vertices, and the fourth color class has 0 elements [11] (See Figure 4.5).

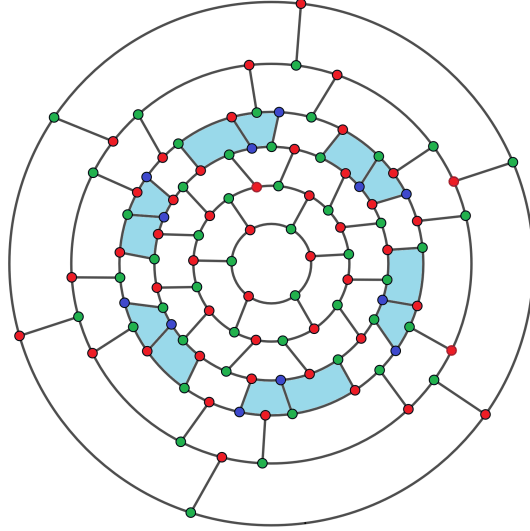


Figure 4.5: An optimal 3-vertex coloring that gives a conformable coloring of  $D_3$ .

The optimal 3-vertex coloring strategy for  $D_3$  consists of coloring the auxiliary cycles, except for the two cycles of the center layer, using two colors alternately, avoiding color conflict in the vertices that are extremes of radial edges between consecutive auxiliary cycles. In the cycles  $C_{12r-6}$  defining the central layer, we introduce a third color by choosing six vertices in each cycle, thus ensuring the parity of this color class and the other color classes, where the fourth color class has 0 vertices.

In 2022, *Nigro et al.* [24] proved that every cubic graph except the complete graph  $K_4$  and the complete bipartite graph  $K_{3,3}$  satisfies the conformable condition through an algorithm that from a 3-vertex coloring gets a fourth color class with cardinality 2. It is known by Brooks' Theorem [8] that exists a 3-vertex coloring that can be achieved in polynomial time for cubic graphs. One way to get such coloring is to sort the vertices of the graph and color greedily each vertex  $v \in V(G)$  with the color  $C_i$ , where  $i = 1, 2, 3$ , of the lowest index not used by the vertices  $u \in V(G)$  that belong to the neighborhood of  $v$ . Moreover, since  $|V(G)|$  is even, there are only two possibilities for the three color classes of this vertex coloring: either the three color classes are even, and so this is a conformable coloring or the three color classes only one of these is even. We will apply the coloring strategy given in [24] to show the conformable condition of the fullerene nanodiscs with  $r$  odd.

**Theorem 46.** *Every nanodisc with odd radius admits a conformable 4-vertex coloring.*

*Proof.* Let  $D_r$  be a fullerene nanodisc with odd  $r$  and  $\mathcal{C} = \{C_1, C_2, C_3, C_4\}$  be a set of colors. By Brooks' Theorem [8], there is a 3-vertex coloring for  $D_r$ , where there are two possibilities for the cardinality of color classes:

- $\mathcal{C}_1, \mathcal{C}_2$  and  $\mathcal{C}_3$  have an even number of vertices, and therefore this vertex coloring is conformable;
- There is only one color class with an even number of vertices.

Suppose, without loss of generality that this single color class is  $\mathcal{C}_2$ . The algorithm that provides a conformable coloring for  $D_r$  is based on the following affirmation.

**Observation 47** (Nigro et al., 2022 [24]). *There is a vertex  $u \in \mathcal{C}_1$  that is not adjacent to a vertex  $v \in \mathcal{C}_3$ .  $\square$ .*

Given this affirmation, we can assign a fourth color to the non adjacent vertices  $v$  and  $u$  and thus obtain a conformable 4-vertex coloring that has  $\mathcal{C}_1 - v, \mathcal{C}_2$  and  $\mathcal{C}_3 - u$  with even size and  $\mathcal{C}_4$  with cardinality 2. Therefore, as all color classes have an even number of vertices, we have a conformable 4-vertex coloring for  $D_r$ , with  $r$  odd. Note that this coloring strategy does not rely on the unicity of  $D_r$ . See Figure 4.6 where from a 3-vertex coloring that is not conformable to the  $D_5$  nanodisc and from the described procedure we obtain a conformable 4-vertex coloring for these graphs.  $\square$

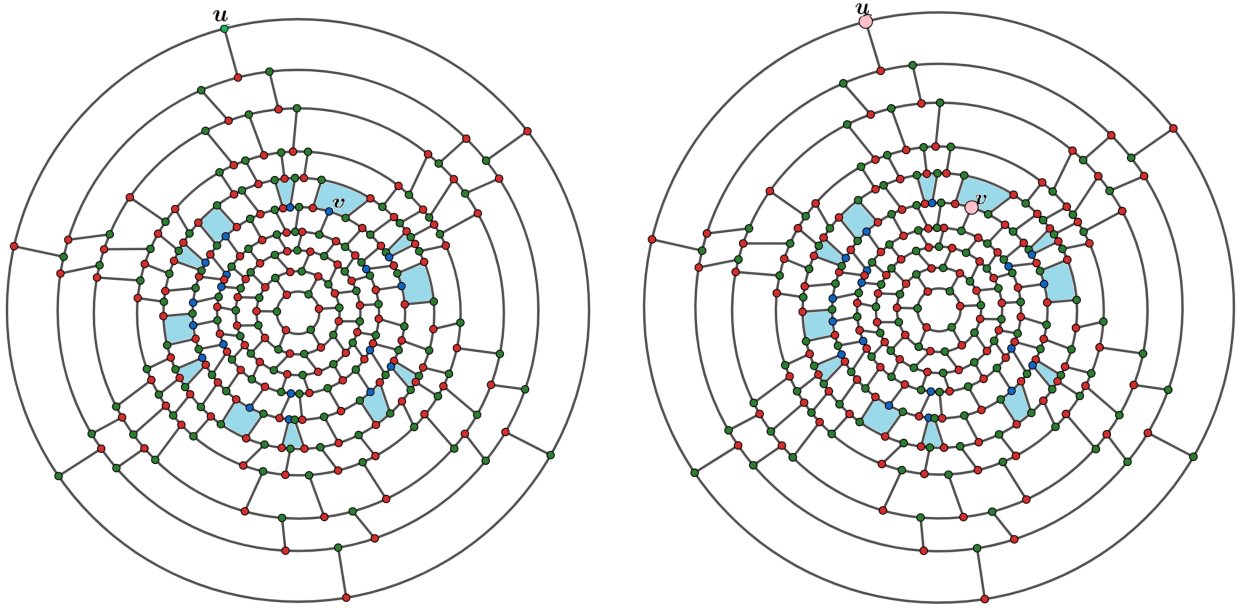


Figure 4.6: On the left, a 3-vertex coloring for  $D_5$ , with  $|\mathcal{C}_1| = 141$ ,  $|\mathcal{C}_2| = 140$ ,  $|\mathcal{C}_3| = 19$  and on the right, a conformable 4-vertex coloring for  $D_5$ , where  $|\mathcal{C}_1| = 140$ ,  $|\mathcal{C}_2| = 140$ ,  $|\mathcal{C}_3| = 18$ ,  $|\mathcal{C}_4| = 2$ . Note that the non-adjacent vertices  $u \in \mathcal{C}_1$  and  $v \in \mathcal{C}_3$  received color  $\mathcal{C}_4$  during the procedure.

Once proven that every fullerene nanodisc is conformable, we seek to improve the above coloring strategy, in favor of obtaining a 3-vertex coloring for odd nanodiscs

where the three color classes have an even number of vertices for some value of the  $r$  parameter, since no  $r$  value has been found whose greedy coloring strategy provides such coloring. Thus, we generalize the conformable coloring obtained for the fullerene nanodisc  $D_3$  [11] in a conformable 4-vertex coloring that extends to every fullerene nanodisc  $D_r$ ,  $r \geq 3$  whose pentagons in the central layer are arranged in pairs. By Lemma 37 it is known that every fullerene nanodisc  $D_r$ ,  $r \geq 3$  has such representation.

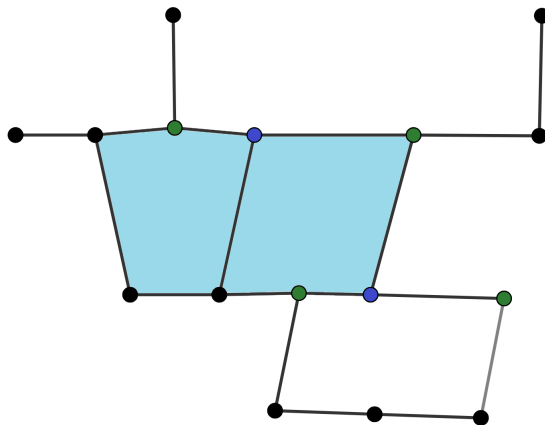


Figure 4.7: A pair of pentagons in the central layer of  $D_r$ ,  $r \geq 3$  and their neighboring vertices.

**Theorem 48.** *Every fullerene nanodisc  $D_r$ ,  $r \geq 3$  whose the pentagons in the central layer are arranged in pairs admits a conformable 4-vertex coloring.*

*Proof.* Let  $C$  and  $C'$  be the auxiliary cycles that make up the central layer of  $D_r$ ,  $r \geq 3$  and  $\mathcal{C} = \{\mathcal{C}_1, \mathcal{C}_2, \mathcal{C}_3, \mathcal{C}_4\}$  be a set of colors. For convenience, in this proof we will denote color  $\mathcal{C}_1$  as green,  $\mathcal{C}_2$  as red,  $\mathcal{C}_3$  as blue and  $\mathcal{C}_4$  as pink.

We select 6 vertices in  $C$  and 6 vertices in  $C'$  and color them with the blue color, as illustrated in Figure 4.7. Next, we color the two vertices that are adjacent to the blue vertex in the  $C$  cycle using color red (green), and in the same pentagon pair, we repeat the process for the blue vertex in  $C'$ . In the following pentagon pair, we use color green (red) to color the vertices that are adjacent to the blue vertices. This process is repeated until all vertices that are adjacent to the blue vertices are colored. This procedure avoids color conflict, as it ensures that radial edge extremes that generate adjacent vertices do not have the same color. It is possible to color the remaining vertices in  $C$  and  $C'$  using the colors red and green alternately and without color conflict, since an even number of vertices remains between each blue vertex and its already colored neighborhood. The other  $D_r$  auxiliary cycles can be easily colored using colors red and green alternately. This strategy has 12 colored vertices with blue color and an even number of colored vertices with colors red and

green. As the pink color has 0 elements, we obtain from the described procedure a conformable 4-vertex coloring for these graphs. See Figure 4.5.  $\square$

The main goal of the study the conformable condition in fullerene nanodiscs is to obtain a 4-vertex coloring that can be extended to a 4-total coloring of  $D_r$ ,  $r \geq 3$ . It is intuitive to think that the conformable colorings obtained induces a 4-total coloring for some subfamilies of  $D_r$ . However, the structure of nanodiscs and its auxiliary cycles give us some restrictions.

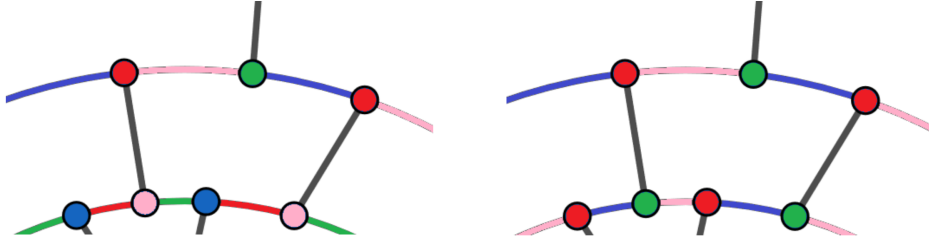


Figure 4.8: Attempt to extend a vertex coloring into a 4-total coloring whose adjacent auxiliary cycles are colored with two colors.

**Lemma 49.** *A vertex coloring of  $D_r$ ,  $r \geq 2$  where two adjacent auxiliary cycles are colored with pairs of colors (distinct or not) does not allow an extension to a 4-coloring of  $D_r$ .*

*Proof.* Please refer to Figure 4.8. Let  $C$  and  $C'$  be two adjacent auxiliary cycles of a nanodisc  $D_r$  and  $\mathcal{C} = \{\mathcal{C}_1, \mathcal{C}_2, \mathcal{C}_3, \mathcal{C}_4\}$  be a set of colors.

Suppose  $C$  is colored with the colors  $\mathcal{C}_1$  and  $\mathcal{C}_2$  and  $C'$  is colored with the colors  $\mathcal{C}_3$  and  $\mathcal{C}_4$ . Therefore, so that there is no color conflict in the cycles, to color the edges of  $C$ , colors  $\mathcal{C}_3$  and  $\mathcal{C}_4$  shall be used, and to color the edges of  $C'$ , colors  $\mathcal{C}_1$  and  $\mathcal{C}_2$  shall be used. Once this procedure is done, it remains to color only the radial edges, which connect  $C$  and  $C'$ , forming a layer of  $D_r$ . However, the 4 colors have already been used in the elements adjacent to the radials, which makes it impossible to color this edge without color conflict. Note that the argument is analogous when  $C$  and  $C'$  are colored with the same color pair, since the same color pair will remain for coloring the edges of the two cycles.  $\square$

Lemma 49 induces important results concerning the conformable colorings already obtained for nanodiscs.

**Corollary 3.** *The conformable 4-vertex coloring given in Theorem 45 does not induce a 4-total coloring for  $D_r$ , with  $r$  even.  $\square$*

**Corollary 4.** *The conformable 4-vertex coloring given in Theorem 46 does not induce a 4-total coloring for  $D_r$ , with  $r$  odd.  $\square$*

**Corollary 5.** *The 3-vertex coloring that is a conformable coloring given in Theorem 48 does not induce a 4-total coloring for  $D_r$  with pentagons arranged in pairs.  $\square$*

## 4.2 Hunting a Type 2 fullerene nanodisc

In the previous section, it was proved that it is not possible to obtain a 4-total coloring from the conformable vertex colorings demonstrated in the Theorems 45, 46 and 48. However, it is possible to establish an upper bound for which these vertex colorings allow an expansion to a total coloring for the nanodisc subfamilies.

Feng and Lin [17] established that the total chromatic number for subcubic graphs is 5 through an algorithm that provides such coloring. In this paper, when  $\Delta = 3$ , are considered the cases where the cubic graph has bridges or not. If  $G$  is a bridgeless cubic graph, by Brooks' Theorem [8] there is a 3-vertex coloring for  $G$ , and by Petersen's Theorem [25]  $G$  has a perfect matching  $M$ . Note that  $G \setminus M$  is a collection of disjoint cycles that can be colored with 4 colors. In this way, a 5-total coloring is obtained using a fifth color class on the edges belonging to the perfect matching  $M$ .

Based on the above results, the following theorems are applicable to the fullerene nanodiscs  $D_r$ , thus finding an upper bound for the conformable colorings obtained.

**Theorem 50.** *The conformable 4-vertex coloring given in Theorem 45 induces a 5-total coloring for  $D_r$ , with  $r$  even.*

*Proof.* Let  $D_r$  be a fullerene nanodisc with  $r$  even and  $\mathcal{C} = \{\mathcal{C}_1, \mathcal{C}_2, \mathcal{C}_3, \mathcal{C}_4\}$  be a 4-vertex coloring of  $D_r$ , as described in Theorem 45. We can assume, without loss of generality that there are  $r$  cycles colored with the color pair  $\mathcal{C}_1$  and  $\mathcal{C}_2$  and  $r$  cycles colored with the color pair  $\mathcal{C}_3$  and  $\mathcal{C}_4$ . In this way, to color the edges of the cycles that have the vertices colored with  $\mathcal{C}_1$  and  $\mathcal{C}_2$  just use the colors  $\mathcal{C}_3$  and  $\mathcal{C}_4$ , and to color the edges of the cycles colored with colors  $\mathcal{C}_3$  and  $\mathcal{C}_4$ , just use the colors  $\mathcal{C}_1$  and  $\mathcal{C}_2$ . By Lemma 49, it is known that radial edges connecting cycles cannot have any of the four color classes. Note that the radial edges form a perfect matching in  $D_r$ . So just include a fifth color class,  $\mathcal{C}_5$  in this perfect matching and so we get a 5-total coloring of  $D_r$ , with  $r$  even. See Figure 4.9 where a 5-total coloring of a nanodisc with even radius is illustrated.  $\square$

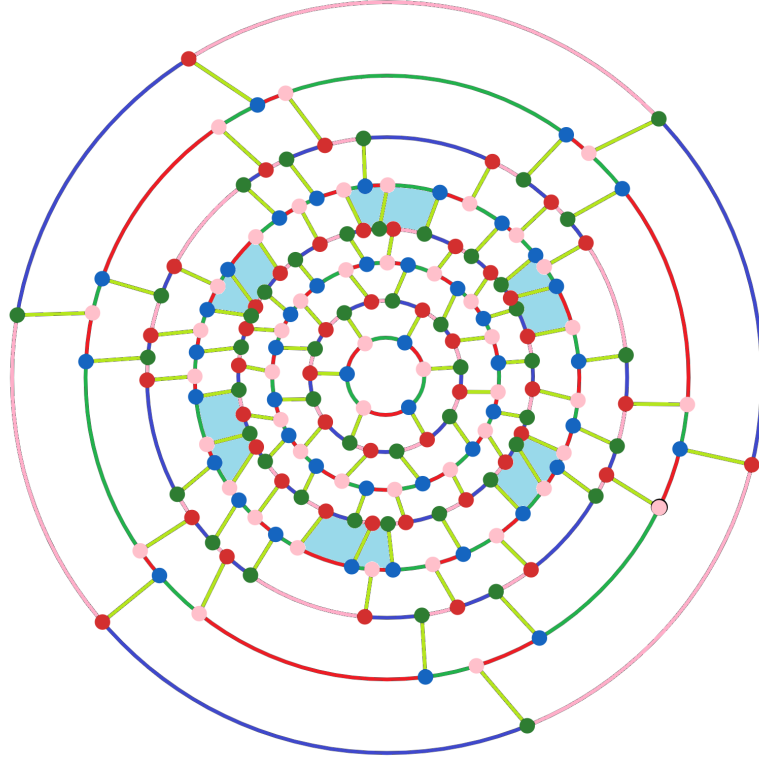


Figure 4.9: A 5-total coloring of  $D_4$ .

**Theorem 51.** *The conformable 4-vertex coloring given in Theorem 46 induces a 5-total coloring for  $D_r$  with  $r$  odd.*

*Proof.* Let  $D_r$  be a fullerene nanodisc with  $r$  odd and  $\mathcal{C} = \{\mathcal{C}_1, \mathcal{C}_2, \mathcal{C}_3, \mathcal{C}_4\}$  be a conformable 4-vertex coloring of  $D_r$ , as described in Theorem 46. Note that in this strategy, we have cycles with vertices colored with two colors, cycles with vertices colored with three colors and as there are two colored vertices with color  $\mathcal{C}_4$ , it is possible that there are auxiliary cycles whose vertices are colored with 4 colors. Note that every auxiliary cycle  $C$  of  $D_r$  has cardinality divisible by 3, and therefore, by the Theorem 17, every auxiliary cycle of  $D_r$  has total chromatic number 3. Thus, each auxiliary cycle  $C$  also admits a 4-total coloring. After this process, it remains to color the radial edges of  $D_r$ . Note that the radial edges form a perfect matching in  $D_r$ . So just include a fifth color class,  $\mathcal{C}_5$  in this perfect matching and so we get a 5-total coloring of  $D_r$ , with  $r$  odd. See Figure 4.10 where a 5-total coloring of a nanodisc with odd radius is illustrated.  $\square$

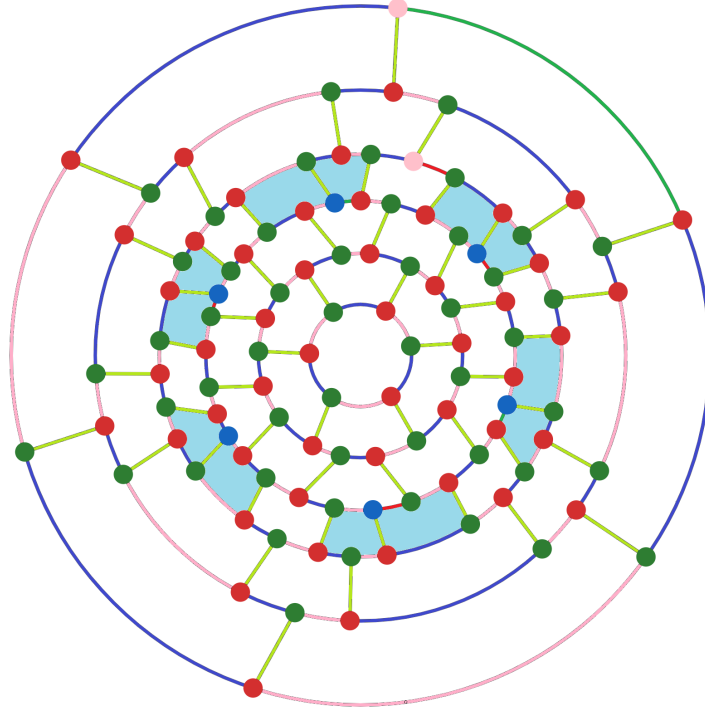


Figure 4.10: A 5-total coloring of  $D_3$ .

**Theorem 52.** *The 3-vertex coloring that is a conformable coloring given in Theorem 48 induces a 5-total coloring for  $D_r$  with pentagons arranged in pairs.*

*Proof.* Let  $D_r$  be a fullerene nanodisc with pentagons arranged in pairs and  $\mathcal{C} = \{\mathcal{C}_1, \mathcal{C}_2, \mathcal{C}_3, \mathcal{C}_4\}$ , be a conformable 4-vertex coloring, where  $|\mathcal{C}_4| = 0$ , as described in Theorem 48. Note that there are  $2r - 2$  cycles whose vertices are colored with colors  $\mathcal{C}_1$  e  $\mathcal{C}_2$ , since the color class  $\mathcal{C}_3$  appears only on 12 vertices in the two cycles that make up the central layer,  $\mathcal{C}_4$  has 0 elements and the other vertices of these cycles are also colored with the colors  $\mathcal{C}_1$  and  $\mathcal{C}_2$ . In this way, to color the edges of the cycles that have the vertices colored with  $\mathcal{C}_1$  and  $\mathcal{C}_2$ , just use the colors  $\mathcal{C}_3$  and  $\mathcal{C}_4$ . On the central layer, just use the color  $\mathcal{C}_1$  on the edges that have as edges colored vertices with the colors  $\mathcal{C}_3$  and  $\mathcal{C}_2$  and use the color  $\mathcal{C}_2$  on the edges that have as edges colored vertices with the colors  $\mathcal{C}_3$  and  $\mathcal{C}_1$ . On the other edges of these cycles, just use the colors  $\mathcal{C}_3$  and  $\mathcal{C}_4$ , since these have colored extremes with  $\mathcal{C}_1$  and  $\mathcal{C}_2$ . After this process, it remains to color the radial edges of  $D_r$ . Note that the radial edges form a perfect matching in  $D_r$ . So just include a fifth color class,  $\mathcal{C}_5$  in this perfect matching and so we get a 5-total coloring of  $D_r$ ,  $r \geq 3$  with pentagons arranged in pairs. See Figure 4.11.  $\square$

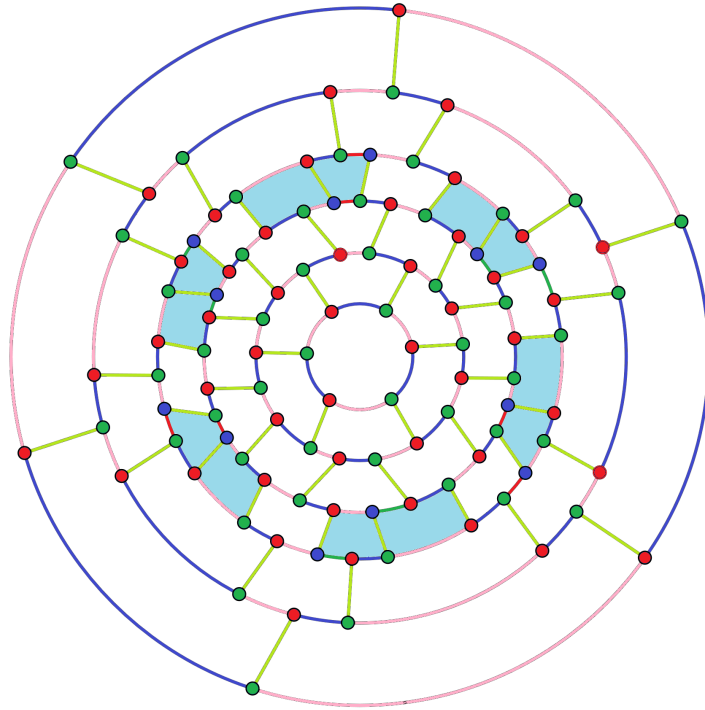


Figure 4.11: A 5-total coloring of  $D_3$ .

In [12] was displayed a 4-total coloring of  $D_2$ , providing the following result.

**Theorem 53.** *The fullerene nanodisc  $D_2$  is Type 1.*

*Proof.* From the unicity established in Section 3.2, we may present in Figure 4.12 a 4-total coloring for  $D_2$  [12]. This is enough to prove that this graph is Type 1.  $\square$

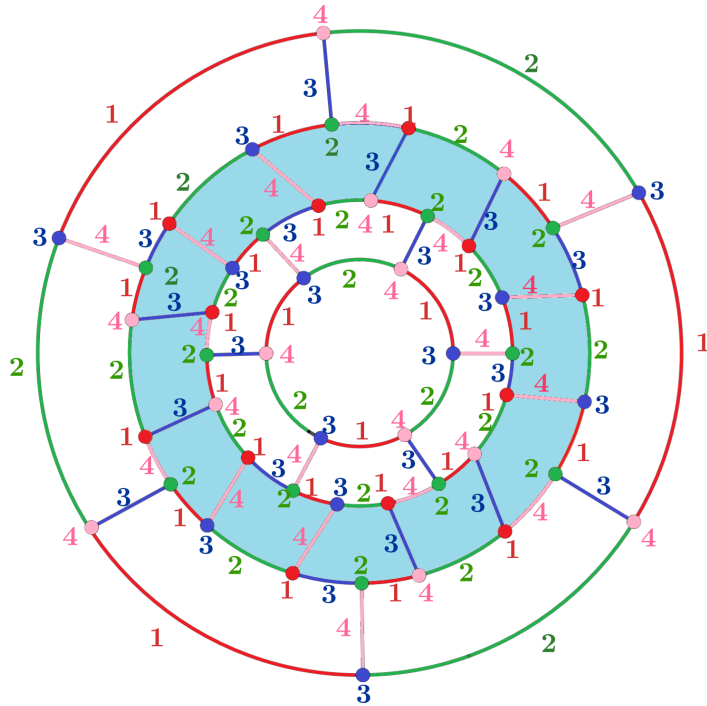


Figure 4.12: A 4-total coloring of fullerene nanodisc  $D_2$ .

Note that in this coloring, the four colors are being used in the vertices, and the perfect matching given by the radials edges has been partitioned into two sets of edges, which receive the colors 3 and 4. By inspection, it is possible to conclude that this coloring is equitable, since there are 18 edges and 12 colored vertices with each color class, resulting in 30 elements of  $D_2$  colored with each color class. It gives exactly  $\frac{1}{4}$  of the number of elements in the graph, a negative evidence to the Question 1. Note that, because it is the only fullerene nanodisc that does not have balanced hexagons and all pentagons of the central layer are arranged side by side, it is a degenerate case. Note that  $D_2$  has the sequence of cycles  $\{C_6, C_{18}, C_{18}, C_6\}$ , which are cycles common to all fullerene nanodiscs. Thus, it is intuitive to think that based on this 4-total coloring obtained for  $D_2$ , we can replicate this strategy for the cycles  $C_6$  and  $C_{18}$  for nanodiscs of radius greater than 2. So far, no strategy investigated has allowed expanding the total coloring obtained to  $D_2$  for the remaining  $D_r$ ,  $r \geq 3$ . In this way, generalizing this coloring to the  $D_r$ ,  $r \geq 3$  and find a 4-total coloring for these nanodiscs has proven to be a challenging problem.

#### 4.2.1 The natural strategy does not work

In this section we prove that the natural strategy to total color first the auxiliary cycles of the nanodisc with 3 colors and then to extend the total coloring by giving

the same color to the remaining radial edges does not work.

In 1996, Yap [36] established the total chromatic number of the cycle graphs  $C_n$ .

**Theorem 54** ([36]). *Let  $G$  be the cycle graph  $C_n$ . Then*

$$\chi''(G) = \begin{cases} 3, & \text{if } n \equiv 0 \pmod{3}; \\ 4, & \text{otherwise.} \end{cases}$$

We will display the algorithm that colors cycles  $C_n$  where  $3|n$ , that is,  $n \equiv 0 \pmod{3}$ . The vertex set of  $G$  is labeled as follows:

$$V(G) = \{v_0, v_1, \dots, v_{n-1}\}.$$

Then, we will define the following color assignment to the elements of  $C_n$ :

$$\begin{aligned} \mathcal{C}(v_i) &= (-i) \pmod{3}, \forall v_i \in V(G); \\ \mathcal{C}(v_i v_{i+1}) &= (\mathcal{C}(v_i) + 1) \pmod{3}, \forall v_i v_{i+1} \in E(G). \end{aligned}$$

Note that by the construction above, the colors 0, 1, 2, ..., 0, 1, 2 will be associated in this order with the elements of the cycle  $v_0, v_0 v_1, \dots, v_{n-1}, v_{n-1} v_0$ . In this way, by making a simple inspection, we can conclude that  $\mathcal{C}$  is a total coloring of  $G$  that uses 3 colors. Since  $C_n$  is 2-regular, we have  $\Delta(C_n) = 2$  and  $\mathcal{C}$  is an optimal coloring of  $C_n$ .

Note that the auxiliary cycles sequence  $\{C_6, C_{18}, \dots, C_{12r-6}, C_{12r-6}, \dots, C_{18}, C_6\}$  that define the layers of a fullerene nanodisc  $D_r$ ,  $r \geq 2$  are cycles where  $n$  is divisible by 3. Thus, it is possible to obtain a 3-total coloring for each subgraph induced by a auxiliary cycle  $C$  of  $D_r$ . See in Figure 4.13 examples of 3-total colorings for auxiliary cycles  $C_n$ , using the above construction.

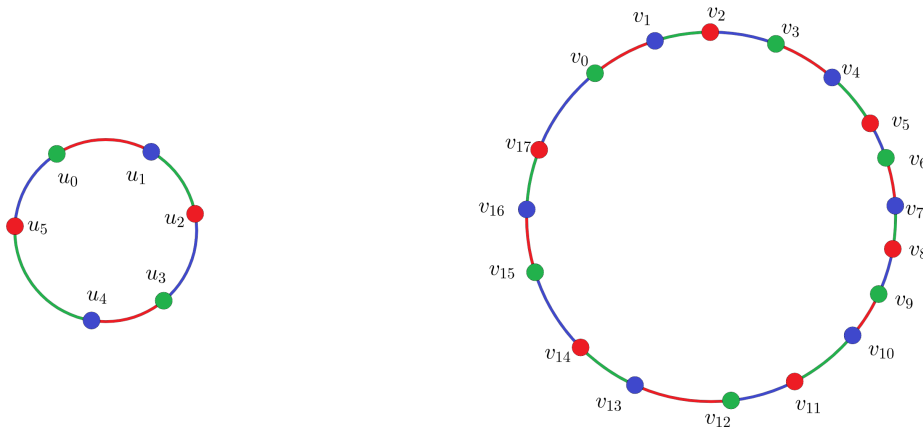


Figure 4.13: A 3-total coloring of  $C_6$  and  $C_{18}$ , respectively.

Note that the radial edges form a perfect matching  $M$  in  $D_r$  and their removal produces  $2r$  disjoint cycles. In this way, it is intuitive to think that it is possible to

get a 3-total coloring for  $D_r \setminus M$  using the coloring algorithm that colors  $C_n$  cycles with  $n$  divisible by 3, and include a fourth color in the edges of  $M$ , and thus get a 4-total coloring for  $D_r$ .

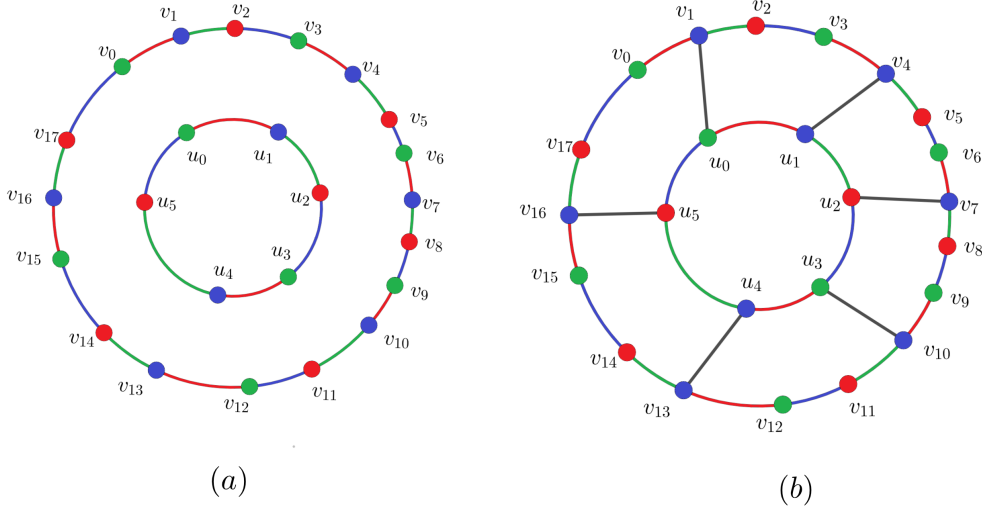


Figure 4.14: (a) A 3-total coloring for  $D_r[C] \setminus M_1$ ; (b) Color conflict after the inclusion of radial edges that form 6 unbalanced hexagons.

**Theorem 55.** *The coloring strategy above does not provide a 4-total coloring for any fullerene nanodisc  $D_r$ ,  $r \geq 2$ .*

*Proof.* Let  $D_r[C]$  be the subgraph of  $D_r$ ,  $r \geq 2$  induced by the vertices of the two adjacent auxiliary cycles  $C_6$  and  $C_{18}$  that make the layer containing six unbalanced hexagons, and  $M_1$  the set of radial edges that connect these two cycles. The removal of  $M_1$  implies two disjoint cycles, namely  $C_6$  and  $C_{18}$ . By the Theorem 54, there is a 3-total coloring for each of the cycles and an algorithm that provides such coloring. We will label the vertices of  $C_6$  and  $C_{18}$  as follows.

$$V(C_6) = \{u_0, u_1, \dots, u_5\}, V(C_{18}) = \{v_0, v_1, v_2, \dots, v_{17}\}$$

See Figure 4.14(a) where we display a 3-total coloring for the disjoint cycles. For convenience, we will denote the color 0 as green, the color 1 as red, and the color 2 as blue. Note that the algorithm described above partitions the vertex set of  $C_{18}$  into three independent sets, namely  $v_{0+3i}$ ,  $v_{1+3i}$  and  $v_{2+3i}$ , with  $0 \leq i \leq 5$ , where the vertices  $v_{0+3i}$  are colored with the color green,  $v_{1+3i}$  with the color red and  $v_{2+3i}$  with the color blue, and the vertices of  $C_6$ , the vertices  $u_0, u_3$  are colored with the color green,  $u_1, u_4$  with the color red and  $u_2, u_5$  with the color blue. To form the six unbalanced hexagons of this layer, we must include the radial edges  $M_1$ . Note that as  $u_0$  and  $v_{0+3i}$  by definition have the same color, it is not possible to have an edge between these vertices. Thus, our initial edge possibilities are  $u_0v_{1+3i}$  or  $u_0v_{2+3i}$ .

Choosing  $v_{1+3i}$ , the radial edges are:  $M_1 = \{u_0v_1, u_1v_4, u_2v_7, u_3v_{10}, u_4v_{13}, u_5v_{16}\}$  (See Figure 4.14(b)). Since all vertices in  $C_6$  are extremes of a radial edge, this will imply that at least one radial edge has two colored vertices with the same color as extremes, causing a color conflict. Note that the argument is analogous if the choice of radial edges has vertex extremes  $v_{2+3i}$  at  $C_{18}$ , since the set of radial edges is  $M_1 = \{u_0v_2, u_1v_5, u_2v_8, u_3v_{11}, u_4v_{14}, u_5v_{17}\}$ . Thus, based on the algorithm described above, it is not possible to obtain a 4-total coloring for the subgraph induced by the vertices of cycles  $C_6$  and  $C_{18}$ . Since this subgraph is common to every nanodisc  $D_r$ ,  $r \geq 2$ , this strategy does not provide a 4-total coloring for any fullerene nanodisc.  $\square$

# Chapter 5

## Conclusion

In this dissertation, we studied the class of fullerene nanodiscs, divided into two lines of analysis: structural and coloring. The choice of this class was motivated by the fact that this class has no classification between Type 1 and Type 2 and by the following conjecture, presented in Chapter 4.

**Conjecture 6** (Brinkmann, Preissmann and Sasaki, 2015 [7]). *There is no Type 2 cubic graph with girth at least 5.*

In Chapter 1, we presented the following question:

**Question 1** (Sasaki, 2013 [30]). *Is there a Type 1 cubic graph such that  $\chi_e'' = 5$  with girth at least 5?*

In Chapter 3 we studied structural properties of fullerene nanodiscs, and we were able to contribute to combinatorial and quantitative results to this class that until then were unknown in the literature. We showed that  $D_2$  and  $D_3$  are unique and  $D_4$  has two non isomorphic representations. From these results, we have been able to develop and use techniques that will be useful in future work. In addition to the techniques developed, the structural analysis of the graph led to the appearance of new questions that we aim to answer in the next works. We will recall the questions proposed in this chapter.

**Question 2.** *The representation of pentagons in pairs given by the Theorem 37 is unique for all fullerene nanodiscs  $D_r$  with  $r \geq 3$ ?*

**Question 3.** *Is there a fullerene nanodisc  $D_r$  whose pentagonal representation is mixed for some  $r \geq 4$ ?*

We believe that Question 2 has a positive answer, as long as Question 3 has a negative answer. As a next step, we intend to investigate the construction of a

$D_r$  nanodisc from its dual  $D_r^*$ , defined in [22, 23] in order to extract properties of  $D_r^*$  that can be transported to their respective planar representation  $D_r$ . A brief exposition on this topic can be found in the Appendix A.

In the Chapter 4, we contributed with a positive evidence to the Conjecture 6 by presenting the first Type 1 fullerene nanodisc, whose 4-total coloring is equitable, which is also an indication that Question 1 has a negative answer. As one of the main results, we proved that the infinite family of fullerene nanodiscs satisfies the conformable property. Although all the techniques used to prove this result did not result in a 4-total coloring for the graph, we will follow this line of analysis, seeking to contribute to the Questions 1 and 6. The hunting continues.

The development of this research culminated in important submissions during the master's degree, such as:

- 2020: Participation in the poster session of the 9th Latin American Workshop on Cliques in Graphs (LAWCG 2020) (see Appendix B);
- 2021: An extended abstract published in the journal *Matemática Contemporânea* (see Appendix C);
- 2021: Participation in the poster session of the IV Workshop de Pesquisa em Computação dos Campos Gerais (WPCCG), promoted by UFTPR (see Appendix D);
- 2022: An extended abstract accepted for participation in the VII Encontro de Teoria da Computação (see Appendix E);
- 2022: An abstract accepted for participation in the next Latin American Workshop on Cliques in Graphs (LAWCG 2022) (see Appendix F).

# References

- [1] ALA'A, K., OTHERS, 1990, "Isolation, separation and characterisation of the fullerenes C 60 and C 70: the third form of carbon", *Journal of the Chemical Society, Chemical Communications*, , n. 20, pp. 1423–1425.
- [2] ANDOVA, V., ŠKREKOVSKI, R., 2013, "Diameter of fullerene graphs with full icosahedral symmetry", *MATCH Commun. Math. Comput. Chem*, v. 70, n. 1, pp. 205–220.
- [3] ANDOVA, V., DOŠLIC, T., KRNC, M., et al., 2012, "On the diameter and some related invariants of fullerene graphs", *Match-Communications in Mathematical and Computer Chemistry*, v. 68, n. 1, pp. 109.
- [4] BEHZAD, M., 1965, *Graphs and their chromatic numbers*. Michigan State University.
- [5] BONDY, J., MURTY, U., 2008, *Graduate Texts in Mathematics 244 - Graph Theory*. Springer.
- [6] BORODIN, O. V., KOSTOCHKA, A. V., WOODALL, D. R., 1998, "Total colourings of planar graphs with large girth", *European Journal of Combinatorics*, v. 19, n. 1, pp. 19–24.
- [7] BRINKMANN, G., PREISSMANN, M., SASAKI, D., 2015, "Snarks with total chromatic number 5", *Discrete Mathematics and Theoretical Computer Science*, v. 17, n. 1, pp. 369–382.
- [8] BROOKS, R. L., 1941, "On colouring the nodes of a network". In: *Mathematical Proceedings of the Cambridge Philosophical Society*, v. 37, pp. 194–197. Cambridge University Press.
- [9] CHARTRAND, G., ZHANG, P., 2008, *Chromatic graph theory*. CRC Press.
- [10] CHETWYND, A. G., HILTON, A., 1988, "Some refinements of the total chromatic number conjecture." *Congressus Numerantium*, v. 66, pp. 195–216.

- [11] DA CRUZ, M., DE FIGUEIREDO, C., SASAKI, D., et al., 2021, “Hunting a Type 2 fullerene nanodisc”, *Matemática Contemporânea*, v. 48, pp. 126–136.
- [12] DA CRUZ, M. M. F., SASAKI, D., COSTA, M. V. T., 2020, “Coloração Total de Nanodiscos de Fullerenos”, *Cadernos do IME-Série Matemática*, , n. 15, pp. 34–53.
- [13] DANTAS, S., DE FIGUEIREDO, C. M., MAZZUOCCOLO, G., et al., 2016, “On the total coloring of generalized Petersen graphs”, *Discrete mathematics*, v. 339, n. 5, pp. 1471–1475.
- [14] DOŠLIĆ, T., 2002, “On some structural properties of fullerene graphs”, *Journal of mathematical chemistry*, v. 31, n. 2, pp. 187–195.
- [15] DOŠLIĆ, T., 2020, “Nice pairs of odd cycles in fullerene graphs”, *Journal of Mathematical Chemistry*, v. 58, n. 10, pp. 2204–2222.
- [16] EULER, L., 1741, “Solutio problematis ad geometriam situs pertinentis”, *Commentarii academiae scientiarum Petropolitanae*, pp. 128–140.
- [17] FENG, Y., LIN, W., 2013, “A concise proof for total coloring subcubic graphs”, *Information Processing Letters*, v. 113, n. 18, pp. 664–665.
- [18] KOSTOCHKA, A. V., 1996, “The total chromatic number of any multigraph with maximum degree five is at most seven”, *Discrete Mathematics*, v. 162, n. 1-3, pp. 199–214.
- [19] KROTO, H. W., HEATH, J. R., O’BRIEN, S. C., et al., 1985, “C<sub>60</sub>: Buckminsterfullerene”, *Nature*, v. 318, n. 6042, pp. 162.
- [20] KUBALE, M., 2004, *Graph colorings*, v. 352. American Mathematical Soc.
- [21] LEIDNER, M., 2014, “A larger family of planar graphs that satisfy the total coloring conjecture”, *Graphs and Combinatorics*, v. 30, n. 2, pp. 377–388.
- [22] NICODEMOS, D., 2017, *Diâmetro de Grafos Fullerenes e Transversalidade de Ciclos Ímpares de Fuleróides-(3, 4, 5, 6)*. Tese de Doutorado, Universidade Federal do Rio de Janeiro/COPPE.
- [23] NICODEMOS, D., STEHLÍK, M., 2017, “Fullerene graphs of small diameter”, *MATCH Communications in Mathematical and in Computer Chemistry*.
- [24] NIGRO, M., FARIA, L., SASAKI, D., 2022, “A conformabilidade dos grafos subcúbicos conexos”, *VII Encontro de Teoria da Computação*.

- [25] PETERSEN, J., 1891, “Die Theorie der regulären graphs”, *Acta Mathematica*, v. 15, n. 1, pp. 193–220.
- [26] ROBERTSON, N., SANDERS, D., SEYMOUR, P., et al., 1996, “A new proof of the four-colour theorem”, *Electronic Research Announcements of the American Mathematical Society*, v. 2, n. 1, pp. 17–25.
- [27] ROCHA-FILHO, R. C., 1996, “Os fulerenos e sua espantosa geometria molecular”, *Química Nova na Escola*, v. 4, pp. 7–11.
- [28] SÁNCHEZ-ARROYO, A., 1989, “Determining the total colouring number is NP-hard”, *Discrete Mathematics*, v. 78, n. 3, pp. 315–319.
- [29] SANTOS, L. J. D., ROCHA, G. P., ALVES, R. B., et al., 2010, “Fulereo [C60]: química e aplicações”, *Química Nova*, v. 33, n. 3, pp. 680–693.
- [30] SASAKI, D., 2013, *Sobre Coloração Total de Grafos Cúbicos*. Tese de Doutorado, Universidade Federal do Rio de Janeiro/COPPE.
- [31] SASAKI, D., DANTAS, S., DE FIGUEIREDO, C. M., et al., 2014, “The hunting of a snark with total chromatic number 5”, *Discrete Applied Mathematics*, v. 164, pp. 470–481.
- [32] TAIT, P. G., 1880, “Remarks on the colouring of maps”. In: *Proc. Roy. Soc. Edinburgh*, v. 10, pp. 501–503.
- [33] VIZING, V. G., 1964, “On an estimate of the chromatic class of a p-graph”, *Discret Analiz*, v. 3, pp. 25–30.
- [34] WANG, W.-F., 2002, “Equitable total coloring of graphs with maximum degree 3”, *Graphs and combinatorics*, v. 18, n. 3, pp. 677–685.
- [35] WEST, D., 1996, *Introduction to graph theory*, v. 2. Prentice hall Upper Saddle River, NJ.
- [36] YAP, H. P., 1996, *Total colourings of graphs*. Springer.
- [37] ZHANG, H., ZHANG, F., 2001, “New lower bound on the number of perfect matchings in fullerene graphs”, *Journal of mathematical chemistry*, v. 30, n. 3, pp. 343–347.
- [38] ZHANG, Y., ZHANG, H., 2021, “Nice pairs of disjoint pentagons in fullerene graphs”, *Journal of Mathematical Chemistry*, v. 59, n. 5, pp. 1316–1331.

# Appendix A

## Fullerene Nanodisc: The definition through its dual

**Definition 36** (Triangulation). *A simple connected planar graph  $G$  in which all its faces have degree three is called **planar triangulation** or simply triangulation. If  $G$  is finite, we say it's a finite triangulation. If  $G$  is infinite and its faces are triangles, then we say it's a infinite triangulation.*

The following result relates planar triangulations and cubic graphs.

**Proposition 56** ([5]). *A simple planar connected graph  $G$  is a triangulation if and only if its dual is a cubic graph.*

We can define a nanodisc through its dual. Let  $T$  be a 6-regular infinite planar triangulation. Let  $N \in V(T)$ , a integer  $r \geq 2$  and  $T_r(N)$  be the subgraph of triangulation  $T$  induced by all vertices at a distance less than or equal to  $r$  of  $N$ . Let  $C$  be the border of  $T_r(N)$ . Note that  $|C| = 6r$  and thus  $C = (u_1, u_2, \dots, u_{6r})$ . Note that  $C$  has six vertices of degree 3 in  $T_r(N)$ . In general, the vertices of degree 3 are given by  $u_{1+pr}$ , with  $0 \leq p \leq 5$ . The other vertices of the outer cycle  $C$  have degree 4 in  $T_r(N)$ . The Figure A.1<sup>1</sup> illustrates two subgraphs with different border sizes, where the vertices that have degree three are highlighted in blue.

---

<sup>1</sup>Figure from [22].

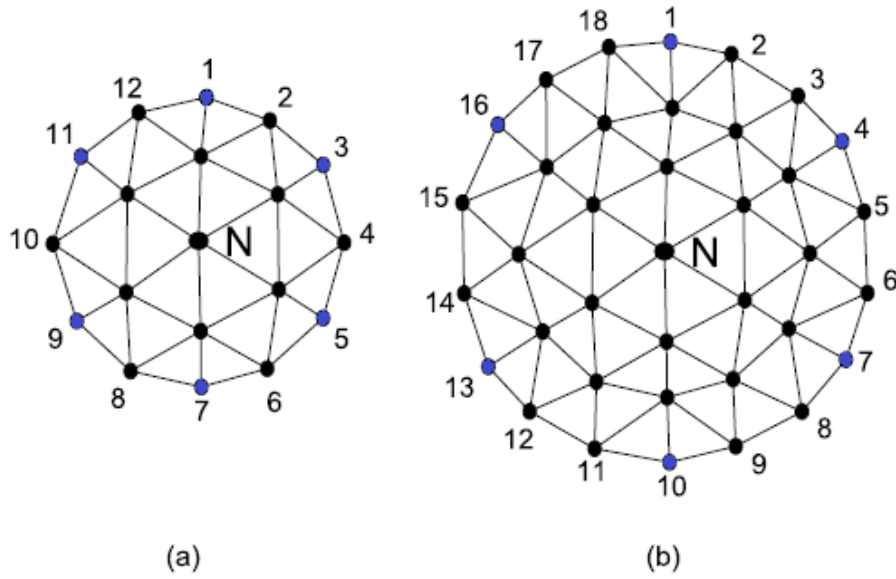


Figure A.1: (a) the subgraph  $T_2(N)$ , where its border consists of 12 vertices, where the vertices of degree 3 are:  $u_1, u_3, u_5, u_7, u_9$  and  $u_{11}$ ; (b), the subgraph  $T_3(N)$ , where its border consists of 18 vertices, where the vertices of degree 3 are:  $u_1, u_4, u_7, u_{10}, u_{13}$  and  $u_{16}$ .

Let  $t$  be a integer such that  $1 \leq t \leq r - 1$ . Consider two copies of the previously determined graph  $T_r(N)$ , so that one copy is centered on vertex  $N$  and the other on a distinct vertex  $S$  of  $N$ , and suppose that  $u_1, u_2, \dots, u_{6r}$  is the border of  $T_r(N)$  and  $v_1, v_2, \dots, v_{6r}$  is the border of  $T_r(S)$ . The dual graph of a nanodisc, represented by  $D_{r,t}^*$ , is obtained from the disjoint union of  $T_r(N)$  and  $T_r(S)$  by identifying the vertices  $u_i$  and  $v_{i+t}$ , for all  $1 \leq i \leq 6r$ , i.e., the indices are taken module  $6r$ . Figure A.2<sup>2</sup> displays the two subgraphs  $T_3(N)$  and  $T_3(S)$  that will generate the  $D_{3,1}^*$  graph.

---

<sup>2</sup>Figure from [22].

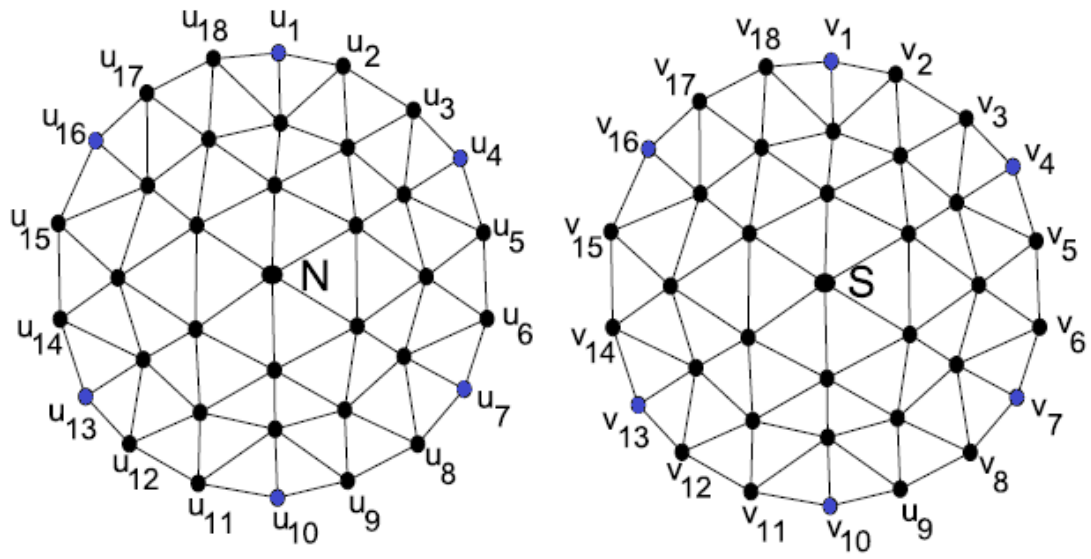


Figure A.2: On the left, the  $T_3(N)$  subgraph. On the right, the  $T_3(S)$  subgraph.

Note that  $r = 3$  and  $t = 1$ . Therefore, the subgraphs will be united so that the vertices  $u_i$  correspond to the vertices  $v_{i+1}$ . For example, the vertex  $u_{18}$  should be superimposed on the vertex  $v_{19}$ , which is equivalent to pasting  $u_{18}$  on the vertex  $v_1$ , since  $19 \cong 1(\text{mod}18)$ . Note that the integer  $t$  controls rotations for vertex identification.

Thus,  $D_{r,t}^*$  is a planar triangulation with all vertices of degree 5 or 6 and its dual is a fullerene nanodisc  $D_{r,t}$ , as illustrated in Figure A.3 an example for  $r = 3$  and  $t = 1$ .

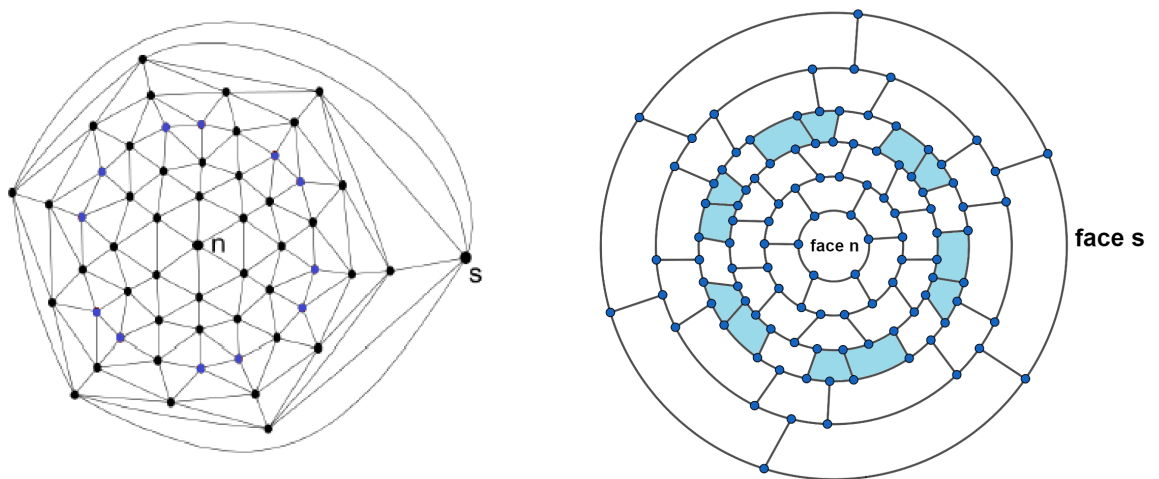


Figure A.3: On the left, the planar triangulation  $D_{3,1}^*$ . On the right, its corresponding fullerene nanodisc  $D_{3,1}$ .

The dual of a nanodisc already brings us an important quantitative result, as we had already proved in Theorem 32.

**Theorem 57.** *The fullerene nanodisc  $D_2$  has only one non isomorphic representation.*

*Proof.* It occurs from the fact that  $t = 1$  for  $r = 2$ . Thus, for two subgraphs  $T_2(N)$  and  $T_2(S)$ , there is only one way to unite the two subgraphs to form the triangulation  $D_{2,1}^*$  and consequently a unique plane representation of  $D_2$ : the nanodisc  $D_{2,1}$ . See Figure 3.1.  $\square$

**Observation 58.** *Note that in the identification of vertices  $u_i$  of the subgraph  $T_r(N)$  with vertices  $v_{i+t}$  of the subgraph  $T_r(S)$ , where  $1 \leq t \leq r - 1$  the superimposition of vertices of degree 3 with vertices of degree 4, when their edges are collapsed, will form 5-vertices, that in the planned representation represent the pentagons of the central layer, and the superposition of two vertices with degree 4, when we collapse the edges, will form 6-vertices, that in the planned representation define the hexagons arranged between the pentagons in the central layer of a nanodisc. We highlight in blue the vertex collages that are responsible for forming 5-vertices in  $D_{r,t}^*$ .*

We can also analyze the rotations generated by the  $t$  parameter to  $r = 3$ , in order to quantify the non isomorphic representations, as proved in the Theorem 36.

**Theorem 59.** *The fullerene nanodisc  $D_3$  has only one non isomorphic representation.*

*Proof.* Please refer to Figure A.2, where we have the two copies  $T_3(N)$  and  $T_3(S)$ , with their respective vertices of degree 3 highlighted in blue. As  $1 \leq t \leq r - 1$ , for  $r = 3$  we have  $t = 1, 2$ . For  $t = 1$ , the identification of the vertices  $u_i \in T_3(N)$  with the vertices  $v_i \in T_3(S)$ ,  $1 \leq i \leq 18$  is made by pasting the vertex  $u_i$  with the vertex  $v_{i+1}$ . Thus, for  $t = 1$ , we have the following vertex identifications:

$$u_1v_2, u_2v_3, u_3v_4, u_4v_5, u_5v_6, u_6v_7, u_7v_8, u_8v_9, u_9v_{10}, u_{10}v_{11}, u_{11}v_{12}, u_{12}v_{13}, u_{13}v_{14}, \\ u_{14}v_{15}, u_{15}v_{16}, u_{16}v_{17}, u_{17}v_{18}, u_{18}v_{19} = u_{18}v_1.$$

For  $t = 1$  we have in  $D_{3,1}^*$  vertices of degree 5 arranged in pairs (the vertices of degree 5 generated by the identification of vertices  $u_1v_2$  and  $u_{18}v_1$  are arranged side by side) with a vertex of degree 6 between each pair. This generates in the central layer of the dual  $D_{3,1}$  pentagons arranged in pairs, with a hexagon between each pair.

For  $t = 2$ , the vertex identification  $u_i \in T_3(N)$  with the vertices  $v_i \in T_3(S)$ ,  $1 \leq i \leq 18$  is done by pasting the vertex  $u_i$  with the vertex  $v_{i+2}$ . Thus, for  $t = 2$ , we have the following vertex identifications:

$$u_1v_3, u_2v_4, u_3v_5, u_4v_6, u_5v_7, u_6v_8, u_7v_9, u_8v_{10}, u_9v_{11}, u_{10}v_{12}, u_{11}v_{13}, u_{12}v_{14}, u_{13}v_{15}, \\ u_{14}v_{16}, u_{15}v_{17}, u_{16}v_{18}, u_{17}v_{19} = u_{17}v_1, u_{18}v_{20} = u_{18}v_2.$$

Note that for  $t = 2$  the vertices of degree 5 are arranged in pairs, containing a vertex of degree 6 between each pair, as well as  $t = 1$ , less than one rotation. This means that both rotations generate the same graph. Thus,  $D_{3,1}^* \cong D_{3,2}^*$ . See Figure 3.1.  $\square$

For nanodiscs with a small radius, it is possible to analyze the rotations given by the  $t$  parameter and thus obtain the amount of non-isomorphic representations of each nanodisc. We will follow the investigation to  $r = 4$ , and as shown in the Theorem 44, we confirm the number of non-isomorphic representations for  $r = 4$ .

**Theorem 60.** *The fullerene nanodisc  $D_4$  has two non isomorphic representations.*

*Proof.* Let  $T_4(N)$  e  $T_4(S)$  be the two subgraphs of the  $T$  triangulation induced by all vertices at a distance less than or equal to 4 of  $N$  and  $S$ , respectively. Note that the boundary of both is composed of 24 vertices, as  $|C| = 6r = 24$ . The vertices of degree 3 in  $T_4(N)$  and  $T_4(S)$  are given for  $u_{1+pr}$  and  $v_{1+pr}$ , respectively, with  $1 \leq p \leq 5$ . Thus, the vertices of degree 3 are:  $u_1, u_5, u_9, u_{13}, u_{17}, u_{21}$ , in  $T_4(N)$ , and  $v_1, v_5, v_9, v_{13}, v_{17}, v_{21}$  in  $T_4(S)$ .

Uma vez que  $1 \leq t \leq r - 1$ , para  $r = 4$  temos  $t = 1, 2, 3$ . Para  $t = 1$ , a identificação dos vértices  $u_i \in T_4(N)$  com os vértices  $v_i \in T_4(S)$ ,  $1 \leq i \leq 24$  é feita colando o vértice  $u_i$  com o vértice  $v_{i+1}$ . So we have:

Since  $1 \leq t \leq r - 1$ , for  $r = 4$  we have  $t = 1, 2, 3$ . For  $t = 1$ , the vertex identification  $u_i$  in  $T_4(N)$  with the vertices  $v_i \in T_4(S)$ ,  $1 \leq i \leq 24$  is done by pasting the vertex  $u_i$  with the vertex  $v_{i+1}$ . So we have:

$$u_1v_2, u_2v_3, u_3v_4, u_4v_5, u_5v_6, u_6v_7, u_7v_8, u_8v_9, u_9v_{10}, u_{10}v_{11}, u_{11}v_{12}, u_{12}v_{13}, u_{13}v_{14}, \\ u_{14}v_{15}, u_{15}v_{16}, u_{16}v_{17}, u_{17}v_{18}, u_{18}v_{19}, u_{19}v_{20}, u_{20}v_{21}, u_{21}v_{22}, u_{22}v_{23}, u_{23}v_{24}, u_{24}v_{25} = \\ u_{24}v_1.$$

Note that for  $t = 1$ , the vertices of degree 5 will be arranged in pairs in  $D_{4,1}^*$ , with a pair of vertices of degree 6 between each pair. This generates in the central layer of the dual  $D_{4,1}$  the pentagons arranged in pairs, and a pair of hexagons between each pair of pentagons.

For  $t = 2$ , the vertex identification  $u_i \in T_4(N)$  with the vertices  $v_i \in T_4(S)$ ,  $1 \leq i \leq 24$  is done by pasting the vertex  $u_i$  with the vertex  $v_{i+2}$ . So we have:

$$u_1v_3, u_2v_4, u_3v_5, u_4v_6, u_5v_7, u_6v_8, u_7v_9, u_8v_{10}, u_9v_{11}, u_{10}v_{12}, u_{11}v_{13}, u_{12}v_{14}, u_{13}v_{15}, \\ u_{14}v_{16}, u_{15}v_{17}, u_{16}v_{18}, u_{17}v_{19}, u_{18}v_{20}, u_{19}v_{21}, u_{20}v_{22}, u_{21}v_{23}, u_{22}v_{24}, u_{23}v_{25} = u_{23}v_1, \\ u_{24}v_{26} = u_{24}v_2.$$

Note that for  $t = 2$ , the rotation disposes in  $D_{4,2}^*$  vertices of degree 5 and 6 appearing alternately. This generates in the central layer of the dual  $D_{4,2}$  the isolated pentagons, with a hexagon between each pair.

For  $t = 3$ , the vertex identification  $u_i \in T_4(N)$  with the vertices  $v_i \in T_4(S)$ ,  $1 \leq i \leq 24$  is done by pasting the vertex  $u_i$  with the vertex  $v_{i+3}$ . So we have:

$$\begin{aligned} &u_1v_4, u_2v_5, u_3v_6, u_4v_7, u_5v_8, u_6v_9, u_7v_{10}, u_8v_{11}, u_9v_{12}, u_{10}v_{13}, u_{11}v_{14}, u_{12}v_{15}, u_{13}v_{16}, \\ &u_{14}v_{17}, u_{15}v_{18}, u_{16}v_{19}, u_{17}v_{20}, u_{18}v_{21}, u_{19}v_{22}, u_{20}v_{23}, u_{21}v_{24}, u_{22}v_{25} = u_{22}v_1, \\ &u_{23}v_{26} = u_{23}v_2, u_{24}v_{27} = u_{24}v_3. \end{aligned}$$

Note that for  $t = 3$ , the vertices of degree 5 will be arranged in pairs in  $D_{4,3}^*$ , with a pair of vertices of degree 6 between each pair. This generates in the central layer of the dual  $D_{4,3}$  the pentagons arranged in pairs, and a pair of hexagons between each pair of pentagons. Note that the rotations obtained for  $t = 1$  and  $t = 3$  generate the same graph less than one rotation. Thus,  $D_{4,1}^* \cong D_{4,3}^*$ . Thus, we have two distinct representations for  $r = 4$ , illustrated in Figure A.4.  $\square$

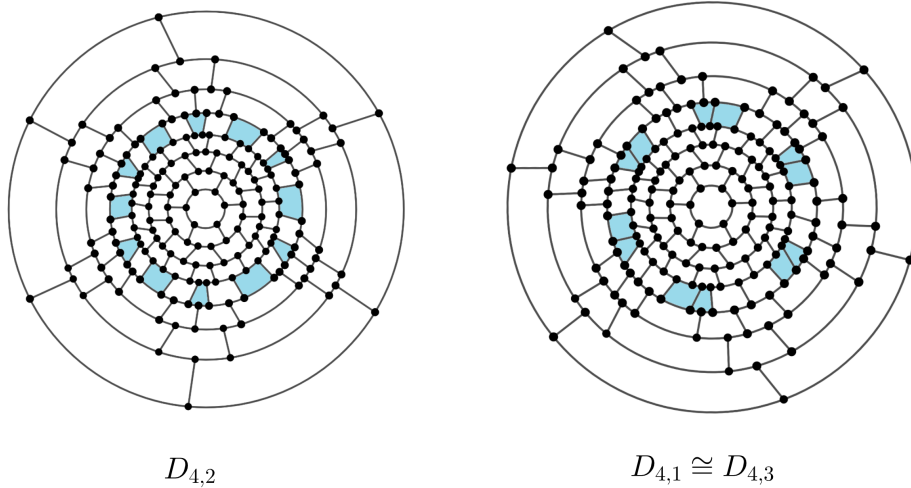


Figure A.4: Two possible representations of fullerene nanodisc  $D_4$ .

In Chapter 3 by Theorems 32, 36 and 44 we obtained quantitative results for  $D_2$ ,  $D_3$  and  $D_4$ , as well as investigating the behavior of hexagonal and pentagonal faces.

We will use the dual of a planned nanodisc  $D_{r,t}^*$  as a new tool to find a more accurate result to find the number of non-isomorphic representations of each nanodisc  $D_{r,t}$ . We will conduct an initial investigation using the dual representation of a planned nanodisc to analyze the behavior of the central layer of the fullerene nanodiscs with  $r = 5$ .

**Theorem 61.** *The fullerene nanodisc  $D_5$  has two non isomorphic representations.*

*Proof.* Let  $T_5(N)$  e  $T_5(S)$  be the two subgraphs of the  $T$  triangulation induced by all vertices at a distance less than or equal to 5 of  $N$  and  $S$ , respectively. Note that the boundary of both is composed of 30 vertices, as  $|C| = 6r = 30$ . The vertices of degree 3 in  $T_5(N)$  and  $T_5(S)$  are given for  $u_{1+pr}$  and  $v_{1+pr}$ , respectively, with  $1 \leq p \leq 5$ . Thus, the vertices of degree 3 are:  $u_1, u_6, u_{11}, u_{16}, u_{21}, u_{26}$ , in  $T_5(N)$ , and  $v_1, v_6, v_{11}, v_{16}, v_{21}, v_{26}$  in  $T_5(S)$ .

For  $t = 1$ , the vertex identification  $u_i \in T_5(N)$  with the vertices  $v_i \in T_5(S)$ ,  $1 \leq i \leq 30$  is done by pasting the vertex  $u_i$  with the vertex  $v_{i+1}$ . So we have:

$$\begin{aligned} &u_1v_2, u_2v_3, u_3v_4, u_4v_5, u_5v_6, u_6v_7, u_7v_8, u_8v_9, u_9v_{10}, u_{10}v_{11}, u_{11}v_{12}, u_{12}v_{13}, u_{13}v_{14}, \\ &u_{14}v_{15}, u_{15}v_{16}, u_{16}v_{17}, u_{17}v_{18}, u_{18}v_{19}, u_{19}v_{20}, u_{20}v_{21}, u_{21}v_{22}, u_{22}v_{23}, u_{23}v_{24}, u_{24}v_{25}, \\ &u_{25}v_{26}, u_{26}v_{27}, u_{27}v_{28}, u_{28}v_{29}, u_{29}v_{30}, u_{30}v_{31} = u_{30}v_1. \end{aligned}$$

Note that for  $t = 1$ , the vertices of degree 5 will be arranged in pairs in  $D_{5,1}^*$ , with three vertices of degree 6 between each pair. This generates in the central layer of the dual  $D_{5,1}$  the pentagons arranged in pairs, and three balanced hexagons between each pair of pentagons.

For  $t = 2$ , the vertex identification  $u_i \in T_5(N)$  with the vertices  $v_i \in T_5(S)$ ,  $1 \leq i \leq 30$  is done by pasting the vertex  $u_i$  with the vertex  $v_{i+2}$ . So we have:

$$\begin{aligned} &u_1v_3, u_2v_4, u_3v_5, u_4v_6, u_5v_7, u_6v_8, u_7v_9, u_8v_{10}, u_9v_{11}, u_{10}v_{12}, u_{11}v_{13}, u_{12}v_{14}, u_{13}v_{15}, \\ &u_{14}v_{16}, u_{15}v_{17}, u_{16}v_{18}, u_{17}v_{19}, u_{18}v_{20}, u_{19}v_{21}, u_{20}v_{22}, u_{21}v_{23}, u_{22}v_{24}, u_{23}v_{25}, u_{24}v_{26}, \\ &u_{25}v_{27}, u_{26}v_{28}, u_{27}v_{29}, u_{28}v_{30}, u_{29}v_{31} = u_{29}v_1, u_{30}v_{32} = u_{30}v_2. \end{aligned}$$

Note that for  $t = 2$  the vertices of degree 5 are isolated in  $D_{5,2}^*$ , and the vertices of degree 6 appear differently between each pentagon. Note that the vertices of degree 6 appear isolated and in pairs between each pentagon. This generates in the central layer of the nanodisc  $D_{5,2}$  isolated pentagons, where the hexagons appear sequentially isolated and in pairs between each pentagon.

For  $t = 3$ , the vertex identification  $u_i \in T_5(N)$  with the vertices  $v_i \in T_5(S)$ ,  $1 \leq i \leq 30$  is done by pasting the vertex  $u_i$  with the vertex  $v_{i+3}$ . So we have:

$$\begin{aligned} &u_1v_4, u_2v_5, u_3v_6, u_4v_7, u_5v_8, u_6v_9, u_7v_{10}, u_8v_{11}, u_9v_{12}, u_{10}v_{13}, u_{11}v_{14}, u_{12}v_{15}, u_{13}v_{16}, \\ &u_{14}v_{17}, u_{15}v_{18}, u_{16}v_{19}, u_{17}v_{20}, u_{18}v_{21}, u_{19}v_{22}, u_{20}v_{23}, u_{21}v_{24}, u_{22}v_{25}, u_{23}v_{26}, u_{24}v_{27}, \\ &u_{25}v_{28}, u_{26}v_{29}, u_{27}v_{30}, u_{28}v_{31} = u_{28}v_1, u_{29}v_{32} = u_{29}v_2, u_{30}v_{33} = u_{30}v_3. \end{aligned}$$

Note that for  $t = 3$  the vertices of degree 5 are isolated in  $D_{5,3}^*$ , and the vertices of degree 6 appear differently between each pentagon. Note that the vertices of degree 6 appear isolated and in pairs between each pentagon. This generates in the central layer of the nanodisc  $D_{5,3}$  isolated pentagons, where the hexagons appear sequentially isolated and in pairs between each pentagon. Note that the rotations

obtained for  $t = 2$  and  $t = 3$  generate the same graph less than one rotation. Thus,  $D_{5,2}^* \cong D_{5,3}^*$ .

For  $t = 4$ , the vertex identification  $u_i \in T_5(N)$  with the vertices  $v_i \in T_5(S)$ ,  $1 \leq i \leq 30$  is done by pasting the vertex  $u_i$  with the vertex  $v_{i+4}$ . So we have:

$$\begin{aligned} &u_1v_5, u_2v_6, u_3v_7, u_4v_8, u_5v_9, u_6v_{10}, u_7v_{11}, u_8v_{12}, u_9v_{13}, u_{10}v_{14}, u_{11}v_{15}, u_{12}v_{16}, u_{13}v_{17}, \\ &u_{14}v_{18}, u_{15}v_{19}, u_{16}v_{20}, u_{17}v_{21}, u_{18}v_{22}, u_{19}v_{23}, u_{20}v_{24}, u_{21}v_{25}, u_{22}v_{26}, u_{23}v_{27}, u_{24}v_{28}, \\ &u_{25}v_{29}, u_{26}v_{30}, u_{27}v_{31} = u_{27}v_1, u_{28}v_{32} = u_{28}v_2, u_{29}v_{33} = u_{29}v_3, u_{30}v_{34} = u_{30}v_4. \end{aligned}$$

Note that for  $t = 4$ , the vertices of degree 5 will be arranged in pairs in  $D_{5,4}^*$ , with three vertices of degree 6 between each pair. This generates in the central layer of the dual  $D_{5,4}$  the pentagons arranged in pairs, and a pair of hexagons between each pair of pentagons. Note that the rotations obtained for  $t = 1$  and  $t = 4$  generate the same graph less than one rotation. Thus,  $D_{5,1}^* \cong D_{5,4}^*$ . Thus, we have two distinct representations for  $r = 5$ , illustrated in Figure A.5.  $\square$

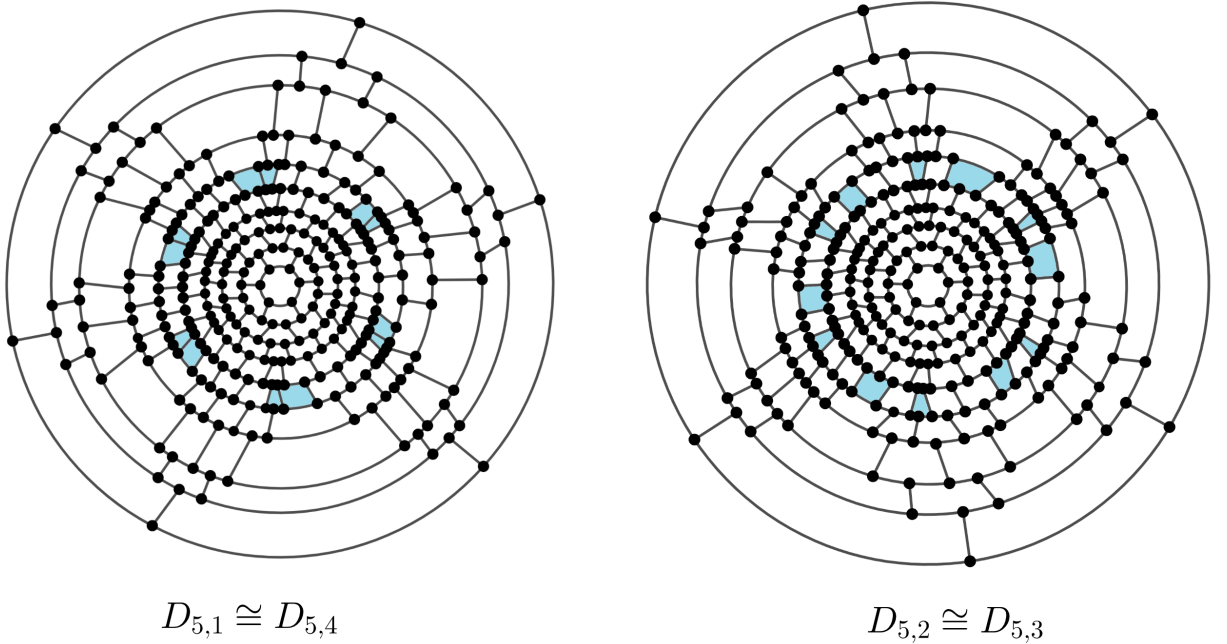


Figure A.5: Two possible representations of fullerene nanodisc  $D_5$ .

So we can define a new subfamily of fullerene nanodiscs: the hybrid nanodiscs.

**Definition 37.** A fullerene nanodisc  $D_r$ ,  $r \geq 5$  is said to be hybrid in hexagons, or simply hybrid, when its central layer admits mixed hexagons between the pentagons. See Figure A.5 the nanodisc  $D_{5,3}$ , an example of a hybrid nanodisc.

From this construction it is possible to conjecture a collection of properties and questions on the dual representations  $D_{r,t}^*$ .

**Conjecture 7.** *Let  $D_{r,t}^*$  be the dual of the fullerene nanodisc  $D_{r,t}$ . If  $r$  is even, then there are  $\frac{r}{2}$  dual isomorphic graphs two by two between them, otherwise there are  $\frac{r-1}{2}$  dual isomorphic graphs two by two between them. That is,  $D_{r,i}^* \cong D_{r,r-i}^*$ , in which  $1 \leq i \leq r-1$ .*

**Question 4.** *Does every nanodisc  $D_r$ ,  $r \geq 5$  have a hybrid representation?*

## Appendix B

Attachment: Poster “A result on total coloring of fullerene nanodiscs” presented at LAWCG 2020

# A RESULT ON TOTAL COLORING OF FULLERENE NANODISCS

Mariana Martins Ferreira da Cruz - COPPE/UFRJ - E-MAIL: mm.marr@hotmail.com

Diana Sasaki Nobrega - IME/UERJ - E-MAIL: diana.sasaki@ime.uerj.br

Marcus Vinicius Tovar Costa - IME/UERJ - E-MAIL: marcus.tovar@ime.uerj.br

9th Latin American Workshop on Cliques in Graphs

## 1. Introduction

A graph is a mathematical model used to represent relationships between objects. The general characters that both of these objects and their relationships can assume, allowed the construction of the so-called Graph Theory, which has been applied to model problems in several areas, such as Mathematics, Physics, Computer Science, Engineering, Chemistry, Psychology and industry. Many parameters associated with these graphs have been discussed to describe the stability of fullerene molecules.

Fullerene graphs are mathematical models for carbon-based molecules experimentally discovered in the early 1980s by Kroto, Heath, O'Brien, Curl and Smalley. Fullerenes are mathematical models for carbon-based molecules experimentally discovered in the early 1980s by Kroto, Heath, O'Brien, Curl and Smalley. Many parameters associated with these graphs have been discussed to describe the stability of fullerene molecules.

By definition, fullerene graphs are cubic, planar, 3-connected with pentagonal and hexagonal faces. The motivation of the present study is to find an efficient method to obtain a 4-total coloring of a particular class of fullerene graphs named fullerene nanodiscs, if it exists.

## 2. Basic Concepts of Graph Theory

This section is based on the reference Bondy and Murty, 2008.

**Definition 1.** A graph  $G = (V(G), E(G))$  is an ordered pair, where  $V(G)$  is a nonempty finite set of vertices and  $E(G)$  is a set of edges disjoint from  $V(G)$ , formed by unordered pairs of distinct elements from  $V(G)$ , that is, for every edge  $e \in E(G)$  there is  $u, v \in V(G)$  such that  $e = \{u, v\}$ , or simply  $e = uv$ .

If  $uv \in E$ , we say that  $u$  and  $v$  are adjacent or that  $u$  is a neighbor of  $v$ , and that the edge  $e$  is incident to  $u$  and  $v$ , and  $u$  and  $v$  are said to be extremities (or ends) of  $e$ . Two edges that have the same end are called adjacent.

The degree of a vertex  $v$  in  $G$ , represented by  $d(v)$ , is the number of edges incident to  $v$ . We denote by  $\delta(G)$  and  $\Delta(G)$  the minimum and maximum degrees respectively, of the vertices of the graph  $G$ .

A graph  $G$  is said **connected** when there is a path between each pair of vertices of  $G$ . Otherwise, the graph is called **disconnected**.

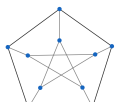


Figure 1: Cubic Graph.

A graph  $G$  is **planar** if there is a representation of  $G$  in the plane so that the edges meet only at the vertices, that is, the edges do not cross. Such a representation of  $G$  is said to be **embeddable** or **planar**. A planar representation divides the plane into regions called **faces**. There is always a single face called **external** or **infinite**, which is not limited (has infinite area). The outer boundary or cycle of a connected planar graph face is a closed walk that limits and determines the face.

Two faces are adjacent if they have a common edge between their boundaries. We denote the boundary of  $f$  by  $\partial(f)$ . If  $f$  is any face, the degree of  $f$ , denoted by  $d(f)$ , is the number of edges contained in the closed walk that defines it. In a planar connected graph with  $f$  faces,  $n$  vertices and  $m$  edges, we have that  $n + f - m = 2$ , which is known as Euler's formula.

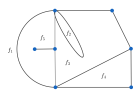


Figure 2: Planar Graph.

## 2.1 Total Coloring

In graph theory, coloring is a color assignment to the graph elements, subject to certain restrictions. The coloring study started with the Four Color Conjecture, which deals with determining the minimum number of colors needed to color a map of real or imaginary countries, so that countries with common borders have different colors. This conjecture was proposed by Francis Guthrie in 1852. After 121 years, the Four Color Conjecture was demonstrated by Kenneth Appel and Wolfgang Haken with the help of a computer. The famous Four Color Theorem is a reference in the area of Graph Theory.

**Definition 2.** A total coloring  $C'$  of a graph  $G$  is a color assignment to the set  $E \cup V$  in a color set  $C = \{c_1, c_2, \dots, c_k\}$ ,  $k \in \mathbb{N}$ , such that distinct colors are assigned to:

- Every pair of vertices that are adjacent;
- All edges that are adjacent;
- Each vertex and its incident edges.

A  $k$ -total coloring of a graph  $G$  is a total coloring of  $G$  that uses a set of  $k$  colors, and a graph is  $k$ -total-colorable if there is a  $k$ -total coloring of  $G$ . We define as the **total chromatic number** of a graph  $G$  the smallest natural  $k$  for which  $G$  admits a  $k$ -total coloring, and is denoted by  $\chi'(G)$ .



Figure 3: Graph with  $i$ -total coloring.

Behzad and Vizing independently conjectured the same upper bound for the total chromatic number.

**Conjecture (Total Color Conjecture (TCC))**

For every simple graph  $G$ ,

$$\chi'(G) \leq \Delta(G) + 2.$$

The TCC is an open problem, but has been checked for several classes of graphs. Knowing that  $\chi'(G) \geq \Delta(G) + 1$ , and from the TCC, we have the following classification: If  $\chi'(G) = \Delta(G) + 1$ , the graph is **Type 1**; and if  $\chi'(G) = \Delta(G) + 2$ , the graph is **Type 2**.

For cubic graphs, the TCC has already been demonstrated, which indicates that these graphs have total chromatic number  $\chi'(G) = \Delta(G) + 1$  or  $\Delta(G) + 2$ . However, the problem of deciding which are Type 1 or Type 2 is difficult.

## 3. Fullerene Graphs

### 3.1 Fullerene: A small history

In 1985 a new carbon allotrope was reported in the scientific community:  $C_{60}$ . A group of scientists, led by Englishman Harold Walter Kroto and Americans Richard Errett Smalley and Robert Curl, trying to understand the mechanism for building long carbon chains observed in interstellar space, discovered a

highly symmetrical, stable molecule, composed of 60 carbon atoms different from all the other carbon allotropes.

The  $C_{60}$  has a structure similar to a soccer hollow ball (Figure 4), with 32 faces, being 20 hexagonal and 12 pentagonal. They decided to name the  $C_{60}$  *buckminsterfullerene*, in honor of American architect Richard Buckminster Fuller, famous for his geodesic dome constructions, which were composed of hexagonal and pentagonal faces.

At the end of the 1980s, other carbon allotrope molecules with similar spatial structure to the  $C_{60}$  were reported called fullerene molecules (Kroto et al., 1985).

The buckminsterfullerene was the first new allotrope form discovered in the 20th century and earned Kroto, Curl and Smalley the Nobel Prize in Chemistry in 1996. Nowadays fullerene molecules are widely studied by different branches of science, from medicine to mathematics. These molecules are supposed to contribute to transport chemotherapy, antibiotics or antioxidant agents and released in contact with deficient cells.

### 3.2 Fullerene Graphs

Each fullerene molecule can be described by a graph where the atoms and the bonds are represented by the vertices and edges of the graph, respectively. In addition, fullerene graphs preserve the geometric properties of fullerene molecules, i.e., fullerene graphs are planar and connected. Moreover, all vertices have exactly 3 incident edges and all faces are pentagonal or hexagonal (Nicolodemos, 2017).



Figure 4: Molecular structure of  $C_{60}$ .

### 3.3 Fullerene Nanodiscs

The fullerene nanodiscs, or nanodiscs of radius  $r \geq 2$  are structures composed of two identical flat covers connected by a strip along their borders. While in the nanodisc lids there are only hexagonal faces, in the connecting strip, 12 pentagonal faces are arranged side by side.

A nanodisc of radius  $r \geq 2$ , represented by  $D_r$ , can be obtained through its flattening. The idea is to arrange the faces in layers around the nearest previous layer starting from a hexagonal face (Nicolodemos, 2017).

The sequence

$$\{1, 6, 12, 18, \dots, 6(r-1), 6r, 6(r-1), \dots, 18, 12, 6, 1\}$$

provides the amount of faces on each layer of nanodisc planning  $D_r$ , while  $r \geq 2$ . In addition, this sequence states that a  $D_r$  nanodisc has  $(6r^2 + 2)$  faces,  $12r$  vertices and  $(2r + 1)$  layers. The 12 pentagonal faces will always be distributed in the same layer with other  $(6r - 12)$  hexagonal faces. This is the key property of fullerene nanodiscs.

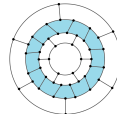


Figure 6: Nanodisc  $D_r$ .

## 4. Goals

To prove that a cubic graph is Type 1, it suffices to show a total coloring with 4 colors. However, to demonstrate that a cubic graph is Type 2, we need to show that it has no total coloring with only 4 colors. Thus, finding Type 2 cubic graphs is more complicated.

We define the girth of a graph  $G$  as the length of its shortest cycle. Until now, every Type 2 cubic graph we know has squares or triangles. So, we could think that there are no Type 2 cubic graphs with girth at least 5. Thus, we investigate the following question.

**Question (Sasaki, 2013)** Does there exist a Type 2 cubic graph with girth at least 5?

Motivated by this question, we analyze the family of fullerene nanodiscs, in search of evidences that can positively or negatively contribute to this question. In this context, we look for an efficient algorithm to find a  $i$ -total coloring of the fullerene nanodisc, if this coloring exists.

## 5. Results

After a few attempts using the brute force method, we were able to obtain a  $i$ -total coloring of the  $D_2$  nanodisc, with  $r = 2$ . Therefore,  $D_2$  is Type 1, which contributes to the evidences that the previously proposed question has a negative answer.

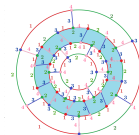


Figure 7: A  $i$ -total coloring of  $D_2$ .

## 6. Conclusion

We will continue the study of total coloring of nanodiscs, looking for an algorithm that gives a total coloring of the graphs of the infinite family of fullerene nanodiscs, also seeking to answer the question previously proposed.

## References

- [1] BONDY, J. A. and Murty, U. S. R., Graduate Texts in Mathematics 244 - Graph Theory, Springer, 2008.
- [2] KROTO, H. et al:  $C_{60}$ : Buckminsterfullerene Nature, 1985.
- [3] NICODEMOS, D. de S. Diâmetro de Grafos Fullerenos e Transversalidade de Círculos Impares de Fullerôides (3, 4, 5, 6). Rio de Janeiro: UFRJ/COPPE, 2017.
- [4] SASAKI, D. Sobre Cobrção Total de Grafos Cúbicos Rio de Janeiro: UFRJ/COPPE, 2013.

## Appendix C

Attachment: Manuscript “Hunting a  
Type 2 fullerene nanodisc”,  
Matemática Contemporânea volume  
48, 2021

# Hunting a Type 2 fullerene nanodisc

M. da Cruz, M. Tovar, C. Figueiredo and D. Sasaki

## Abstract

A total coloring assigns colors to the vertices and edges of a graph without conflicts. The Total Coloring Conjecture is settled for cubic graphs, but not to all regular graphs nor to arbitrary planar graphs. We investigate the total coloring of fullerene nanodiscs, a subclass of cubic planar graphs with girth 5 arising in Chemistry, motivated by a conjecture about the nonexistence of a Type 2 cubic graph of girth at least 5. We provide a combinatorial description and then a conformable coloring for small fullerene nanodiscs.

## 1 Introduction

A total coloring  $C^T$  of a graph  $G$  is a color assignment from set  $E \cup V$ , such that distinct colors are assigned to: every pair of vertices that are adjacent; all edges that are adjacent; and each vertex and its incident edges. Clearly, a total coloring of a graph  $G$  requires at least  $\Delta(G) + 1$  colors, where  $\Delta(G)$  is the maximum degree of  $G$ . A  $k$ -total coloring of a graph  $G$  is a total coloring that uses a set of  $k$  colors, and the graph is  $k$ -total colorable if it admits a  $k$ -total coloring. The total chromatic number of  $G$  is the smallest natural  $k$  for which  $G$  admits a  $k$ -total coloring, and it is denoted by  $\chi''(G)$ . Behzad and Vizing [2, 16] independently conjectured

---

*2000 AMS Subject Classification:* 05C10, 05C15, 92E10.

*Keywords and Phrases:* Graph Theory, Total Coloring, Fullerenes, Nanodiscs.

This research was supported by CAPES, CNPq and FAPERJ.

20 the Total Coloring Conjecture (TCC) that for any simple graph  $G$ , we have  
21  $\chi''(G) \leq \Delta(G) + 2$ . If  $\chi''(G) = \Delta(G) + 1$ , then the graph is Type 1; if  
22  $\chi''(G) = \Delta(G) + 2$ , then the graph is Type 2. The TCC is open for regular  
23 graphs, and has been verified for some particular classes of graphs. For  
24 cubic graphs that are graphs where every vertex has degree 3, the TCC has  
25 already been settled [8], but it is not yet settled for all planar graphs [10].  
26 Deciding whether a cubic bipartite graph is Type 1 is NP-complete [13].

27 We investigate the total coloring problem considering cubic planar graphs  
28 with large girth that model chemical structures: the fullerene nanodiscs.  
29 The length of the shortest cycle in a graph is called girth and has been  
30 considered for total coloring planar graphs [3]. Our goal is to study a con-  
31 jecture proposed by Brinkmann, Preissmann and Sasaki [4] which states  
32 that every Type 2 cubic graph has girth less than 5, and suggests that  
33 the girth of a graph is a relevant parameter in the study of total color-  
34 ing. The hunting of special Type 2 cubic graphs has been considered for  
35 nonplanar graphs as well [15]. We contribute by giving a combinatorial  
36 description of the small fullerene nanodiscs, and then by showing that they  
37 are conformable, a necessary step towards proving that they are Type 1.

## 38 2 Fullerene graphs

39 To motivate the choice of the studied graph class, we first give a histori-  
40 cal account of the discovery of the carbon molecule which can be modeled  
41 through a special cubic planar graph of girth 5, and then establish a com-  
42 binatorial description of our target class.

### 43 2.1 Fullerene: A graph class modeling a molecule

44 In attempt to understand the spectroscopy data obtained from astro-  
45 nomical objects as giant red carbon stars, which indicates the formation  
46 of long chains of carbon atoms, Harold Kroto and coworkers [9] performed  
47 a series of experiments vaporizing and cooling highly pure carbon samples  
48 discovering a new carbon allotrope highly symmetrical stable molecule,

49 composed of 60 tertiary carbon atoms. As the only way to maintain this  
 50 amount of carbon atoms stable, Richard Smalley proposed a spheroid  
 51 structure similar to a geodesic dome built by the Architect Buckminster  
 52 Fuller, with 32 faces, being 20 hexagonal and 12 pentagonal (see Figure 1)  
 53 later named by them as “ $C_{60}$  buckminsterfullerene”, or simply “buckyball”  
 54 since the molecule structure is shaped like a soccer ball. For this contri-  
 55 bution Harold Kroto, Robert Curl and Richard Smalley earned the 1996  
 56 Chemistry Nobel Prize. Fullerene molecules are widely studied by differ-  
 57 ent branches of science, from medicine to mathematics. These molecules  
 58 are supposed to contribute to transport chemotherapy, antibiotics or an-  
 59 tioxidant agents, and are released in contact with deficient cells [14]. At  
 60 the end of the 1980s, other carbon allotrope molecules with similar spatial  
 61 structure to the  $C_{60}$  were reported to be called fullerene molecules, defined  
 62 as polyhedral carbon cages in which  $sp^2$ -carbons are directly bonded to  
 63 three neighbors in an arrangement of five- and six-membered rings [1].

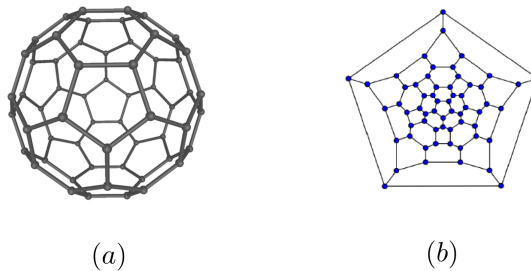


Figure 1: molecular structure (a) and fullerene graph (b) of  $C_{60}$ .

64 Each fullerene molecule can be described as a planar graph in which  
 65 the atoms and the bonds are represented by the vertices and edges of  
 66 the graph, respectively, preserving the geometric properties of the original  
 67 fullerene molecule. Thus, we define a fullerene graph as cubic, planar, 3-  
 68 connected graph whose faces are pentagonal or hexagonal (see Figure 1).  
 69 The famous Euler’s formula for connected planar graphs  $n + f - m = 2$   
 70 relates the number  $f$  of faces, the number  $m$  of edges and the number  $n$   
 71 of vertices, and implies that every fullerene graph must contain exactly  
 72 12 pentagons, and that the smallest fullerene graph is the well known

dodecahedron with 20 vertices where all faces are pentagons [11].

## 2.2 Fullerene nanodiscs

We shall consider a particular family of fullerene graphs. According to the 3-dimensional structure, the fullerene nanodiscs, or nanodiscs of radius  $r \geq 2$ , are structures composed of two identical flat covers connected by a strip along their borders. While in the nanodisc covers there are only hexagonal faces, in the connecting strip, besides the hexagonal faces, additional 12 pentagonal faces are arranged. Please refer to Figure 2 where the smallest fullerene nanodisc graphs are depicted. In each fullerene nanodisc graph, we highlight in the connecting strip the 12 pentagons.

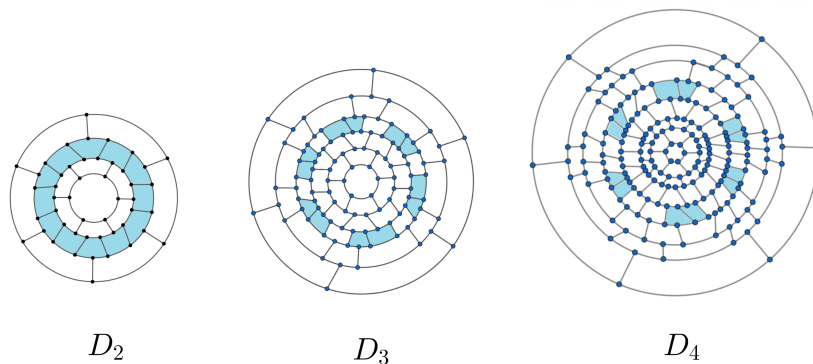


Figure 2: The smallest fullerene nanodisc graphs.

A nanodisc graph of radius  $r \geq 2$ , denoted by  $D_r$ , has its faces arranged into layers, one layer next the nearest previous layer starting from an hexagonal cover until we reach the other hexagonal cover [12]. The sequence  $\{1, 6, 12, \dots, 6(r-1), 6r, 6(r-1), \dots, 12, 6, 1\}$  provides the amount of faces on each layer of the nanodisc graph  $D_r$ . Note that there is an odd number of  $2r+1$  layers, and we call the layer with  $6r$  faces the central layer. For  $D_2$  the layer sequence is  $\{1, 6, 12, 6, 1\}$ , for  $D_3$  is  $\{1, 6, 12, 18, 12, 6, 1\}$  and for  $D_4$  is  $\{1, 6, 12, 18, 24, 18, 12, 6, 1\}$  (see Figure 2). The auxiliary cycle sequence provides the sizes of the auxiliary cycles that define the layers  $\{C_6, C_{18}, \dots, C_{12r-6}, C_{12r-6}, \dots, C_{18}, C_6\}$ . For example, for  $D_2$  the cycle sequence is  $\{C_6, C_{18}, C_{18}, C_6\}$ , for  $D_3$  is  $\{C_6, C_{18}, C_{30}, C_{30}, C_{18}, C_6\}$ , and

94 for  $D_4$  is  $\{C_6, C_{18}, C_{30}, C_{42}, C_{42}, C_{30}, C_{18}, C_6\}$  (see Figure 2). A nanodisc  
 95 graph  $D_r$  contains  $12r \times r$  vertices and  $18r \times r$  edges.

96 The 12 pentagonal faces are distributed in the central layer among its  
 97  $6r$  faces with the other  $(6r - 12)$  hexagonal faces. This is the key property  
 98 of fullerene nanodiscs [12]. Note that the central layer is defined by two  
 99 auxiliary cycles, each of size  $12r - 6$ . The 5 vertices of each pentagon  
 100 are partitioned such that 3 vertices appear consecutively in one cycle and  
 101 2 vertices appear consecutively in the other cycle. We say that two pen-  
 102 tagons in the central layer are partitioned in the same way if each pentagon  
 103 has 3 vertices in the same cycle  $C_{12r-6}$ . For  $r \geq 2$ , in a  $D_r$ , we may have  
 104 choice to distribute and to partition the 12 pentagonal faces. Our first  
 105 result imposes restrictions to the way the pentagons are partitioned in the  
 106 central layer of a nanodisc graph and ensures that there is a unique  $D_2$ .

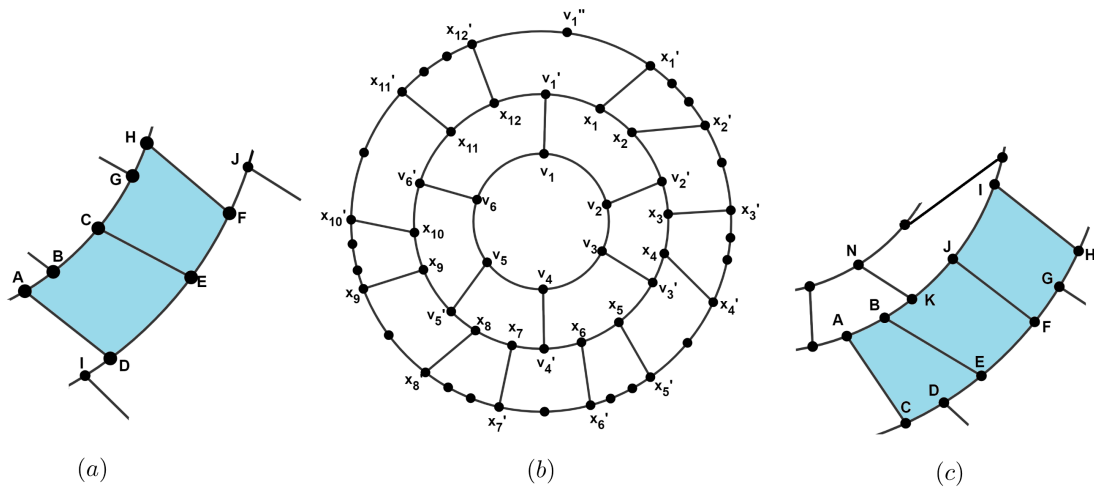


Figure 3: (a) Two consecutive pentagons partitioned in the same way;  
 (b) Labels of the vertices in three cycles of  $D_3$ ; (c) Three consecutive  
 pentagons in the central layer of  $D_3$ .

107 **Proposition 2.1.** *A nanodisc  $D_r$ ,  $r \geq 2$ , cannot have two consecutive*  
 108 *pentagons in the central layer partitioned in the same way.*

109 *Proof.* In Figure 3(a), we show two pentagons (namely  $ABCED$  and  
 110  $CGHFE$ ) partitioned in the same way and arranged side by side in the

111 central layer of  $D_r$ , so that vertices  $A, B, C, G$  and  $H$  belong to the same  
 112 auxiliary cycle and the other vertices  $D, E$  and  $F$  belong to the other.

113 Consider the layer adjacent to the central layer, where one of its defining  
 114 cycles contains vertices  $D, E, F$ . By considering vertices  $I$  and  $J$  adjacent  
 115 respectively to  $D$  and  $F$  in the cycle  $C_{12r-6}$ , we find a path containing  
 116 five consecutive vertices  $I, D, E, F, J$  in the In Figure 3(a), we show two  
 117 pentagons (namely  $ABCED$  and  $CGHFE$ ) partitioned in the same way  
 118 and arranged side by side in the central layer of  $D_r$ , so that vertices  
 119  $A, B, C, G$  and  $H$  belong to the same auxiliary cycle and the other vertices  
 120  $D, E$  and  $F$  belong to the other.

121 Consider the layer adjacent to the central layer, where one of its defining  
 122 cycles contains vertices  $D, E, F$ . By considering vertices  $I$  and  $J$  adjacent  
 123 respectively to  $D$  and  $F$  in the cycle  $C_{12r-6}$ , we find a path containing  
 124 five consecutive vertices  $I, D, E, F, J$  in the cycle, leading to a contra-  
 125 diction that  $I, D, E, F, J$  must lie in a forbidden face.cycle, leading to a  
 126 contradiction that  $I, D, E, F, J$  must lie in a forbidden face. ■

127 Observe that there are two ways of partitioning a hexagon in a layer de-  
 128 fined by auxiliary cycles  $C$  and  $C'$ . We may place 3 vertices of the hexagon  
 129 in each auxiliary cycle, or place 4 vertices of the hexagon in one auxiliary  
 130 cycle say  $C$  and the other 2 vertices in  $C'$ . Our next results consider  $D_3$   
 131 and impose restrictions to the way the hexagons are partitioned and the  
 132 pentagons are distributed, and ensure that there is a unique  $D_3$ .

133 **Proposition 2.2.** *In  $D_3$ , the layers consisting of 12 hexagons cannot have*  
 134 *two consecutive hexagons partitioned in the same way.*

135 *Proof.* Please refer to Figure 3(b). Label as  $v_i$  the vertices of the inner  
 136  $C_6$  of  $D_3$  that define radial edges with vertices  $v'_i$  in the next cycle  $C_{18}$ .  
 137 The inner  $C_6$  and the next  $C_{18}$  build a layer consisting of 6 hexagons.  
 138 In the  $C_{18}$ , we must distribute 12 additional vertices  $x_i$  in pairs, between  
 139 the  $v'_i$ , as follows:  $x_1$  and  $x_2$  between  $v'_1$  and  $v'_2$ ,  $x_3$  and  $x_4$  between  $v'_2$   
 140 and  $v'_3$ , ..., and  $x_{11}$  and  $x_{12}$  between  $v'_6$  and  $v'_1$ . All 6 hexagons in the  
 141 inner layer have 2 vertices appearing consecutively in the inner cycle  $C_6$

142 and 4 vertices appearing consecutively in the next cycle  $C_{18}$ . The vertices  
 143  $x_i$  define radial edges with 12 vertices  $x'_i$  in the next cycle  $C_{30}$ . We have  
 144 a hexagon defined by three vertices  $x_{12}, v'_1, x_1$  in the  $C_{18}$ , and vertices  
 145  $x'_{12}, x'_1$ , plus  $v''_1$  between them, in the  $C_{30}$ . The two hexagons that lie on  
 146 each side of the hexagon must be partitioned such that 2 vertices appear  
 147 consecutively in the  $C_{18}$  and 4 vertices appear consecutively in the  $C_{30}$ . ■

148 **Proposition 2.3.** *In  $D_3$ , the central layer cannot have three consecutive*  
 149 *pentagons.*

150 *Proof.* From Proposition 2.1, we cannot have two consecutive pentagons  
 151 in the central layer partitioned in the same way, so we have in Figure 3(c)  
 152 three consecutive pentagons so that between two pentagons partitioned in  
 153 the same way, there is a pentagon partitioned in a different way.

154 The central layer of the  $D_3$  is defined by two cycles  $C_{30}$ . Consider in  
 155 Figure 3(c) five vertices  $A, B, K, J$  and  $I$  that are consecutive in a  $C_{30}$ , and  
 156 observe that among them only vertex  $K$  is adjacent to a vertex  $N$  in a  $C_{18}$ .  
 157 So the two consecutive hexagons, of the layer defined by  $C_{30}$  and a  $C_{18}$ ,  
 158 containing vertices  $A, B, K, J$  and  $I$ , and additionally the vertex  $N$ , must  
 159 be partitioned in the same way, which contradicts Proposition 2.2. ■

160 In the central layer of  $D_3$ , we have 12 pentagons distributed among 6  
 161 hexagons. By Proposition 2.1, we cannot have two consecutive pentagons  
 162 partitioned in the same way. By Proposition 2.3, we cannot have three  
 163 consecutive pentagons. So, among the 6 hexagons, the 12 pentagons must  
 164 appear in pairs of consecutive pentagons where each pair is not partitioned  
 165 in the same way. See the unique  $D_3$  in Figure 2.

### 166 3 Conformable coloring of fullerene nanodiscs

167 The smallest Type 2 cubic graph is  $K_4$ , and another known Type 2  
 168 cubic graph is the generalized Petersen graph  $G(5, 1)$  [5], and both have  
 169 squares or triangles, as well as all Type 2 cubic graphs found so far [7]. The  
 170 evidence found in the work of Brinkmann et al. [4] suggests the conjecture

171 that every Type 2 cubic graph has a girth less than 5, and searches were  
 172 started for Type 1 and Type 2 fullerene graphs, which are graphs with  
 173 girth 5, but so far only Type 1 fullerene graphs have been obtained [11].

174 A necessary step towards proving that a cubic graph is Type 1 is to  
 175 define a 4-vertex coloring where the cardinality of each vertex color class  
 176 has the same parity when compared to the cardinality of the entire vertex  
 177 set. Such special vertex coloring is called conformable [5]. From the  
 178 unicity established in Subsection 2.2 for  $D_2$  and  $D_3$ , we may present in  
 179 Figure 4: (a) a 4-total coloring for  $D_2$  [6], and (b) an optimal 3-vertex  
 180 coloring for  $D_3$  that satisfies the requirement to be a conformable 4-vertex  
 181 coloring since each of the 4 color classes has an even number of elements.

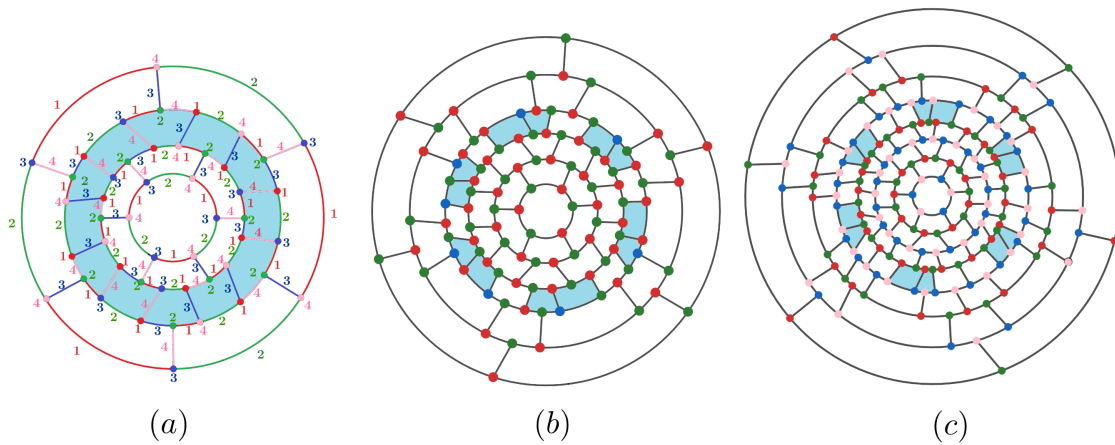


Figure 4: (a) A 4-total coloring of  $D_2$ ; (b) A 3-vertex coloring that is a 4-conformable coloring of  $D_3$ ; (c) A 4-conformable coloring of  $D_4$ .

182 Another strategy is to take advantage that the auxiliary cycles have  
 183 even length and color alternately with colors 1 and 2 the cycle  $C_6$  defining  
 184 the inner layer, with colors 3 and 4 the next cycle  $C_{18}$ , and so on. The  
 185 strategy does not rely on the unicity of  $D_r$ , for  $r > 3$ , and defines a  
 186 conformable 4-vertex coloring for even radius as proved next. Our current  
 187 goal is to generalize the 3-vertex coloring that is a 4-conformable coloring  
 188 of  $D_3$  presented in Figure 4(b) to an arbitrary nanodisc of odd radius.

189 **Theorem 3.1.** *Every nanodisc with even radius admits a conformable*

190 *4-vertex coloring.*

191 *Proof.* Please refer to Figure 4(c). In a  $D_r$  with even  $r$ , consider the 4-  
192 vertex coloring that gives colors 1 and 2 to the outer cycle  $C_6$ , colors 3 and  
193 4 to the next cycle  $C_{18}$ , until we reach the central layer, where colors 3 and  
194 4 are given to cycle  $C_{12r-6}$  and colors 1 and 2 are given to the next cycle  
195  $C_{12r-6}$ , continue in this fashion until colors 3 and 4 are given to the inner  
196 cycle  $C_6$ . Note that each cycle provides an odd number of colored vertices  
197 with the same color, and that every color class has the same number of  
198 vertices and that this number is even, given by  $3r \times r$ . ■

## 199 Acknowledgment

200 We are grateful to two reviewers for their careful reading with many sug-  
201 gestions which contributed to the presentation of the extended abstract.

## 202 References

- 203 [1] K. Ala'a, J. P. Hare, H. Kroto, and R. Taylor, *Isolation, separation*  
204 *and characterisation of the fullerenes  $C_{60}$  and  $C_{70}$ : the third form of*  
205 *carbon*, Journal of the Chemical Society, Chemical Communications  
206 **20** (1990), pp. 1423–1425.
- 207 [2] M. Behzad, *Graphs and Their Chromatic Numbers*, PhD Thesis,  
208 Michigan University (1965).
- 209 [3] O. V. Borodin, A. V. Kostochka and D. R. Woodall, *Total colourings*  
210 *of planar graphs with large girth*, European Journal of Combinatorics  
211 **19** (1998), 19–24.
- 212 [4] G. Brinkmann, M. Preissmann and D. Sasaki, *Snarks with total chro-*  
213 *matic number 5*, Discrete Mathematics and Theoretical Computer  
214 Science **17** (2015), pp. 369–382.
- 215 [5] A. G. Chetwynd and A. J. W. Hilton, *Some refinements of the total*  
216 *chromatic number conjecture*, Congressus Numerantium **66** (1988),  
217 pp. 195–216.
- 218 [6] M. M. F. da Cruz, D. Sasaki, and M. V. T. Costa, *Coloração Total*  
219 *de Nanodiscos de Fulerenos*, Cadernos do IME-Série Matemática **15**  
220 (2020), pp. 34–53.
- 221 [7] S. Dantas, C. M. H. de Figueiredo, G. Mazzuocolo, M. Preissmann,  
222 V. F. dos Santos, and D. Sasaki, *On the total coloring of generalized*  
223 *Petersen graphs*, Discrete Mathematics **339** (2016) pp. 1471–1475.

- 224 [8] A. V. Kostochka, *The total chromatic number of any multigraph with*  
225 *maximum degree five is at most seven*, Discrete Mathematics **162**  
226 (1996), pp. 199–214.
- 227 [9] H. W. Kroto, J. R. Heath, S. C. O'Brien, R. F. Curl, and R. E.  
228 Smalley, *C<sub>60</sub>: Buckminsterfullerene*, Nature **318** (1985), pp. 162–163.
- 229 [10] M. Leidner, *A larger family of planar graphs that satisfy the total*  
230 *coloring conjecture*, Graphs and Combinatorics **30** (2014), pp. 377–  
231 388.
- 232 [11] D. S. Nicodemos, *Diâmetro de Grafos fulerenos e Transversalidade*  
233 *de Ciclos Ímpares de Fuleróides-(3, 4, 5, 6)*, Tese de doutorado. Rio  
234 de Janeiro: COPPE/UFRJ (2017).
- 235 [12] D. Nicodemos and M. Stehlík, *Fullerene graphs of small diameter*,  
236 MATCH Communications in Mathematical and in Computer Chem-  
237 istry **77** (2017), pp. 725–728.
- 238 [13] A. Sánchez-Arroyo, *Determining the total colouring number is NP-*  
239 *hard*, Discrete Mathematics **78** (1989), pp. 315–319.
- 240 [14] L. J. Santos, G. P. Rocha, R. B. Alves, and R. P. de Freitas, *Fulereno*  
241 *[C<sub>60</sub>]: química e aplicações*, Química Nova **33** (2010), pp. 680–693.
- 242 [15] D. Sasaki, S. Dantas, C. M. H. de Figueiredo, M. Preissmann, *The*  
243 *hunting of a snark with total chromatic number 5*, Discrete Applied  
244 Mathematics **164** (2014), pp. 470–481.
- 245 [16] V. Vizing, *On an estimate of the chromatic class of a p-graph*, Discret  
246 Analiz **3** (1964), pp. 25–30.

M. da Cruz

Rio de Janeiro Federal University  
(COPPE/UFRJ)

Rio de Janeiro, Brazil.

mmartins@cos.ufrj.br

D. Sasaki

Rio de Janeiro State University  
(IME/UERJ)

Rio de Janeiro, Brazil.

diana.sasaki@ime.uerj.br

247

M. Tovar

Rio de Janeiro State University  
(IME/UERJ)

Rio de Janeiro, Brazil.

marcus.tovar@ime.uerj.br

C. Figueiredo

Rio de Janeiro Federal University  
(COPPE/UFRJ)

Rio de Janeiro, Brazil.

celina@cos.ufrj.br

## Appendix D

Attachment: Poster “Fullerene nanodiscs: from Chemistry to Combinatorics” presented at WPCCG 2021



WPCCG 2021

Workshop de Pesquisa em Computação dos Campos Gerais

FULLERENE NANODISCS: FROM CHEMISTRY TO COMBINATORICS

Mariana Martins Ferreira da Cruz - PESC/UFRJ - E-MAIL: mm.marr@hotmail.com
Celina Miraglia Herrera de Figueiredo - PESC/UFRJ - E-MAIL: celina@cos.ufrj.br
Diana Sasaki Nobrega - IME/UERJ - E-MAIL: diana.sasaki@ime.uerj.br
Marcus Vinicius Tovar Costa - IME/UERJ - E-MAIL: marcus.tovar@ime.uerj.br

4th Workshop de Pesquisa em Computação dos Campos Gerais (WPCCG 2021)



1. Fullerene Graphs

1.1 Fullerene: A graph class modeling a molecule

In 1985 a new carbon allotrope was reported in the scientific community: C60. A group of scientists, led by Englishman Harold Walter Kroto and Americans Richard Errett Smalley and Robert Curl, trying to understand the mechanisms for building long carbon chains observed in interstellar space, discovered a highly symmetrical, stable molecule, composed of 60 carbon atoms different from all the other carbon allotropes.

The C60 has a structure similar to a soccer hollow ball (Figure 1), with 32 faces, being 20 hexagonal and 12 pentagonal. They decided to name the C60 buckminsterfullerene, in honor of American architect Richard Buckminster Fuller, famous for his geodesic dome constructions, which were composed of hexagonal and pentagonal faces.



Figure 1: Molecular structure of C60.

At the end of the 1980s, other carbon allotrope molecules with similar spatial structure to the C60, were reported called fullerene molecules [1].

The buckminsterfullerene was the first new allotropic form discovered in the 20th century, and earned Kroto, Curl and Smalley the Nobel Prize in Chemistry in 1996. Nowadays fullerene molecules are widely studied by different branches of sciences, from medicine to mathematics. These molecules are supposed to contribute to transport chemotherapy, antibiotics or antioxidant agents and released in contact with deficient cells.

1.2 Fullerene Graphs

Each fullerene molecule can be described as a planar graph in which the atoms and the bonds are represented by the vertices and edges of the graph, respectively, preserving the geometric properties of the original fullerene molecule. Thus, we define a fullerene graph as cubic, planar, 3-connected graph whose faces are pentagonal or hexagonal (Figure 2).

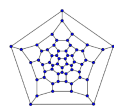


Figure 2: Fullerene graph of C60.

1.3 Fullerene Nanodiscs

The fullerene nanodiscs, or nanodiscs D\_r, of radius r >= 2, are structures composed of two identical flat covers connected by a strip along their borders. While in the nanodisc covers there are only hexagonal faces, in the connecting strip, besides the hexagonal faces, additional 12 pentagonal faces are arranged. Please refer to Figure 3 where the smallest fullerene nanodisc graphs are depicted. In each fullerene nanodisc graph, we highlight in the connecting strip the 12 pentagons.

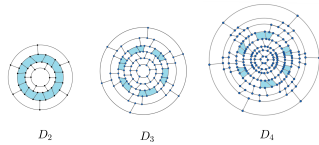


Figure 3: The smallest fullerene nanodisc graphs.

A nanodisc graph of radius r >= 2, denoted by D\_r, has its faces arranged into layers, one layer next to the nearest previous layer starting from an hexagonal cover until we reach the other hexagonal cover [2]. The sequence {1, 6, 12, ..., 6(r-1), 6r, 6(r-1), ..., 12, 6, 1} provides the amount of faces on each layer of the nanodisc graph D\_r. Note that there is an odd number of 2r-1 layers, and we call the layer with 6r faces the central layer. For D\_2 the layer sequence is {1, 6, 12, 6, 1}, for D\_3 is {1, 6, 12, 18, 12, 6, 1} and for D\_4 is {1, 6, 12, 18, 24, 18, 12, 6, 1} (see Figure 3). The auxiliary cycle sequence provides the sizes of the auxiliary cycles that define the layers {C\_6, C\_6, ..., C\_{12}, ..., C\_{6r}, C\_6}. For example, for D\_2 the cycle sequence is {C\_6, C\_6, C\_6, C\_6}, for D\_3 is {C\_6, C\_6, C\_6, C\_6, C\_6, C\_6}, and for D\_4 is {C\_6, C\_6, C\_6, C\_6, C\_6, C\_6, C\_6, C\_6} (see Figure 3). A nanodisc graph D\_r contains 12r x r vertices and 18r x r edges.

2. Combinatorial Results

The 12 pentagonal faces are distributed in the central layer among its 6r faces with the other (6r - 12) hexagonal faces. This is the key property of fullerene nanodiscs [2]. Note that the central layer is defined by two auxiliary cycles, each of size 12r - 6. The 5 vertices of each pentagon are partitioned such that 3 vertices appear consecutively in one cycle and 2 vertices appear consecutively in the other cycle. We say that two pentagons in the central layer are partitioned in the same way if each pentagon has 3 vertices in the same cycle C\_{12r-6}. For r >= 2, in a D\_r, we may have choice to distribute and to partition the 12 pentagonal faces.

Lemma 1: A nanodisc D\_r, r >= 2, cannot have two consecutive pentagons in the central layer partitioned in the same way.

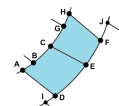


Figure 4: Two consecutive pentagons partitioned in the same way.

Observe that there are two ways of partitioning a hexagon in a layer defined by auxiliary cycles C and C'. We may place 3 vertices of the hexagon in each auxiliary cycle to obtain a balanced hexagon, or we may place 4 vertices of the hexagon in one auxiliary cycle say C' and the other 2 vertices are placed in C' to obtain an unbalanced hexagon. The following results are obtained through the rigidity of the construction of the layers of a nanodisc.

Lemma 2

Consider the fullerene nanodisc D\_r, r >= 2, and its layers consisting of 6 hexagons. All the hexagons in these layers are unbalanced.

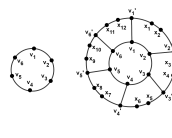


Figure 5: Construction of layer consisting of 6 hexagons in a fullerene nanodisc D\_r, r >= 2.

Theorem 1. Lemmas 1 and 2 ensure that D\_3 shown in Figure 3 is unique.

Lemma 3

In D\_r, r >= 3, the layers consisting of 12 hexagons cannot have two consecutive hexagons partitioned in the same way.

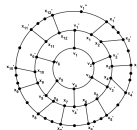


Figure 6: Construction of layer consisting of 12 hexagons in a fullerene nanodisc D\_r, r >= 3.

Lemma 4

The fullerene nanodisc D\_r, r >= 3, cannot have three consecutive pentagons in the central layer.

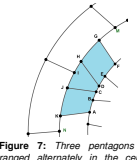


Figure 7: Three pentagons arranged alternately in the central layer of D\_r.

In the central layer of D\_r, we have 12 pentagons distributed among 6 hexagons. By Lemma 1, we cannot have two consecutive pentagons partitioned in the same way. By Lemma 4, we cannot have three consecutive pentagons. So, among the 6 hexagons, the 12 pentagons must appear in pairs of consecutive pentagons where each pair is not partitioned in the same way.

Theorem 2. Lemmas 1, 3 and 4 ensure that D\_3 shown in Figure 3 is unique.

Lemma 5

Consider the fullerene nanodisc D\_r, r >= 4, and its layers containing 18 hexagons. Between each pair of unbalanced hexagons, there is a pair of consecutive balanced hexagons.

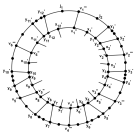


Figure 8: Construction of layer consisting of 18 hexagons in a fullerene nanodisc D\_r, r >= 4.

In the central layer of D\_r, we have 12 pentagons distributed among 12 hexagons. By Lemma 1, we cannot have two consecutive pentagons partitioned in the same way. By Lemma 5, we cannot have three consecutive pentagons. So, we have two forms to distribute the pentagons and the hexagons:

- The pentagons and the hexagons are distributed alternately.
Among the 12 hexagons, the 12 pentagons in pairs of two consecutive pentagons such that each pair is not partitioned in the same way.

Theorem 3. The two non isomorphic nanodiscs D\_r are shown in Figure 9.

In order to describe the number of non isomorphic nanodiscs D\_r, we introduce an auxiliary parameter, 0 <= r <= r-1, defined as the number of hexagons arranged between the pentagons in the central layer, and denote the nanodisc by D\_{r,i} (see Figure 9).

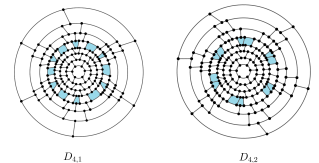


Figure 9: The two non isomorphic fullerene nanodiscs D\_{r,i}

References

[1] KROTO, H. et al. C60: Buckminsterfullerene Nature, 1985.
[2] NICODEMOS, D. de S. Diâmetro de Grafos Fullerenos e Transversalidade de Ciclos Impares de Fullerenos (3, 4, 5, 6). Rio de Janeiro: UFRJ/COPPE, 2017.

3. Acknowledgment



## Appendix E

Attachment: Extended abstract “The conformable condition for Nanodiscs”  
to be presented at ETC 2022

# The conformable condition for Nanodiscs

Mariana M. F. da Cruz<sup>1</sup>, Celina M. H. de Figueiredo<sup>1</sup>, Diana Sasaki<sup>2</sup>, Marcus T. Costa<sup>2</sup>

<sup>1</sup>Programa de Engenharia de Sistemas e Computação (PESC)  
Rio de Janeiro Federal University (UFRJ) – Cidade Universitária, Rio de Janeiro – Brazil

<sup>2</sup>Instituto de Matemática e Estatística (IME)  
Rio de Janeiro State University (UERJ) – Maracanã, Rio de Janeiro – Brazil

{mmartins,celina}@cos.ufrj.br, {diana.sasaki,marcus.tovar}@ime.uerj.br

**Abstract.** We investigate the total coloring of fullerene nanodiscs, a subclass of cubic planar graphs with girth 5 arising in Chemistry, motivated by a conjecture about the nonexistence of a Type 2 cubic graph of girth at least 5. We give a combinatorial description and then a conformable coloring for an infinite family of fullerene nanodiscs.

## 1. The large girth Type 1 conjecture

A  $k$ -total coloring of a graph  $G$  is a color assignment from set  $E \cup V$ , where  $E$  denotes the set of edges and  $V$  denotes the set of vertices of the graph, such that distinct colors are assigned to: every pair of vertices that are adjacent; all edges that are adjacent; and each vertex and its incident edges. The total chromatic number  $\chi''(G)$  is the smallest natural  $k$  for which  $G$  admits a  $k$ -total coloring. Behzad and Vizing [Behzad 1965, Vizing 1964] independently conjectured the Total Coloring Conjecture (TCC) that for any simple graph  $G$ , we have  $\chi''(G) \leq \Delta(G) + 2$ . If  $\chi''(G) = \Delta(G) + 1$ , then the graph is Type 1; if  $\chi''(G) = \Delta(G) + 2$ , then the graph is Type 2. The TCC has been verified for some particular classes of graphs, including cubic graphs [Kostochka 1996].

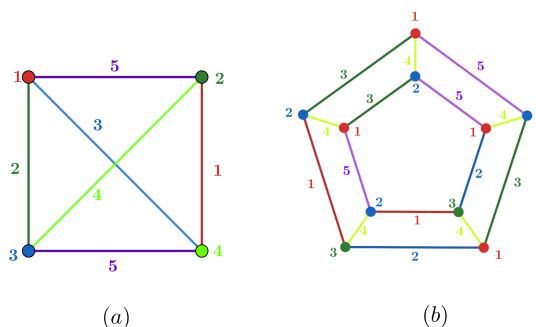


**Figure 1.** (a) A Type 2 girth 3 cubic graph; (b) a Type 2 girth 4 cubic graph.

Every known Type 2 cubic graph has a girth 3 or 4 (See Figure 1). So, it is natural to think that there are no Type 2 cubic graphs with girth at least 5. Thus the following conjecture was proposed [Brinkmann et al. 2015]:

**Conjecture 1.** *There is no Type 2 cubic graph with girth at least 5.*

We will then define a special vertex coloring which is a necessary condition for a graph to be Type 1.

**Lemma 1** ([Chetwynd and Hilton 1988]). *Let  $G$  be a regular graph.  $G$  is conformable if and only if it has a vertex coloring with  $\Delta + 1$  colors and each color class has the same parity of  $|V(G)|$ .*

By Lemma 1, a necessary step towards proving that a cubic graph is Type 1 is to define a 4-vertex coloring where the cardinality of each vertex color class is even. Deciding whether an arbitrary graph is Type 1 is NP-complete [Sánchez-Arroyo 1989], even restricted to cubic graphs. Therefore, extending a conformable coloring to a  $(\Delta + 1)$ -total coloring is also NP-complete.

**Lemma 2** ([Chetwynd and Hilton 1988]). *If  $G$  is a Type 1 graph, then  $G$  is conformable.*

## 2. The nanodiscs are graphs of girth 5

The fullerene nanodiscs, or nanodiscs  $D_r$  of radius  $r \geq 2$ , are structures composed of two identical flat covers, made with only hexagonal faces, connected by a strip along their borders constructed with additional 12 pentagonal faces. Figure 2 shows nanodiscs, where we highlighted with blue color in the connecting strip the 12 pentagonal faces.

The sequence  $\{1, 6, 12, 18, \dots, 6(r - 1), 6r, 6(r - 1), \dots, 18, 12, 6, 1\}$  provides the amount of faces on each layer of the nanodisc graph  $D_r$ . The 12 pentagonal faces are distributed in the central layer among its  $6r$  faces with the other  $(6r - 12)$  hexagonal faces [Nicodemos 2017]. The auxiliary cycle sequence  $\{C_6, C_{18}, \dots, C_{12r-6}, C_{12r-6}, \dots, C_{18}, C_6\}$  provides the sizes of the auxiliary cycles that define the layers. A nanodisc contains  $12r^2$  vertices,  $18r^2$  edges and has girth 5.

## 3. All even radius nanodiscs are conformable

A strategy to color the vertices of  $D_r$  is to take advantage that the auxiliary cycles have even length and color alternately with colors 1 and 2 the cycle  $C_6$  defining the inner layer, with colors 3 and 4 the next cycle  $C_{18}$ , and so on. The strategy does not rely on the unicity of  $D_r$ , and defines for even radius a 4-vertex coloring that is conformable. See Figure 2.

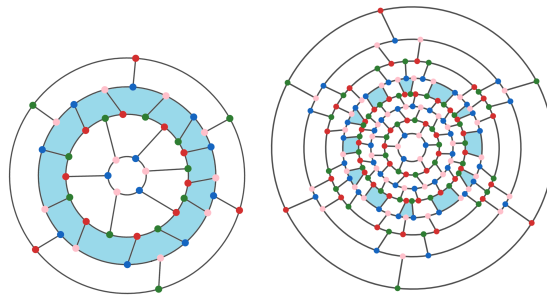


**Figure 2. Conformable colorings for  $D_2$  and  $D_4$ , respectively.**

**Theorem 1** ([da Cruz et al. 2021]). *Every nanodisc with even radius admits a conformable coloring.*

*Proof.* In a  $D_r$  with even  $r$ , consider the 4-vertex coloring that gives colors 1 and 2 to the outer cycle  $C_6$ , colors 3 and 4 to the next cycle  $C_{18}$ , until we reach the central layer, where colors 3 and 4 are given to cycle  $C_{12r-6}$  and colors 1 and 2 are given to the next cycle  $C_{12r-6}$ , continue in this fashion until colors 3 and 4 are given to the inner cycle  $C_6$ . There are  $2r$  cycles, and each color appears in  $r$  cycles. Each color class has the same even number  $3r^2$  of vertices.  $\square$

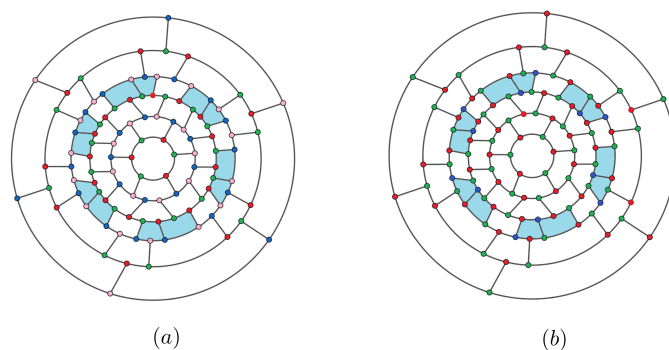


**Figure 3.** (a) A 4-vertex coloring that does not give a conformable coloring of  $D_3$ ; (b) an optimal 3-vertex coloring that gives a conformable coloring of  $D_3$ .

Note that for  $r$  odd this 4-vertex coloring is not conformable, since  $3r^2$  generates an odd number of vertices for each color class (See Figure 3(a)). Thus, seeking to prove that all  $D_r$  nanodiscs are conformable, we further studied the  $D_3$  nanodisc and obtained an optimal 3-vertex coloring that gives a conformable 4-vertex coloring, since each of the three color classes has an even number of vertices, and the fourth color class has 0 elements (See Figure 3(b)).

**Theorem 2** ([da Cruz et al. 2021]). *The nanodisc  $D_3$  is conformable.*

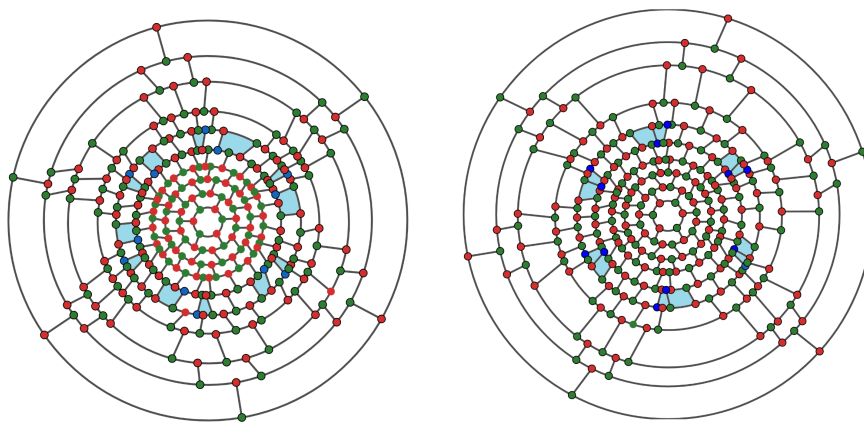


**Figure 4.** 3-vertex colorings of the two non-isomorphic instances of  $D_5$ .

The optimal 3-vertex coloring strategy for  $D_3$  consists of coloring the auxiliary cycles, except for the two cycles of the center layer, using two colors alternately, avoiding color conflict in the vertices that are extremes of radial edges between consecutive auxiliary cycles. In the cycles  $C_{12r-6}$  defining the central layer, we introduce a third color by choosing six vertices in each cycle, thus ensuring the parity of this color class and the other color classes, where the fourth color class has 0 vertices. Recently, we have found two non-isomorphic instances for the fullerene nanodisc  $D_5$ . We verified the coloring strategy described above in both, which culminated in the following result (See Figure 4).

**Theorem 3.** *The two non-isomorphic instances of nanodisc  $D_5$  are conformable.*

## 4. Current work

Our current goal is to generalize the 3-vertex coloring strategy that gives a conformable coloring of  $D_3$  presented in Figure 3(b) and of  $D_5$  presented in Figure 4 to an arbitrary nanodisc of odd radius. We were not able to extend the conformable vertex colorings defined in Section 3 for a 4-total coloring of those fullerene nanodiscs. We need to further investigate the structure of the class, looking for a suitable conformable vertex coloring that extends to a 4-total coloring of  $D_r$ , in order to prove that every fullerene nanodisc is Type 1, as has already been proven for  $D_2$  [da Cruz et al. 2021]. See Figure 5.

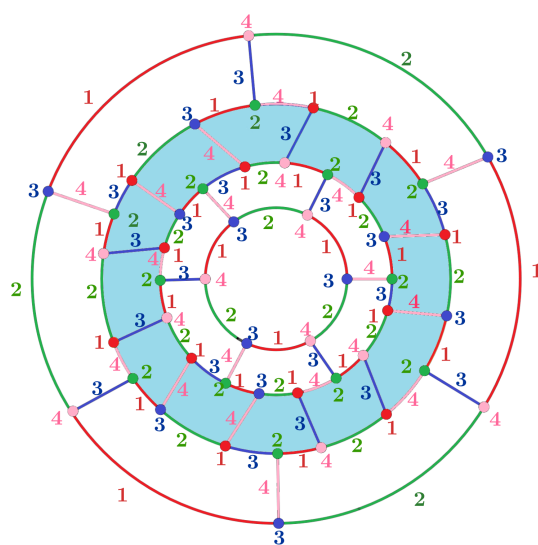


Figure 5. A 4-total coloring of  $D_2$ .

## References

- Behzad, M. (1965). *Graphs and their chromatic numbers*. Michigan State University.
- Brinkmann, G., Preissmann, M., and Sasaki, D. (2015). Snarks with total chromatic number 5. *Discrete Mathematics and Theoretical Computer Science*, 17:369–382.
- Chetwynd, A. and Hilton, A. (1988). Some refinements of the total chromatic number conjecture. *Congressus Numerantium*, 66:195–216.
- da Cruz, M., de Figueiredo, C., Sasaki, D., and Costa, M. (2021). Hunting a Type 2 fullerene nanodisc. *Matemática Contemporânea*, 48:126–136.
- Kostochka, A. V. (1996). The total chromatic number of any multigraph with maximum degree five is at most seven. *Discrete Mathematics*, 162:199–214.
- Nicodemos, D. (2017). *Diâmetro de Grafos Fulerenes e Transversalidade de Ciclos Ímpares de Fuleróides-(3, 4, 5, 6)*. PhD thesis, Universidade Federal do Rio de Janeiro.
- Sánchez-Arroyo, A. (1989). Determining the total colouring number is NP-hard. *Discrete Mathematics*, 78(3):315–319.
- Vizing, V. (1964). On an estimate of the chromatic class of a p-graph. *Discret Analiz*, 3:25–30.

## Appendix F

Attachment: Abstract “Hunting a conformable fullerene nanodisc that is not 4-total colorable” accepted for participation in LAWCG 2022

# Hunting a conformable fullerene nanodisc that is not 4-total colorable

M. da Cruz <sup>1,\*</sup> C. Figueiredo <sup>1</sup> D. Sasaki <sup>2</sup> M. Tovar <sup>2</sup> D.  
Nicodemos <sup>3</sup>

<sup>1</sup> Rio de Janeiro Federal University (UFRJ)

<sup>2</sup> Rio de Janeiro State University (UERJ)

<sup>3</sup> Colégio Pedro II (CPII)

---

*Keywords: Total Coloring, Fullerene Nanodiscs, Conformable Graphs*

---

Fullerene nanodiscs  $D_r$  are mathematical models for carbon-based molecules experimentally found in the early eighties, which are cubic, 3-connected, planar graphs with pentagonal and hexagonal faces. The planar embedding of  $D_r$  has its faces arranged into layers, one layer next to the nearest previous layer starting from a hexagonal cover until we reach the other hexagonal cover. The distance between the inner (outer) layer and the central layer, where lie 12 pentagonal faces, is given by the radius parameter  $r \geq 2$ .

A total coloring of a graph assigns colors to the vertices and edges such that adjacent or incident elements have different colors. The long-standing Total Coloring Conjecture is settled for cubic graphs, implying that every cubic graph admits a 5-total coloring. However, the recognition of 4-total colorable cubic graphs is a challenging problem. Since every known cubic graph that is not 4-total colorable has girth at most 4, it has been conjectured that every cubic graph with girth at least 5 is 4-total colorable. A necessary step toward proving that a cubic graph admits a 4-total coloring is to define a conformable coloring, which is a 4-vertex coloring where the cardinality of each vertex color class has the same parity as the cardinality of the entire vertex set. A graph that admits a conformable coloring is called conformable.

We prove that every fullerene nanodisc is conformable. Although every conformable coloring we were able to exhibit does extend to a 5-total coloring, we are still looking for a suitable conformable coloring that might extend to the desired 4-total coloring. In parallel with these investigations, we present combinatorial contributions referring to the structure of fullerene nanodiscs.